Cross-talk between inflammation and mitochondria in X-linked adrenoleukodystrophy (X-ALD): an integrative approach towards different therapies

Janani Parameswaran

TESI DOCTORAL UPF / 2017

Director de la tesi

Dr. Aurora Pujol Onofre

(Neurometabolic Disease Laboratory-IDIBELL)

DEPARTAMENTO DE CIENCIAS EXPERIMENTALES

Y DE LA SALUD

UNIVERSIDAD POMPEU FABRA

Dedicated to my Dad

ACKNOWLEDGEMENT

At the outset I would like to express my sincere and deep gratitude to my supervisor Dr. Aurora Pujol for the confidence reposed on me and given a platform to commence my doctorate .

Further I would like to express my thanks to Dr. Stéphane Fourcade for extending his helping hands to me by all means during the tenure to complete this task and to finish writing the thesis. I gratefully acknowledge the help of all the dignitaries of funding sources who helped for my survival and completion of this stupendous task my PhD degree.

Every member of the Neurometabolic disease Laboratory has contributed their share immensely to my personal and professional welfare during the tenure of my stay at Barcelona. I would like to convey my special thanks to Jone and Xavi Ortega, whose support and motivation during my initial years of PhD has been a great boon to me. I express a very big thanks to all the past and present laboratory colleagues with whom I have had a great pleasure to work with - Montse, Juanjo, Agatha, X Joya, Nathalie, Harmurt, Cristina, Laia, Jordi, Edgard, Laia Garcia, Laura and the most fabulous PhD squad Laia Morato, Andrea, Patri, Sanjib, Pablo, Devesh and Leire and to remain grateful for their immense contribution to complete my assignment. The group has given me a source of friendship as well as good advice and collaboration. I am grateful to the funny "coffee group" also in particular, which always turns me to be cheerful and happy during the tougher days. A special acknowledgement goes to Imma, who was a nice friend ever since we began to interact. My period of stay at IDIBELL was made enjoyable for the larger part due to the presence of many friends and groups in Genetica Molecular. I am very much thankful to all of them. Also, I would like to thank people from outside the lab - Ekin, Sandra, Veena for sharing special moments with me during my PhD life.

A special group from my bachelor's and master's university is not mentioned yet, because they deserve their own part: I praise their enormous amount of help thoughout these years. Thank you Priyam, Monisha, Roobini, Arul, Varun, Murali and Prabhakaran.

I would like to express my heartfelt thanks to my family for all their love and encouragement. For my parents who raised me with a love of science and supported me in all my pursuits. Words cannot express how grateful I am to them for all of the sacrifices that you have made on my behalf. I would also like to thank my grandparents your blessings made me sustained so far.

Lastly, I would like to remain grateful ever to each and every one who has helped, guided and rendered all sorts of services to me in completing my doctroate.

.

Abstract

Lack of function of ALDP in mouse leads to a late onset disease, characterized by spastic paraparesis and degeneration of corticospinal tracts, without signs of inflammatory demyelization resembling AMN patients.

Taking advantage of this mice model and using primary glia cultures, we investigated the role of inflammation (mainly the pro and anti-inflammatory pattern) in X-ALD mice spinal cord and studied the contribution of microglia and astrocytes in disease pathogenesis. We found X-ALD mice spinal cord shows an inflammatory imbalance at 12 months of age. Similar observations were found in case of X-ALD mice primary microglia. In addition, we found mitochondria as the source of ROS in X-ALD mice microglia when insulted with C26:0.

Activation of CB_2 receptor prevents microgliosis and recovers all the altered parameters in X-ALD mice and thus halts axonal degeneration. Similar neuroprotective effects were observed with Methylene blue by targeting mitochondria.

Resum

La ausencia de función de ALDP en ratón conduce a una enfermedad tardía caracterizada por paraparesia espástica y degeneración del tracto corticoespinal sin signos de desmielinización inflamatoria, semejante a pacientes con AMN.

Aprovechando este modelo y utilizando cultivos primarios de glía, hemos investigado el rol de la inflamación en la médula espinal del ratón X-ALD y la contribución de microglía y astrocitos en la patogénesis de la enfermedad.
Hemos observado que la médula espinal muestra un desequilibrio inflamatorio a los 12 meses de edad. El mismo patrón se ha encontrado en cultivos primarios de microglía provenientes del mismo modelo, identificando además a la mitocondria como su fuente de ROS, tras tratarla con C26:0.

Se han observado efectos neuroprotectores tales como la prevención de microgliosis y la recuperación de todos los parámetros alterados en los ratones los X-ALD, tanto activando los receptores CB2 como atacando dianas mitocondriales con azul de metileno.

Preface

X-linked adrenoleukodystrohpy (X-ALD) is the most common peroxisomal disorder and monogenic leukodystrophy with the incidence 1:17000, caused by loss of function of the peroxisomal transporter ABCD1. The defective function of the ABCD1 transporter leads to VLCFA accumulation due to decreased β-oxidation of these fatty acids in peroxisomes mainly hexacosanoic acid (C26:0). Despite being a single-gene disease, X-ALD is a complex inherited syndrome in which the same mutation in the *ABCD1* gene can lead to clinically very distinct phenotypes from adrenal insufficiency to fatal cerebral demyelination. Abcd1-null mice (*Abcd1*$^{-}$) develop a late onset axonal degeneration in the spinal cord and locomotor disability without active signs of inflammatory demyelination in brain resembling the most common phenotype in humans, adrenomyeloneuropathy (AMN). The animals show early oxidative damage, mitochondrial dysfunction and impaired bioenergetic and redox homeostasis.

In this thesis, we sought to investigate the contribution of microglia and astrocytes in disease pathogenesis and to explore novel therapeutic targets with the existing and new studies derived from this mouse model. In the first study, with the application of both *in-vivo* and *in-vitro* approaches, we identified a general inflammatory imbalance in X-ALD mice. We analyzed the M1 and M2 inflammatory profile in our mouse model with background knowledge of M1 and M2 induction in PBMC and plasma from AMN patients. We identified a mixed inflammatory profile in *Abcd1*$^{-}$ mice spinal cord associated with upregulation of most of the pro and anti-inflammatory cytokines and chemokines. Further, we speculate whether these inflammatory responses come from microglia, as they are key players of many neurodegenerative disorders that contribute the major role in neurodegeneration. We found a similar inflammatory pattern like spinal cord as these cultures display an inflammatory imbalance at baseline and show more severe inflammatory profile with exogenous C26:0. These inflammatory responses are characterized by up-regulation of some cytokines and chemokines in *Abcd1*$^{-}$ mice microglia like *Tnf-α, Il1β* and *Ccl5* at baseline and further elevation of cytotoxic factors *like Cd86, iNOS* and *Cox2* upon C26:0. Moreover, we found mitochondria as the major source of ROS when *Abcd1*$^{-}$ mice microglia is loaded with exogenous C26:0. Similar toxic effects of C26:0 was found, when treated on astrocytes cultures. However, no

baseline differences were seen in case of astrocytes either in ROS and inflammation indicating microglia could play an important role in progression of the disease.

In the second study, we found an altered endocannabionoid system with upregulated CB_2 levels in X-ALD spinal cord and in primary microglia. With these data, we hypothesized that modulation of inflammatory responses and regulating microglia activation via CB_2 would be a beneficial therapeutic approach for treating X-ALD. Activation of CB_2 prevents microgliosis but not astrocytosis and halts axonal degeneration together with improved locomotor disability. We also found normalization of almost all altered parameters includes inflammatory imbalance, mitochondrial dysfunction and bio-energetic failure previously observed in X-ALD mice. Moreover, we found that CB_2 activation also inhibits C26:0 driven inflammation and ROS production in primary *Abcd1*$^{-}$ mice microglia. These altogether indicates us that CB_2 activation may provokes these neuroprotective activities via modulation of microglia activity.

In third study, we used Methylene blue as a target drug for the treatment of X-ALD as many existing reports shown to exert protective effects via modulating mitochondria activity. Here we showed that apart Methylene blue is able to induce mitochondrial biogenesis and respiration in X-ALD mice. Also, we demonstrated that Methylene is able to modulate the activity of DRP1. We found that MB treatment reduces the activated DRP1 levels in *Abcd1*$^{-}$ mice spinal cord. To corroborate these results with *in-vitro* studies, we checked the effect of MB on activity of DRP1 on mitochondria network. We demonstrated that MB treatment inhibits C26:0 induced ROS production and prevents the translocation of DRP1 to mitochondria, thus maintaining the integrity of mitochondria network. Further, we also observed that MB treatment improves locomotors disability and halts axonal degeneration.

Collectively, the findings of this doctoral thesis suggest that the above two drugs targeting inflammation and mitochondria may be potential therapies for the treatment of X-ALD and also for the other neurodegenerative disorders that share the common pathogenic features.

Table of contents

LIST OF ABBREVIATION

2-AG	2-Arachidonoylglycerol
ABC	ATP-binding cassette
AD	Alzheimer's disease
ADP	Adenosine diphosphate
AEA	Anandamide
ALS	Amyotrophic lateral sclerosis
AMN	Adrenomyeloneuropathy
AMP	adenosine monophosphate
ARE	Antioxidant response element
ATP	Adenosine triphosphate
Aβ	Amyloid-β
BBB	Blood brain barrier
C26:0	Hexacosanoic acid
cAMN	Cerebral adrenomyeloneuropathy
ccALD	Childhood cerebral adrenoleukodystrophy
CB1	Cannabinoid receptor 1
CB2	Cannabinoid receptor 2
cDNA	Complementary deoxyribonucleic acid
CEL	Carboxyethyl lysine
CML	Carboxymethyl lysine
CNS	Central nervous system
CoA	Coenzyme A
COX2	Cyclooxygenase 2
CTL	Control
DAGLα	Diacylglycerol lipase alpha
DAGL β	Diacylglycerol lipase beta
DKO	Abcd1/Abcd2double knockout
DNA	Deoxyribonucleic acid
EAE	Experimental autoimmune encephalomyelitis
EC	Endocannabinoid
ER	Endoplasmic reticulum
FAAH	Fatty acid amide hydrolase
FAD	Flavin adenine dinucleotide
FADH2	Flavin adenine dinucleotide (reduced form)
GSA	Glutamic semialdehyde
GSH	Reduced glutathione
HD	Huntington's disease
HSCT	Hematopoietic stem cell transplantation
IF	Immunofluorescence
IHC	Immunohistochemistry
IL	Interleukin
IVR	Intervening region
LA	Lipoic acid

MAGL	Monoacylglycerol lipase
MDA	Malondialdehyde
MDAL	MDA-lysine
MIM	Mitochondrial inner membrane
MRI	Magnetic resonance imaging
mRNA	Messenger ribonucleic acid
mtDNA	Mitochondrial DNA
NAC	N-acetyl-L-cysteine
NAD+	Nicotinamide adenine dinucleotide
NADH	Nicotinamide adenine dinucleotide (reduced form)
NADPH	Nicotinamide adenine dinucleotide phosphate, (reduced form)
NAPE-PLD	N-acyl phosphatidylethanolamine-specific phospholipase D
OSCSC	Organotypic spinal cord slice cultures
OXPHOS	Oxidative phosphorylation
PBMC	Peripheral blood mononuclear cells
PD	Parkinson's disease
R.C.R	Respiratory control ratio
RNS	Reactive nitrogen species
ROS	Reactive oxygen species
UPS	Ubiquitin proteasome system
VLCFA	Very long-chain fatty acids
WAT	White adipose tissue
WT	Wild-type
X-ALD	X-linked adrenoleukodystrophy

INTRODUCTION

1 Introduction

1.1 X-ALD: knowledge about the disease

1.1.1 X-ALD History

The first description about X-linked Adrenoleukodystrophy (X-ALD) was presented by Haberfeld and Spieler in 1910. They showed that a 6 year old boy had developed hyper-pigmentation, impaired visual activity followed by spastic paraparesis, lost his ability to speak and walk and eventually died at the age of 7. An older brother had died of a similar illness at the age of 8. The neuropathological post-mortem analysis described a diffuse involvement of the cerebral hemispheres with a severe demyelination combined with perivascular accumulation of lymphocytes and plasma cells (Schilder, 1924). In 1923, Siemerling and Creutzfeldt described a similar case, but with adrenal gland involvement (Siemerling and Creutzfeldt, 1923). The disease was first named Schilder´s disease and later, in 1970, Blaw coined the term adrenoleukodystrophy.

Few years later, it was demonstrated that these inclusions were enriched in cholesterol esterified with saturated very long-chain fatty acids (VLCFA) (Igarashi et al., 1976). In the 80's, high VLCFA levels were detected in cultured skin fibroblasts and plasma (Moser et al., 1981). Accumulation of VLCFA in plasma is still nowadays used as pathognomonic marker of the disease (Moser and Moser, 1999). Later on, it was demonstrated that white blood cells and cultured skin fibroblasts had an impaired capacity to degrade VLCFA (Singh et al., 1987) and the gene mutated in X-ALD was mapped to Xq28 (Migeon et al., 1981). The evidence that bone-marrow derived cells are able to degrade VLCFA set the proof of concept for bone-marrow transplantation for X-ALD patients (Aubourg et al., 1990). In the 90's, *ABCD1* was identified by positional cloning as the defective gene in X-ALD (Mosser et al., 1993). This crucial discovery allowed the generation of mouse models in 1997 (Forss-Petter et al., 1997, Kobayashi et al., 1997, Lu et al., 1997) and the successful lentiviral-mediated gene therapy in 2009 (Cartier et al., 2009).

1.1.2 Gene and mutation

X-ALD patients carry a mutation in *ABCD1* (Mosser et al., 1993). *ABCD1,* the defective gene in X-ALD, consists of 10 exons and encodes for a protein of 745 amino acids named ALD protein (ALDP). ALDP is localized in the peroxisomal membrane. This protein is a member of the ATP binding cassette (ABC) transmembrane transporter super family, which typically consists of six hydrophobic transmembrane domains and two hydrophobic nucleotide-binding folds (Dean and Allikmets, 2001). The peroxisomal ABC transporters have been designated in the subgroup D, which includes four members *ABCD1, ABCD2, ABCD3* and *ABCD4*. *ABCD1* is expressed strongly in the glia and the adrenal cortex and *ABCD2* is the closest gene to *ABCD1* and encodes for the ALD-related protein (ALDRP) (Ferrer et al., 2005). ALD and ALDRP show 66% identity, with overlapping functions, but a mirror expression in most tissues (Pujol et al., 2004). ABCD2 is strongly expressed in neurons and the adrenal medulla. *ABCD3* encodes for PMP70 and *ABCD4* for PMP70/69R (Kamijo et al., 1990, Shani et al., 1997). Although *ABCD4* was initially considered a peroxisomal transporter the actual localization are the lysosomes (Coelho et al., 2012). Members of the ABCD family are encoded as half-transporters with 6 transmembrane domains and a single binding fold. Thus, they function as either homodimers or as heterodimers with other members of the ABCD group. Homodimerization of ALDP and heterodimerization of ALDP with ALDRP or PMP70 have been described *in vitro* ((Braiterman et al., 1998). Finally a recent study showed ABCD1 and ABCD2 oragnized in tetramers (Geillon et al., 2017).

1.1.3 Biochemistry

ABCD1 is an integral peroxisomal membrane protein with the ATP-binding domain located towards the cytoplasmic surface of the peroxisomal membrane (Contreras et al., 1996). Peroxisomes are ubiquitous subcellular organelles, derived from the endoplasmic reticulum (Schluter et al., 2006). Peroxisomal functions include hydrogen peroxide (H_2O_2) detoxification, plasmalogens biosynthesis and degradation of purines, polyamines and amino acids. Moreover, peroxisomes are responsible of β-oxidation of VLCFA, fatty acids (FA) with aliphatic tails longer than 22 carbons (Wanders and Waterham, 2006). The peroxisomal β -oxidation system involves four enzymatic steps

of (1) dehydrogenation, (2) addition of H_2O to the resulting double bond, (3) oxidation of the -hydroxyacyl-coA to a ketone and (4) thiolytic cleavage by coenzyme A (CoA). At the end of each cycle of four reactions, one acetyl-CoA (Ace-CoA) is released from the end of the FA, giving a shortened acyl-CoA ester, which can undergo subsequent rounds of β-oxidation. As peroxisomes are not able to degrade completely fatty acyl-CoA, the shortened acyl-CoA chain is shuttled to mitochondria for full oxidation (Kemp and Wanders, 2010).

In X-ALD, there is an increased content of VLCFA, mainly tetracosanoic (C24:0) and hexacosanoic (C26:0) acids, in cholesterol esters and complex lipids such as gangliosides, phosphatidylcholine, sphingomyelin, cerebrosides and sulfatides (Igarashi et al., 1976, Moser et al., 1981, Wiesinger et al., 2013). This accumulation is caused by an impaired capacity of the peroxisomes to degrade VLCFA (Fourcade et al., 2009). VLCFA are metabolically inactive and thio-esterification to CoA (VLCFA-CoA) is necessary for the initiation of the peroxisomal β-degradation. Thereby, initially it was hypothesized that the gene defective in X-ALD had VLCFacyl-CoA synthetase activity. Experimental evidence that *ABCD1* is the defective gene in X-ALD came from complementation studies. The expression of the wild-type *ABCD1* in fibroblast from X-ALD patients restored VLCFA β-oxidation and reduces VLCFA levels (Cartier et al., 1995, Shinnoh et al., 1995). In yeast Saccharomyces cerevisiae, ABC half-transporters (Pxa1p and Pxa2p) form a heterodimer in peroxisomes and import acyl-coA esters. The inability of yeast mutants lacking these genes to growth in a medium with oleic acid is partially restored when ALDP is expressed (van Roermund et al., 2008). These experiments demonstrated that ALDP transports acyl-CoA esters across the peroxisomal membrane (Hettema et al., 1996, van Roermund et al., 2008, Wanders et al., 2007). In summary, VLCFA accumulation is caused by mutations in *ABCD1* gene, which impair the import of VLCFA-CoA into the peroxisomes (**Fig. 1**).

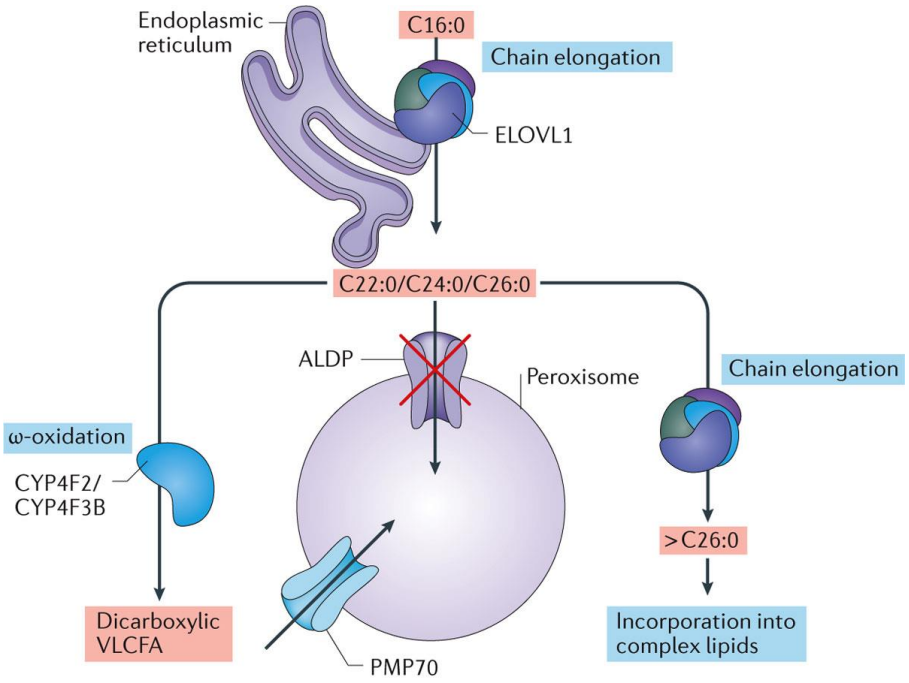

Figure 1. Very long-chain fatty acids (VLCFA) are synthesized via chain-elongation of long-chain fatty acids by ELOVL1, the human VLCFA-specific elongase. A deficiency in ALDP impairs peroxisomal import and β-oxidation of VLCFA. (Kemp, S. 2016).

1.1.4 X-ALD phenotypes

X-ALD is the most common peroxisomal disorder and monogenic leukodystrophy with the incidence of 1 in 17000 newborns. X-ALD presents from clinical manifestation in white matter of CNS and adrenal gland. The main hallmark in X-ALD is the accumulation of VLCFA mainly C26:0 in target organs like CNS and adrenal glands (also found in plasma and human fibroblasts). Despite being a single-gene disease, X-ALD displays a complex range of clinical phenotypes. The two main distinct phenotypes have described below:

1. Childhood cerebral ALD (ccALD): It is characterized by strong inflammatory demyelination with autoimmune responses leading to death within few years. It is most progressive form of X-ALD and affects mainly boys between ages of 5 to 12 years. Initially, main symptoms are behavioral or learning deficits, which usually lead to attention deficit or hyperactivity diagnosis. Next, progressive

impairment of cognition, behaviour, vision, hearing. This phenotype affects the 35% of X-ALD patients.

2. Adrenomyeloneuropathy (AMN): It is the most frequent manifestation of X-ALD and affects adult patients. AMN patients present peripheral neuropathy and distal axonopathy involving corticospinal tracts of the spinal cord but not brain neuroinflammation or major demyelination with spastic paraparesis as major symptoms. Virtually all patients with X-ALD who reach adulthood develop AMN. However, approximately 20% of the AMN patients develop an additional cerebral demyelination (cerebral AMN, cAMN), which can progress as in patients with CCALD (de Beer et al., 2014).

1.1.5 Animal models for X-ALD

In 1997, three different groups developed three independent X-ALD mouse models, by inactivating *Abcd1* gene (Forss-Petter et al., 1997, Kobayashi et al., 1997, Lu et al., 1997). Despite, all the above three models display accumulation of VLCFA which is the main biochemical hallmark of the disease, they do not develop cerebral demyelination or brain inflammation, characteristic of ccALD. However, around 18 months of age, these mice develop a late onset AMN-like phenotype. This phenotype is characterized by spastic paraparesis due to degeneration of corticospinal tracts, without signs of inflammatory demyelination in the brain. Axonal pathology is found in sciatic nerves and spinal cord, including slower sciatic nerve conduction and motor behaviour abnormalities in rotarod, bar cross and treadmill tests (Pujol et al., 2002). *ABCD1*-deficient mice have been instrumental in dissecting pathomechanisms of AMN (Fourcade et al., 2008, Galino et al., 2011, Launay et al., 2015, Launay et al., 2013, Launay et al., 2017, Lopez-Erauskin et al., 2013a, Morato et al., 2013, Morato et al., 2015). In an attempt to obtain a more severe phenotype (ccALD), *ABCD1/ABCD2* double-deficient mice (*Abcd1*$^{-}$/*Abcd2*$^{-/-}$) were generated, although they do not develop brain inflammation or demyelination either. The neuropathology in these mice is also restricted mainly to the spinal cord and, due to the contribution of *ABCD2*, the dorsal root ganglia, resulting in a sensory neuropathy. Nevertheless, these defects are more pronounced and start at 12 months of age, earlier than upon *ABCD1* deficiency alone (Pujol et al., 2002), setting up a suitable preclinical model

for testing disease-modifying drugs (Launay et al., 2017, Lopez-Erauskin et al., 2011, Morato et al., 2013, Morato et al., 2015). Furthermore, since *Abcd1*$^{-}$ mouse does not present a progressive phenotype that leads to cerebral demyelination and neuroinflammation, it underscores the hypothesis that considers that genetic and/or environmental factors trigger the onset of cerebral forms of X-ALD.

1.1.6 Therapies for X-ALD

Currently, the therapeutic opportunities for X-ALD are unsatisfied. Here some of the possible therapeutic strategies are listed below:

1. As 70% of X-ALD patients develop adrenal insufficiency, X-ALD diagnosed boys and men should be monitored by measuring adrenocorticotropic hormone (ACTH) levels in plasma and with the ACTH stimulation test. Then, if necessary, they must be treated with steroid replacement, in the same way as for other forms of primary adrenal insufficiency (Moser and Mahmood, 2007).

2. Lorenzo's oil is a 4:1 mixture of oleic (C18:1ω9) and erucic (C22:1ω9) acids, which competes for the fatty acid elongation system, preventing the synthesis of saturated VLCFA. Oral administration of this oil, combined with moderate reduction of fat in the diet, reduces plasma levels of VLCFA within four weeks (Moser et al., 1987), so it was a promising therapeutic strategy in the 80s-90s. Nevertheless, VLCFA levels in brain do not change (Rasmussen et al., 1994) and further studies proved that Lorenzo's oil administration does not stop the progression of X-ALD (Aubourg et al., 1993, van Geel et al., 1999). Even though a study with 89 asymptomatic boys with normal MRI showed that Lorenzo's oil might prevent cerebral demyelination (Moser et al., 2005), there is no definitive evidence for the efficacy of Lorenzo's oil in the prevention of the onset of cerebral ALD.

3. Lovastatin, a cholesterol-lowering drug, normalizes VLCFA levels in X-ALD fibroblasts and in plasma of X-ALD patients (Singh et al., 1998, Singh et al., 2004). However, in a placebo-controlled trial, it did not lower C26:0 levels in

peripheral-blood cells, and its effect on plasma VLCFA were attributed to be a consequence of a non-specific decrease in the level of low-density lipoprotein (LDL)-cholesterol (Engelen et al., 2010).

4. Bezafibrate gave hope for therapy, as it reduces *de novo* C26:0 synthesis, by competitive inhibition of ELOVL1 in X-ALD fibroblasts (Engelen et al., 2012a), but it does not lower VLCFA levels in plasma or lymphocytes of X-ALD patients (Engelen et al., 2012b).

5. Immunomodulators or immunosuppressants aimed to reduce brain inflammation have not worked in X-ALD. Neither cyclophosphamide nor subcutaneous injections of interferon (IFN)-β1a nor intravenous immunoglobulins injection stopped the progression of the disease (Cappa et al., 1994, Korenke et al., 1997, Naidu et al., 1988).

6. Pharmacological induction of *ABCD2* gene expression: Since overexpression of *ABCD2* in X-ALD fibroblasts and in *Abcd1*$^{-}$ mice prevents VLCFA accumulation (Flavigny et al., 1999, Netik et al., 1999, Pujol et al., 2004), ABCD2-inducing drugs were proposed as a therapeutic option for X-ALD. Nevertheless, 4-phenylbutyrate (4- PBA) (Kemp et al., 1998, McGuinness et al., 2001, Moser et al., 2000), fenofibrate (Albet et al., 1997, Fourcade et al., 2001) and valproic acid (Fourcade et al., 2010) had little success when tested.

7. Antioxidant supplementation: Given the important role of oxidative stress in X-ALD, antioxidant therapies were tested in the X-ALD animal models. A combination of antioxidants (vitamin E, N-acetylcysteine and lipoic acid) halts axonal degeneration and prevents locomotor deficits in *Abcd1*$^{-}$ mice (Lopez-Erauskin et al., 2011). These results from our group, have led to a phase II clinical trial in AMN patients with a cocktail of antioxidants (NCT01495260). High-dose of antioxidants resulted in the normalization of several protein and DNA oxidative damage biomarkers and a significant reduction of several inflammation markers such as chemokines and lipid mediators. In addition, the

results showed a significant reduction in central motor conduction time in both legs (upper motorneuron), and an improvement in the six-minute walking test (6MWT) in eight out of ten patients (M. Ruiz, personal communication).

8. Apart from these therapeutic strategies, the only useful therapy for cerebral X-ALD is bone marrow transplantation (Aubourg et al., 1990). HSCT (Hematopoietic stem cell transplantation) arrests neuroinflammation, probably through an improvement in microglial functions, as these cells derive from bone marrow progenitors (Eglitis and Mezey, 1997). HSCT can only be performed at an early stage of the disease, meaning a score of ≤9 in the X-ALD MRI Severity Scale (Loes et al., 2003) and no neurologic or neuropsychological deficits. Because of this, monitoring of X-ALD boys is so important. In these conditions the 5-years survival is above 90% (Mahmood et al., 2007, Miller et al., 2011). Anyway, HSCT remains associated with high risks of morbidity and mortality, and it is not easy to find a matching donor. The absence of biomarkers that can predict the evolution of cerebral disease together with the fact that HSCT performed in childhood does not seem to prevent myelopathy and peripheral neuropathy in adulthood (van Geel et al., 2015) makes mandatory the search of new therapies for X-ALD patients.

9. A recent alternative to allogeneic HSCT is gene therapy, by transplantation of genetically corrected autologous CD34+, with encouraging results in the first two treated boys, in which this therapy has impeded the progression of the disease (Cartier et al., 2009).

1.1.7 The role of VLCFA in pàthogenesis of X-ALD

The exact mechanism that connects VLCFA accumulation with the axonal degeneration in AMN, or neuroinflammation and demyelination in ccALD remains elusive. Several mechanisms of VLCFA-induced cytotoxicity have been proposed. VLCFA that are incorporated in complex lipid such as gangliosides and phosphatidylcholine might have disruptive effects on structure, stability and function of cell membranes. In agreement with this, C26:0 increases the membrane microviscosity in erythrocytes of patients with

cerebral ALD and AMN (Knazek et al., 1983), and in adrenocortical cells from X-ALD patients, altering their capacity to secrete cortisol (Whitcomb et al., 1988). Whereas the accumulation of VLCFA in myelin components, such as the proteolipid protein (PLP), would destabilize myelin sheaths (Bizzozero et al., 1991). Consistently the amounts of VLCFA were found to be higher in normal appearing white matter and iPSCs oligodendrocytes from ccALD patients compared with AMN patients (Asheuer et al., 2005; Jang et al., 2011). Thus, the initial phase of spontaneous onset of demyelination might be directly related to the level of VLCFA in the myelin sheath (Berger et al., 2014). An important factor that could be involved in the conversion into a rapidly progressive inflammatory demyelination in cerebral ALD, is the capacity of VLCFA to activate an immune response through CD1, the major lipid antigen presenters (Ito et al., 2001). Gangliosid and proteolipid containing VLCFA have been suggested as self-lipid antigens for eliciting auto immunity (Berger et al., 2014). However, the wide spectrum of X-ALD phenotypes and the lack of demyelination in Abcd1 null mice, in spite of VLCFA accumulation in brain (Forss-Petter et al., 1997; Lu et al., 1997) suggest the presence of additional VLCFA-related mechanisms underlying the progression from a metabolic disease (AMN) to the fatal neuroinflammatory disease (CCALD) (Singh and Pujol, 2010). The current model suggests that VLCFA accumulation initiates a sequence of toxic phenomena, including oxidative stress as “first hit”, inflammation as “second hit” and peroxisome dysfunction as “third hit”, that participate in the onset and progression of the disease.

1.2 Hallmarks of X-ALD

As described before X-ALD is rare fatal neurometabolic disease caused by mutation in single gene *ABCD1* characterized by striking variations in clinical phenotypes. With the help of moude model of X-ALD, *Abcd1*$^{-}$ mice that resembles the most common phenotype of X-ALD (AMN) we revealed several dyregulated pathways underlying the pathogenesis of disease. A schematic diagram showing all the dysregulated pathways and noxious effect of C26:0 on different target cellular components have been described in (**Fig. 2**). Some of the hallmarks are described below in brief.

1.2.1 Impaired mitochondria biogenesis and function in X-ALD

Mitochondria are cytoplasmic cellular organelles compartmentalized by two lipid membranes: outer mitochondrial membrane and inner mitochondrial membrane. The outer one is porous and allows the passage of molecules between the inner membrane and cytosol. The inner membrane provides efficient barrier for the ionic flow and covers the mitochondrial matrix. Mitochondria are controlled by nuclear and mitochondrial genomes. They contain a circular genome, mtDNA, which encodes 13 out the 1500 mitochondrial proteins, while the rest are encoded in the nucleus. They perform several vital cellular functions including ATP production *via* OXPHOS system, scavenging free radicals, intracellular calcium regulation and alteration of oxidation and reduction potential of cells. One of the major physiological features of mitochondria is the generation of transmembrane potential across the mitochondrial inner membrane. Thus the substrates like pyruvate, end product of glycolysis enter the tricarboxylic acid cycle (TCA) and maintain the reduced state of the $NADH/NAD^+$ and $FADH_2/FAD$ couples. And the electron released are then supplied to respiratory chain, passes through five different complexes (CI-V) generating a potential gradient across the inner membrane which eventually drives ATP-synthase to form ATP from ADP.

Despite of X-ALD being peroxisomal origin, based on the published evidences it has been considered as a secondary mitochondrial disorder. Many accumulating *in-vitro* and *in-vivo* studies have shown mitochondrial dysfunction in adrenal cortex and spinal cord X-ALD (Lopez-Erauskin et al., 2013b, McGuinness et al., 2003). Functional analysis in X-ALD mice and human patients revealed a common metabolic abnormality signature which includes mitochondrial dysfunction (Schluter et al., 2012). Reduced mitochondrial DNA and mitochondrial protein levels were reported in the white matter of autopsy brain from patients with X-ALD (Fourcade et al., 2008, Morato et al., 2013, Singh and Pujol, 2010). Furthermore, from our laboratory we demonstrated that *Abcd1*$^-$ mice shows low mtDNA copy number associated with downregulation of mitochondrial biogenesis pathway driven by PGC-1α, PPARγ and reduced expression of mitochondrial proteins cytochrome c, NDUFB8 and VDAC (Morato et al., 2015). In addition, using X-ALD human fibroblasts and *ex-vivo* spinal cord slices from *Abcd1*$^-$ mice, excess of VLCFA induces mtDNA oxidation with impaired OXPHOS system

triggered by mitochondrial ROS (Lopez-Erauskin et al., 2013b). The molecular mechanism by which the excess of VLCFA triggers oxidative stress from the mitochondria in X-ALD is not completely clear. It was hypothesized that C26:0 could replace the lateral chains of phospholipids of the inner mitochondrial membrane and physically interfere with the OXPHOS system, inducing electron leakage and ROS production. Besides, a disturbed calcium signaling was observed in *Abcd1*$^{-}$ astrocytes, displayed a lower intracellular calcium reaction in response to acute VLCFA application and higher calcium intake by *Abcd1*$^{-}$ astrocytes mitochondria (Kruska et al., 2015). Beneficial effects were seen by boosting mitochondria biogenesis via PPARγ activation with pioglitazone (Morato et al., 2013) by SIRT1 activation with resveratrol or by SIRT1 over expression (Morato et al., 2015). These approaches have shown to recover axonal degeneration associated locomotor disabilities in X-ALD mice.

In contrast, no mitochondrial abnormalities have been observed in isolated mitochondria from muscles and brain, indicates the hypothetical mechanism that these organs were not primarily affected in the disease like spinal cord and also due to the heterogeneity within the cells or tissue types that are more or less susceptible to VLCFA insult (Oezen et al., 2005). Similar unchanged reports on mitochondria DNA and protein levels were seen in cortex and liver (Morato et al., 2013).

1.2.2 Impaired mitochondria dynamics in X-ALD

With existing studies from our laboratory, we revealed that mitochondria malfunction and redox homeostasis are highly interconnected and play vital roles in etiopathogenesis of X-ALD. To further focus more deeply the mechanism behind mitochondria function, very recently in our laboratory we studied mitochondria dynamics, as it is key factor that mediates and amplifies mitochondria and neuronal dysfunction (Przedborski, 2011; Su et al., 2010). VLCFA mediated shift towards mitochondria fission were observed by the involvement of DRP1 recruitment to mitochondria. Moreover, C26:0 induced DRP1 levels caused mitochondria fragmentation in X-ALD fibroblasts in redox dependent manner. These effects were not seen when control fibroblasts were insulted with C26:0, indicating ALDP lack of function leads to impaired mitochondrial dynamics. These results were in agreement with the *in-vivo* data showing high DRP1 levels in mice spinal cord at 14 months of age (Patrizia thesis: Impairment of mitochondrial dynamics

in X-linked adrenoleukodystrophy) without changes at 3 months. Thus mitochondrial dynamics impairment appears as a late onset event in X-ALD progression and is not involved in the earlier stage of the disease. Furthermore, overexpression of Drp1 levels were found in the motor neurons of Abcd1 mice spinal cord compared with WT. Thus, *Abcd1*$^{-}$ mice shows mitochondrial dynamics imbalance and suggest a shift toward mitochondrial fission. Drp1 dysregulation could be involved in axonal degeneration in X-ALD, like others neurodegenerative diseases (Chen and Chan, 2009; Cho et al., 2013; Knott et al., 2008; Su et al., 2010). Drugs targeting this imbalance would be a suggested therapy to prevent the disease progression.

1.2.3 Neuroinflammation in X-ALD

Although AMN patients do not exert an over brain inflammatory demyelination, low grade degree of inflammation was found with the induction pro and anti-inflammatory cytokines and chemokines. In addition, by using the functional genomics approaches on the *Abcd1 null* model, we unraveled a signature characterized by oxidative stress, mitochondrial dysregulation, adipocytokine signaling, and chronic inflammation routes, including NFkβ activation with production of proinflammatory cytokines (such as IL1β, TNFα) detected in spinal cords (Schluter et al., 2012). Moreover, a similar degree of inflammation was seen in plasma and PBMC from AMN patients showing a mixed pattern with up-regulated and down-regulated of pro and anti inflammatory cytokines and chemokines (Ruiz et al., 2015). These findings provide a basis to argue that a low-grade proinflammatory reaction initiated by VLCFA and present in the mouse models and in AMN patients, may adopt a more aggressive profile should a second (or third or several) hit appear (Singh and Pujol, 2010) during disease progression. The molecular mechanism that causes the transformation of AMN to the cerebral inflammatory demyelination form reassembling cAMN and ccALD is still unknown. Thus, a suitable animal model for ccALD would be beneficial to study the etiology and to investigate deeply the molecular mechanism underlying this transformation and further serves as a tool for the development of therapeutic strategies for the lethal stages of this disorder.

Microglia as in other neurodegenerative diseases thought to play a crucial role in X-ALD (described in detail under neuroinflammation chapter). These come from the fact showing the arrest of demyelination in X-ALD patients by gene therapy and bone

marrow transplantation (Aubourg et al., 1990, Cartier et al., 2009). Autologous CD34+ cells were removed and replaced by genetically corrected cells by lenti-viral vector encoding wild type *ABCD1*. In addition from our laboratory, we showed microgliosis and astrocytosis as one of the main pathological features of X-ALD in our mice model (Pujol et al., 2002). Subsequently, accumulation of VLCFA induces microglia activation and triggers the massive productioin of the proinflammatory cytokines like TNFα and IL1β (Khan et al., 1998), creating a vicious cycle that worsens the pathology of X-ALD. Morover, recently using an integrated-omics approach to identify novel biomarkers and altered network dynamics that possibly driving, the disease. We combined an untargeted metabolome assay of plasma and peripheral blood mononuclear cells (PBMC) of AMN patients, which used liquid chromatography coupled to quadrupole-time-of-flight mass spectrometry (LC-Q-TOF), with a functional genomics analysis of spinal cords of *Abcd1*$^{-}$ mouse. The results uncovered altered nodes in lipid-driven proinflammatory cascades, such as glycosphingolipid and glycerophospholipid synthesis, governed by the β-1,4-galactosyltransferase (B4GALT6), the phospholipase 2γ (PLA2G4C) and the choline/ethanolamine phosphotransferase (CEPT1) enzymes. Confirmatory investigations revealed a non-classic, inflammatory profile, consisting on the one hand of raised plasma levels of several eicosanoids derived from arachidonic acid through PLA2G4C activity, together with the proinflammatory cytokines *IL6, IL8, MCP-1* and *TNF-α*. Thus, we illustrated an unreported connection between ABCD1 dysfunction, glyco- and glycerolipid-driven inflammatory signaling and a fine-tuned inflammatory response underlying a disease considered non-inflammatory. Thus strategies modulating microglial inflammatory responses would be the considerable target to halt the disease progression.

1.2.4 Oxidative stress and impaired anti-oxidant system

Oxidative stress' is a processes resulting from an imbalance between the excessive formation of ROS and limited antioxidant defences. Reactive oxygen species (ROS) are highly reactive molecules which contain oxygen. ROS are generated as by-products of cellular metabolism, primarily in the mitochondria. A build up of reactive oxygen species in cells may cause damage to DNA, RNA, and proteins, and may cause cell

death. Reactive oxygen species are free radicals. Also called oxygen radical. ROS are balanced with antioxidant systems to keep their level constant in living organisms.

Oxidative stress is one of the most common feature involved in the X-ALD disease progression (Fourcade et al., 2008, Fourcade et al., 2010, Lopez-Erauskin et al., 2012, Petrillo et al., 2013). Increased oxidative damage in the spinal cord of X-ALD mice and in human fibroblast has been found marked by upregulation of markers of direct carbonylation to proteins (GSA and AASA), protein glycoxidation and lipoxidation (CEL and CML) and protein lipoxidation (Fourcade et al., 2008). Some of these markers are already found to be altered in the *Abcd1*$^{-}$ mice at 3.5 months of age, suggesting that oxidative stress is an early etiologic factor in the disease pathogenesis. Further, we showed VLCFA insult drives mitochondria ROS and reduces GSH levels and decreases the inner mitochondrial membrane potential in X-ALD human fibroblast (Fourcade et al., 2008, Lopez-Erauskin et al., 2013b). Similar observations have been found in *in vitro* models of neurons, oligodendrocytes and astrocytes (Baarine et al., 2015, Hein et al., 2008).

In addition, blunted antioxidant responses were found in X-ALD mice showing decreased expression of the antioxidants enzymes SOD1 and SOD2 and a reduced levels of GSH in the spinal cord of *Abcd1*$^{-}$ mice (Fourcade et al., 2008). Very recently, we found an aberrant inactivation of *Nrf2*-dependent anti-oxidant pathway characterized by low *Nrf2* levels in X-ALD mice spinal cord associated with down-regulation of target genes like *Hmox, Nqo1* and *Gstα3.* Further, we demonstrated an altered NRF2-dependent response under oxidative conditions in X-ALD patient´s fibroblasts (thesis: NRF2 and RIP140 as new therapeutic targets for X-ALD: Control of redox/metabolic homesotasis and inflmmation). This energetic and redox imbalance is prevented by the administration of a cocktail of antioxidants (Galino et al., 2011, Lopez-Erauskin et al., 2011) (**Fig. 2**).

Another study uncovered that oxidative damage compromises the energy metabolism in X-ALD mice. It was found that the oxidative modification of proteins specifically affects five key enzymes of glycolysis and tricarboxylic acid cycle (TCA): aldolase A, phosphoglycerate kinase, pyruvate kinase, dihydrolipoamide dehydrogenase and mitochondrial aconitase. This was associated with decreased enzyme activities of

pyruvate kinase, leading to lowered levels of ATP, NADH and reduced glutathione (GSH), and increase in NADPH (Galino et al., 2011). All these alteration, appear in spinal cords of Abcd1 null mice prior to development of neurological symptoms, and result in a situation of energetic failure that may be a pathogenic factor, at least in adult forms of X-ALD (Fourcade et al., 2014). Importantly, treatment of *Abcd1*$^{-}$ mice with a combination of antioxidants (N-acetylcysteine, α- lipoicacid, and vitamin E) neutralize oxidative damage to proteins, preserved bioenergetic homeostasis, halted signs of axonal degeneration in immunohistological stainings and prevented locomotor impairment (Lopez-Erauskin et al., 2011). These results provide conceptual proof of C26:0 induced oxidative stress as a major causative disease-driving factor in X-ALD (**Fig. 2**).

1.2.5 Ubiquitin-proteasome system (UPS) dysfunction

The UPS has a pivotal role in the rapid clearance of damaged, misfolded or aggregated proteins in both healthy and diseased state (ref). Functional studies have pointed out a dysregulation of proteasomal gene expression and activity before disease onset in the mouse model of X-ALD (Launay et al., 2013). Further along in disease progression, it was observed the induction of catalytic subunits of the immunoproteasome, concomitant with a redoxdependent recruitment of immunoproteasomes to mitochondria when fibroblasts are exposed to C26:0. All these events are prevented by the treatment of Abcd1-null mice with antioxidant (Launay et al., 2013). The results suggested a possible role of UPS and immunoproteasomes as first line of defense against oxidative damage to the mitochondria by elimination of oxidized mitochondrial proteins, thereby improving mitochondrial viability and turnover.

1.2.6 ER stress

Moreover, very recently a redox dependent ER stress was found by our laboratory in X-ALD mice spinal cord and in X-ALD human fibroblasts. These dysregulation was characterized by the activation of three main ER stress sensors: PERK, ATF6 and IRE1 causing an early engagement of UPR (unfolded protein response). An induced UPR found in the brain samples of X-ALD patients characterized by upregulation of PERK

and eIF2α phosphorylation with induced ATF4 levels in the affected areas of ccALD and cAMN (Launay et al., 2017). Further we observed the activation of PERK pathway in the affected white matter of CCALD and cAMN patients with no changes in IRE1 or ATF6 pathways. In case of X-ALD mice spinal cord, an early phenomenon with a strong activation of the ATF6 pathway was seen at three months of age and a later activation of the PERK and ATF6 but not IRE1 pathways (Launay et al., 2017).
Further, we demonstrated that the bile acid tauroursodeoxycholate (TUDCA) abolishes UPR activation, which results in improvement of axonal degeneration and its associated locomotor impairment in Abcd1^{-}/Abcd2$^{-/-}$ mice.

1.2.7 Autophagy malfunction

Impaired autophagic flux together with autophagolysosomal formation were detected in *Abcd1*$^{-}$ mice spinal cords. This was associated with decreased levels of the autophagolysosomes marker p62 and authophagy marker LC3II. The mechanism appeared to be an aberrant overactivation of the mammalian target of rapamycin (mTOR) pathway, mediated by VLCFA excess. The induction of autophagic flux through the rapamycin ester temsirolimus (inhibitor of mTOR) preserved proteasome function, maintain the redox and metabolic homeostasis, and successfully arrested axonal degeneration in X-ALD mice (Launay et al., 2015)

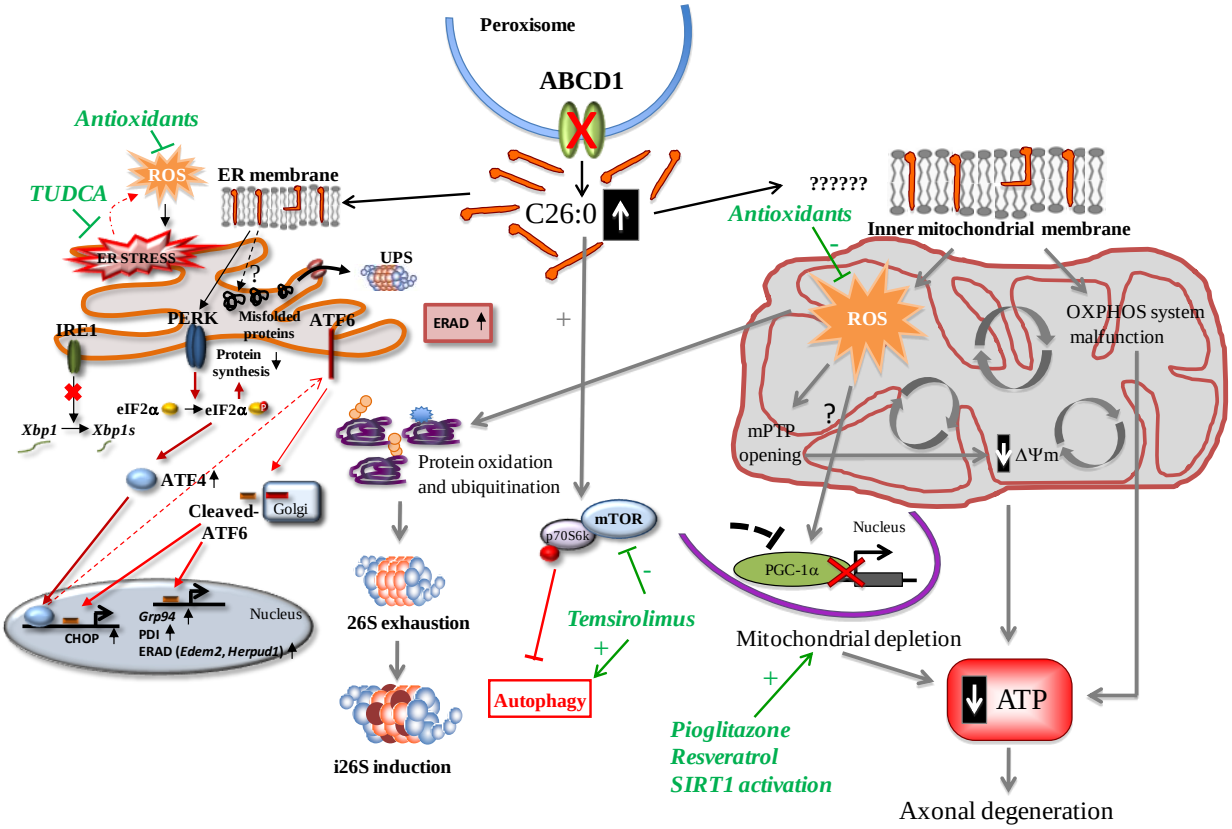

Figure 2. Model recapitulating the noxious effects of C26:0 excess on mitochondria, redox homeostasis, ER and proteolytic machineries in the X-ALD cell.

In X-ALD, excess of C26: leads to the production of intramitochondrial ROS from the electron transport chain probably by an unknown mechanism. The consequences are mitochondrial dysfunction resulting in loss of □□m and ATP production, mPTP opening, inhibition of mitochondria biogenesis via the SIRT1/PGC-1/PPAR□ pathway, and ultimately axonal degeneration. VLCFA-dependent ROS inhibit UPS and autophagy process and produces ER stress, with axonal degeneration as fatal outcome. The pathogenic cascade can be abrogated: i) by a combination of antioxidants; ii) by activating SIRT1 or boosting mitochondria biogenesis with pioglitazone or resveratrol; iii) by activating autophagy via mTOR inhibition with TEMS; iv) by inhibiting ER stress with TUDCA. These results provide potential therapies to be translated into clinical trials for AMN patients.

1.3 Mitochondrial dynamics and neurological disorders

Here I will explain more in detail about mitochondria and inflammation related to other neurological disorders as these two are major topics studied in my thesis. Mitochondria are dynamic in nature that continuously move, fuse and undergoes division. These movements are shown to be essential for function, maintenance and distribution of mitochondria. Given the high energy dependence properties of neurons, they are particularly vulnerable to mitochondrial dysfunction (Su et al., 2013). Indeed, defects in

mitochondrial fusion and fission primarily affect neuronal functions. Several human neurological diseases are caused by mutations in the core proteins involved in mitochondrial fusion and fission which includes OPA1 causes dominant optic atrophy, MFN2 is linked to peripheral neuropathy Charcot-Marie-Tooth type 2A (CMT2A) and alterations in DRP1 leads to neonatal lethality. OPA1 and Autosomal Dominant Optic Atrophy Human genetic studies identified OPA1 as the gene mutated in the autosomal dominant optic atrophy (DOA), Kjer's type (Alexander et al., 2000; Delettreet al., 2000). This is the most common form of dominant optic atrophy caused by heterozygous mutations in OPA1. Pathological analysis indicates that DOA is caused by degeneration of the retinal ganglion cells leading to atrophy of the optic nerve. More recent clinical studies indicate that a part retinal ganglios a wider range of cell types result vulnerable to mitochondrial dysfunction associated with OPA1 haplo-insufficiency (Delettre et al., 2002). Other cells can be affected by the disease producing extraocular clinical features that include neurosensory hearing loss, ataxia, myopathy, and peripheral neuropathy (Yu- Wai-Man et al., 2010). Here in this thesis we talked more in detail about DRP1, as it has shown to play a key in mitochondrial dynamics of X-ALD mice. Drp1 is highly expressed in brain and mutation in this gene leads to neuronal impairment. Due to its vital role in survival of post-mitotic neurons, purkinje DRP1 KO neurone shows accumulated oxidative stress, induced mitophagy and deffective mitochondrial respiration. These mice mice display locomotor problems after 6 months of age showing the importance of DRP1 in neurone survival. (Kageyama 2012).Inherited diseases that are directly linked to essential fission components have not been described. However, a study reported the case of a newborn girl that carried a heterozygous dominant-negative mutation of the DRP1 gene that resulted in an Ala395-to-Asp (A395D) substitution in the middle domain of the protein. The girl died 37 days after birth and exhibited severe pleiotropic defects, including microcephaly, abnormal brain development, optic atrophy and a mildly elevated plasma concentration of VLCFA (Waterham et al., 2007). More recent clinical study associated DRP1 mutation also shown to linked with refractory epilepsy (Vanstone et al., 2016). Detailed physiological importance of mitochondrial fission in vertebrates was clarified by the generation of tissue-specific Drp1 KO mice. These studies showed that mice lacking the mitochondrial fission GTPase Drp1 have developmental abnormalities, particularly in the forebrain, and die at embryonic stage. Neural cell-specific Drp1 KO mice die shortly after birth as a result of brain hypoplasia and cell death. Primary cultured neuronal cells

from Drp1 KO mouse embryos showed a decreased number of neurites and fail to form stable synapse structure, leading to neurodegeneration (Ishihara et al., 2003, Wakabayashi et al., 2009). These defects reflect the importance of Drp1-dependent mitochondrial fission within highly polarized cells such as neurons.

1.3.1 Mitochondrial fission and neurodegeneration

The regulation of mitochondrial dynamics process represents an important mechanism controlling neuronal cell fate and impairment of mitochondrial dynamics appears to be implicated in a much broader set of inherited and age-associated neurodegenerative diseases (Knott et al., 2008; Su et al., 2010). Defects in either fusion or fission, leading to mitochondrial fragmentation, may limit mitochondrial motility, decrease energy production and increase oxidative stress, thereby promoting cell dysfunction (Luo et al., 2015). Disruption of the fusion-fission balance have been proposed as potential cause of mitochondrial dysfunction, which is an early event in the pathogenesis of most common neurodegenerative diseases such as AD, PD, HD and ALS (Knott et al., 2008; Su et al., 2010). In all these pathologies have been described modifications altering DRP1 activity (Costa and Scorrano, 2012; Elgass et al., 2013; Reddy et al., 2011). The mechanisms involved in this process are reported in the follow section.

Imbalance in mitochondrial dynamics toward mitochondrial fragmentation in concert with increased expression of mitochondrial fission genes and decreased expression in mitochondrial fusion genes, have been reported in AD. It was suggested that Aβ and phosphorylated tau interact with DRP1 in AD neurons. This causes extensive mitochondrial fragmentation and leads to neuronal and synaptic damage associated to the disease (Calkins et al., 2011; Manczak et al., 2011, 2012; Wang et al., 2009).

Parkinsonian neurotoxins induce mitochondrial fragmentation and neuronal cell death, which can be prevented by genetic inhibition of Drp1 or fusion induction (Barsoum et al., 2006; Gomez-Lazaro et al., 2008; Meuer et al., 2007). More recent is the demonstration that the PD-related LRRK2 mutant interact with Drp1 and phosphorylates it at Thr595 resulting in aberrant mitochondrial fragmentation possibly leading to aberrant autophagy and neuronal damage. These defects are corrected with selective inhibition of Drp1 (Jheng et al., 2012). Another study showed that in mammalian cells which lack the PD-related gene PINK1, Drp1 dephosphorylation by

calcineurin leads to decreased mitochondrial connectivity (Sandebring et al., 2009). Moreover it was described that Drp1-deficient cells are protected from mitochondrial dysfunction induced by PINK1/Parkin silencing, indicating that increased mitochondrial fission contribute to this phenotype (Irrcher et al., 2010). However, it was reported that mitochondria fragmentation can occur in a Drp1-independent manner by direct interaction of α-synuclein with mitochondria membranes (Nakamura et al., 2011). Expression of the mutant huntingtin protein (mHtt) triggers mitochondrial fragmentation by interaction with Drp1 and increase its enzymatic activity in HD transgenic mouse models and in brains of HD patients, thereby causing neuronal cell death (Shirendeb et al., 2012; Song et al., 2011). Inactivation of Drp1 by using the dominant-negative Drp1 K38A mutant rescues the mitochondrial fragmentation (Song et al., 2011). Moreover mHtt can also activate Drp1 by calcineurin mediated dephosphorylation at Ser637 (Costa et al., 2010). Mitochondrial dysfunction displayed by the mutant SOD1 (G93A) transgenic mouse model of ALS, associate with reduced mitochondrial length, impaired mitochondrial axonal transport and neuronal cell death (Bilsland et al., 2010; Kong and Xu, 1998).These defective phenotypes are rescued by suppressing Drp1 activity (Song et al., 2013).

1.4 Neuroinflammation

Inflammation is an active host defense mechanism of multi-cellular organisms against diverse insults (pathogens or injury) to inhibit and counteract the detrimental effects caused by them. The ability to distinguish the foreign from self and abnormal from normal is the most fascinating aspect of inflammation in central nervous system (CNS). Almost all the CNS disorders displays inflammatory component but the precise functions of inflammation are indefinitely explained as the resulting inflammatory responses may modulate the neurodegenerative pathway either in a detrimental or beneficial fashion. Under physiological conditions microglia exhibit a deactivated phenotype where it produces neurotrophic factors and maintain the CNS homeostasis. Upon insults or pathogens, microglia turns to an activated phenotype and promotes an inflammatory response to initiate the repair mechanism. This process is usually self limiting and gets to the normal form once the damage has been repaired. Overt activation of these cells cause sustained inflammation associated with abundant

production of cytotoxic factors which ultimately ends to cell death (Aldskogius et al., 1999, Wyss-Coray and Mucke, 2002). Thus the imbalance between the protective and destructive functions of microglia might contribute to neuronal death in many neurodegenerative diseases.

1.4.1 Effector cells "microglia and astrocytes"

Microglia are resident macrophages in CNS originate from hematopoietic stem cells in the yolk sac during early embryogenesis where they constantly survey the microenvironment. Microglia provides the first line of defense of innate immune mechanism when injury or disease occurs. Due to the heterogeneity existence of microglia population in brain parenchyma, the concept of classical and alternative activation of macrophages has applied to microglia **(Fig. 3).** Classical activation so called ¨M1¨ state or phenotype is associated with the production of pro-inflammatory cytokines and chemokines like *Il1β, Tnfα, Cxcl10* and *Ccl2*, reactive oxygen and nitrogen species and proteases. On the other side ¨M2¨ phenotype includes alternative activation and acquired deactivation associated with M2 genes like *Il10*, *Tgfβ1, Arg1, Mrc1* and *Ym1* that promote ant-inflammation and tissue repair (Colton and Wilcock, 2010, Colton, 2009). However, it is not very clear whether these phenotypes co-exist and implies morphological differences between them. Indeed it is important to note that most of the experimental evidences of these phenotypes comes from purely isolated cultures and is failed to reproduce by *in-vivo* studies reviewed recently by Richard explaining the limitations of phenotypic mechanism applied in these cultures (Ransohoff, 2016). Accumulating evidence has acknowledged the microglia-mediated neuroinflammation as a critical contributor to the pathogenesis of neurodegenerative diseases (Heneka et al., 2015, Herrera et al., 2015, Tang and Le, 2016).

Astrocytes are another important glia cell that shares the developmental pathway with neurons and oligodendrocytes. They are large ramified cells of neuroectodermal origin, performs several vital functions like immune defense, support, synaptic plasticity and integrity of blood brain barrier (Alvarez et al., 2013). Astrocytes play a crucial role in higher neural processing, and actively serve to maintain the neuronal health. Astrocytes are shown to produce potentially neurotoxic molecules, including proinflammatory

cytokines, glutamate, nitric oxide, and ROS under diverse brain injury conditions (Hashioka et al., 2015). Astrocytes execute these harmful effects during chronic neuro-inflammation mostly via NF-kB and STAT3 pathways that control the expression of numerous proinflammatory and neurotoxic mediators (Brambilla et al., 2009). LPS-stimulated astrocytes are reported to produce increased level of proinflammatory cytokines such as TNF-a, IL-1b, and IL-6, but decreased level of anti-inflammatory cytokines such as IL-10. Similarly, IFN-γ stimulated adult human astrocytes are reported to exert potent neurotoxicity in vitro (Hashioka et al., 2015). Reported studies showed reactive astrocytes in the EAE-induced animals are the principal source of CCL20, which promotes the migration of Th17 cells (Ambrosini et al., 2003). Inflammatory activation of astrocytes has been implicated in a wide variety of brain injury and neurodegenerative conditions, including MS, AD, PD, and HD (Hsiao et al., 2013, Lindner et al., 2015, Mayo et al., 2014). Reactive astrocytes may have a dual role in the propagation of ischemic brain damage (Rusnakova et al., 2013). The role played by reactive astrocytes under specific condition depends on their polarized phenotype and their interaction with the surrounding neurons and microglia (Kang et al., 2012). A recent study defined the signaling networks controlling reactive astrogliosis, which can be a promising target for the treatment of diverse CNS injuries and pathologies (LeComte et al., 2015).

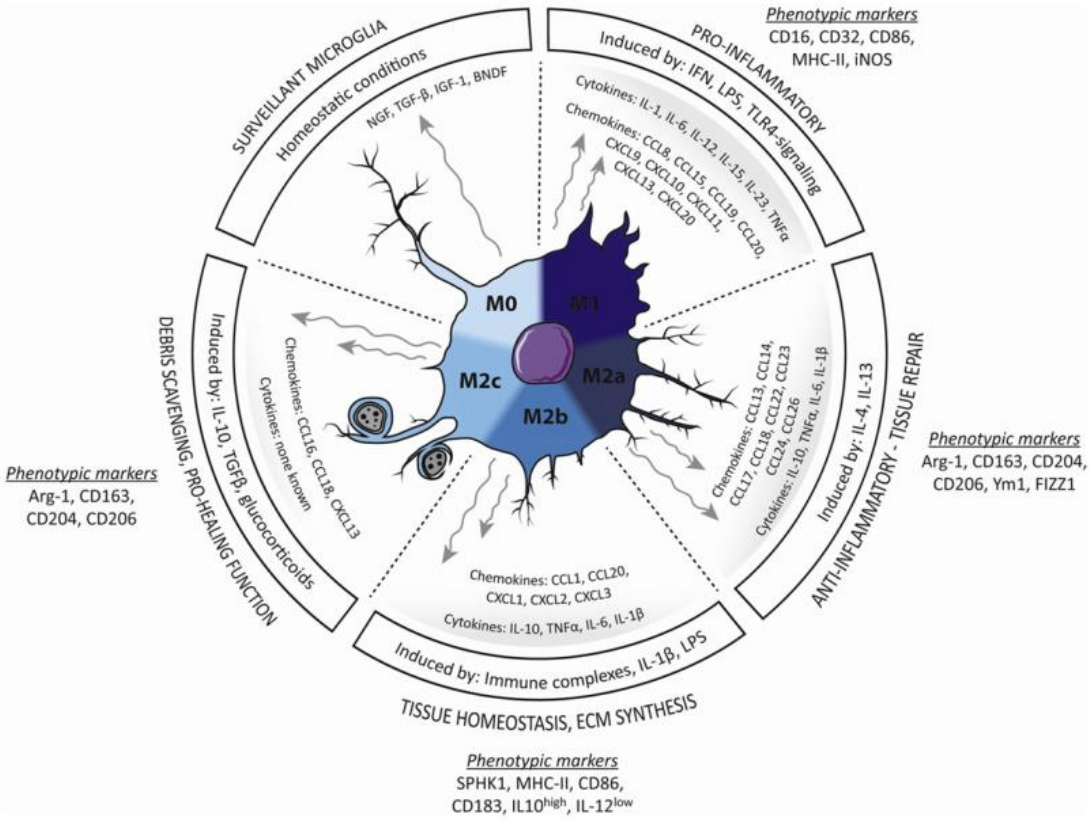

Figure 3. Microglia phenotypes, markers and actions

Proposed morphological changes, phenotypic markers, and secreted cytokines and chemokines in M0, M1, M2a, M2b and M2c microglia phenotypes. Surveillant microglia (M0), classically activated (M1) and alternatively activated (M2a, M2b and M2c). (Mecha et al., 2016).

1.4.2 Chronic inflammation and Neurodegenerative diseases

Mounting evidences indicate that microglia activation is the principal component of neuroinflammation which provides the first line of defense in CNS parenchyma against various insults. Neuroinflammation thus constitutes innate and adaptive immune responses that involve plethora factors including cytokines, chemokines and neurotrophic factors managed by microglia and other CNS cells like astrocytes together with involvement of immune cells that infiltrate CNS during injury (**Fig. 4**).

After the application of different stimulus like pathogens or virus, stroke and injury, CNS mediates a controlled and rapid inflammatory response to initiate the reparative

process with the help of resident immune cells. Such immediate responses are called ¨acute inflammation¨ mainly involves the participation of activated microglia and astrocytes (termed as microgliosis and astrocytosis). These responses are required to kill the pathogens and recover the damage caused by the insult and further cause a shift from pro-inflammatory environment to anti-inflammatory for removing the debris and reconstructing the extracellular matrix (Varin and Gordon, 2009). Sustained inflammatory responses and failure of shifting leads to massive production of ROS, RNS and cytokines causing damage to healthy neurons ultimately ends with massive neurodegeneration (Kigerl et al., 2009). In contrast, chronic inflammation is often considered as long term and self perpetuating inflammatory response associated with prolonged microglia activation. This activation involves the continuous release of pro-inflammatory mediators, cytokines and ROS associated mainly with wide range of neurodegenerative diseases. Unlike acute inflammation, these inflammatory responses are often detrimental and enhance the infiltration of peripheral macrophages thus maintain the inflammatory milieu within CNS. Thus, in most of the neurodegenerative diseases macrophages mediates persistent low grade inflammatory component rather than strong self limited response against injury as seen in non chronic inflammatory diseases like atherosclerosis (Rivest, 2009).

The role of inflammation in many neurological disorders has been under debate as many studies have shown inflammation as deleterious and beneficial for the disease pathology. Here I have described more in detail with reported examples about chronic inflammation as X-ALD is a chronic inflammatory disorder associated with neurodegeneration. Jimenez and colleagues had demonstrated that microglia from APP/PS1 mice, a transgenic mouse model of AD shows an M2 profile at early stage (6 months) as a responsive mechanism and displays a shift towards M1 phenotype at the stage of 18 months associated with the enhancement of pro-inflammatory and cytotoxic factors together with down regulation of M2 marker YM1 making the disease worsen (Jimenez et al., 2008). On other side, intra-hippocampal injections of LPS to APP/PS1 transgenic mice lowers the abeta accumulation together with moderate microglia activity providing a beneficial treatment for halting the Alzheimer disease (DiCarlo et al., 2001). Similar controversial cases have been in multiple sclerosis showing that lysolecithin injected MS mice model shows a shift from M1 to M2 dominant response in microglia and peripheral macrophages during the initiation of remyelination (Miron

et al., 2013). In contrast a mixed profile of microglia was observed in cuprizone model of MS during de and re-myelination states (Voss et al., 2012). Thus the modulating the neuroinflammation rather suppressing would be the useful strategy for treatment of many neurodegenerative diseases.

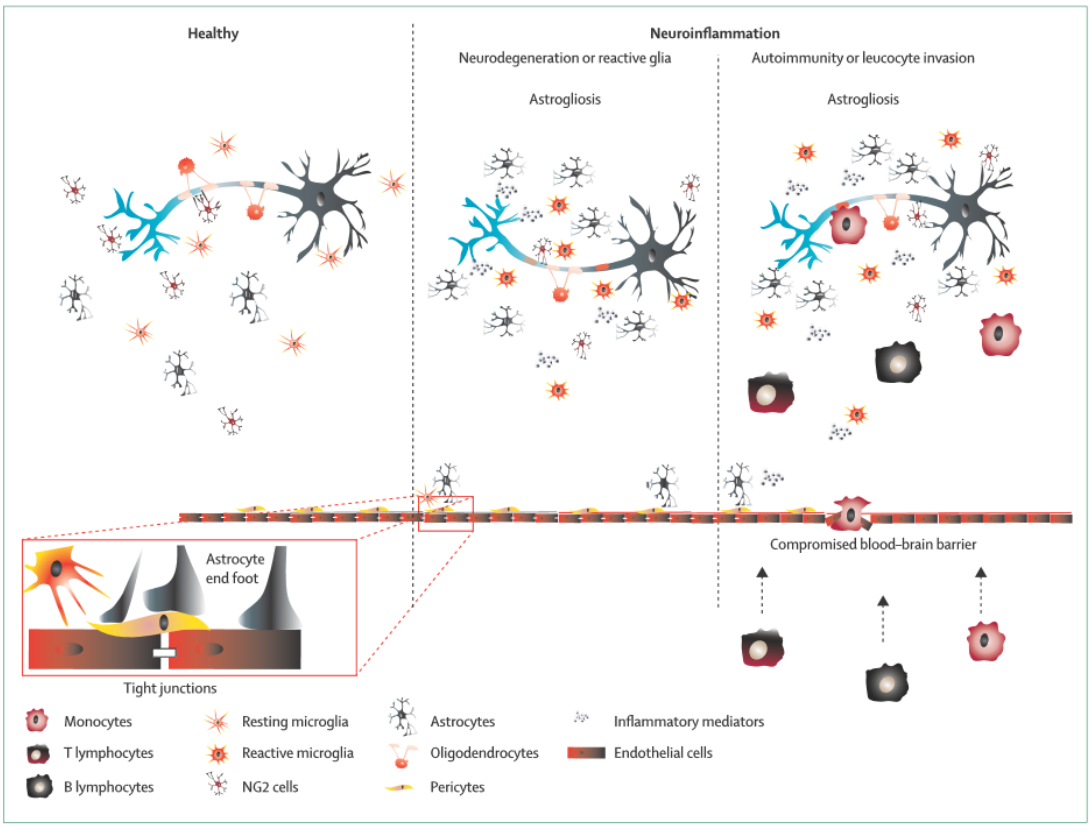

Figure 4. Involvement of various cell types in CNS inflammation

Under pathological conditions, resident CNS cells like astrocytes and microglia become activated, proliferate and display an inflammatory signature. In some inflammatory CNS diseases, peripheral macrophages cross BBB and invade CNS. Lymphocytes with recombined antigen receptors (T cells and B cells) can also penetrate the CNS and target CNS-resident antigens in many inflammatory diseases. (Waisman et al., 2015).

1.5 The endocannabinoid system (ECS)

Over the past decade, the anecdotal use of Cannabis plants has been increased throughout the world. Cannabinoids are naturally occurring compounds present in the

plant Cannabis Sativa. There are about 80 cannabinoids identified in Cannabis extract of which the most well studied compound is Δ^9–tetrahydrocannabinol (THC, the major psychotropic component in the flowers). Other constituents include Cannabinol, cannabidiol, cannabigerol and other related acids. Despite of wide therapeutic uses of THC for the treatment of emesis in patients with cancer undergoing chemotherapy, promoting appetite in patients with AIDS, treatment of menstrual irregularity, dysmenorrhoea, cannabis extracts were finally considered as an effective therapeutic targets for many neurodegenerative diseases after a decade of pre-clinical trials on THC and CBD. The accumulating evidence given from different animal models greatly increased our understanding the mechanism of action of THC and provides the support for targeting endocannabinoid to treat chronic inflammatory and neurodegenerative diseases.

After twenty years of discovery of THC, Allyn Howllet and her colleagues showed that exogenous exposure of THC to murine neuroblastoma cells inhibit the activity of adenylate cyclase by binding to specific receptors (REF). A year later in 1998 the first guanine-nucleotide binding protein (G-protein) coupled receptor (GPCR) activated by THC so called cannabinoid receptor type 1 (CB_1) was discovered and cloned in 1990. The second GPCR was from human immune cells and named cannabinoid receptor type 2 (CB2). The existence of these two receptors put forward the hypothesis of presence of endogenous ligands or can be called as ¨enodcannabinoids¨ (eCBs). These were shortly discovered as the derivatives of non-oxidative metabolism of polyunsaturated fatty acids after the invention of CB_1 and CB_2 receptors. N-arachidonoyl-ethanolamine (Anandamide) and 2-arachidonoyl-glycerol (2-AG) are the two best studied eCBs so far. Thus these enodcannabinoids together with enzymes involved in their biosynthesis and degradation and the two cannabinoids receptors form the “eCB” system.

1.5.1 Cannabinoid receptors

The CB_1 and CB_2 cannabinoid receptors belong to the large family of GPCRs, with seven transmembrane domains connected by three extracellular and three intracellular loops, an extracellular N-terminal tail and an intracellular C-terminal tail. CB_1 receptors are mainly expressed throughout the brain by many different cell types of neuron (both glutamatergic & GABAergic) and at lower levels by glial cells (Howlett et al., 2002). It

is the most abundant GPCR in mammalian brain thus referred to as ¨brain cannabinoid receptor. CB_1 is most frequently coupled to $G_{I/O}$ proteins and less to $G_{q/11}$ type. Thus the stimulation of CB_2 either by endogenous or exogenous ligands activates mitogen-activated protein kinase (MAPK) activity and inhibits adenylate cyclase and cyclic AMP-protein kinase A (PKA) signaling. Activation of CB_1 receptor also found to inhibit presynaptic N-type calcium channels and stimulates inwardly rectifying potassium channels, thereby reducing the neurotransmission. (Turu and Hunyady, 2010). CB_2 receptor is mainly expressed in the periphery lymphoid tissues and by myeloid cells. In brain, CB_2 is barely detectable although they seem to be present in some neuronal populations. However, CB_2 receptor expression can be induced in microglia under pathological conditions. Similar to CB_1, CB_2 receptors are also coupled to G-protein and mediate the signal transduction by inhibiting adenylate cyclase and voltage gated calcium channels.

1.5.2 Biosynthesis and degradation pathways of endocannabinoids

ECS comprises a growing number of lipid mediators. Among these, AEA and 2-AG are the two major endocannabinoids whose metabolic pathways have been well investigated. Synthesis of AEA can occur via three distinct routes: 1) direct conversion of N-arachidonoylphosphatidyl-ethanolamines (NArPE) to AEA by the presence of NAPE-PLD (NAPE-phospholipase D); 2) Deacylation of NArPE by ABHD4 and the hydrolysis of glycerophosphoethanolamine by GDE1; 3) via PLC-mediated hydrolysis of NArPEs to yield phosphoanandamide, which is in turn dephosphorylated to AEA by a phosphatase, such as PTPN22 (Di Marzo, 2011). Recent studies suggested these biosynthetic pathways may compensate to each other when either one of these are lacking. The other endocannabinoid, 2-AG is synthesized from the hydrolysis of 2-arachidonoyl-containing diacylglycerols (DAG) by either of two enzymes known as sn-1-specific DAGL α or β. Mice lacking either DAGL-α or -β revealed that DAGL-α plays a primary role for 2-AG synthesis in the brain; conversely, DAGL-β is often active at the peripheral level, although its expression in the brain has been reported (Bisogno et al., 2003). The DAG precursors for 2-AG biosynthesis are in turn the product of the hydrolysis of membrane phospholipids, and particularly of sn-2-

arachidonoyl-PIP2 species by PLCβ. However, DAG precursors for 2-AG have also been suggested to originate also from phosphatidic acid hydrolysis (**Fig 5**).

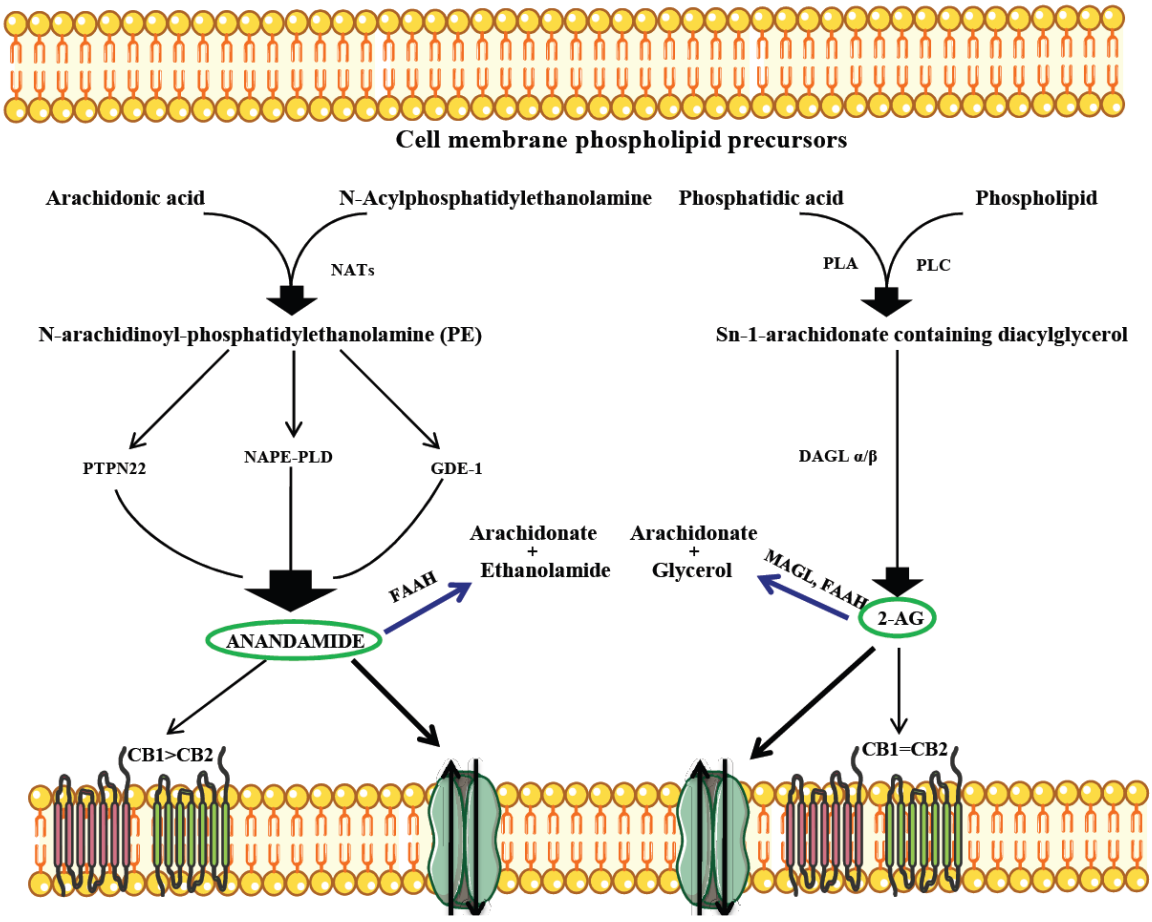

Figure 5. Bio-sythesis and degradation pathway of AEA and 2 AG.

Thick arrow denotes biochemical synthesis of two main endocannabinoids AEA and 2 AG from the membrane precursors in the presence of respective enzymes. The arrows in blue denote the inactivation of AEA and 2 AG in the presence of hydrolytic enzymes. (Adapted from Fabio Arturo Iannotti 2016).

1.5.3 Endocannabinoid system: effective role in neurodegenerative diseases

With the growing evidence on the neuroprotective role of enodcannabinods, many studies have focused on identifying molecular targets within eCB system that could lead to fight against the most prevalent neurodegenerative disorders. Due to the pleiotropic activities of endocannabinoids , the aspect of being potential neuroprotectant is

particularly important in neurodegenerative disorders since the involvement of different insults like inflammation, mitochondria dysfunction, oxidative stress and excitotoxicity causing neuronal damage or death are modulated by eCB signaling system. Moreover, in most of the physiological and pathological conditions, ECS shown to play a pre-homeostatic role, facilitated by the fact that endocannabinoids are biosynthesized and released on demand and activate their receptors when and where needed either as an adaptive endogenous response or as a non-adaptive response mechanism. Thus, three possible therapeutic strategies could apply based on modulation of ECS. i) pharmacological or genetic manipulation of cannabinoid receptors ii) administration of exogenous endocannabinoids or cannabinoids and iii) elevating the levels of endocannabinoids by using hydrolysis inhibitors. Several experimental studies have proved to modulate the pathogenesis of disease by applying either approach described above. **Table 1** shows the protective effects of ECS on different neurodegenerative diseases. In the contempt of having several protective effects derived by CB_1 receptors. CB_1 mediated psychoactive effects have served to limit their development in clinical practices (Maldonado et al., 2011). Thus the use of compounds targeting CB_2 receptor which is devoid of psychoactive effects could make CB_2 receptor as a safe and well tolerated therapeutic target in many neurodegenerative diseases. In this thesis we have applied the second strategy as therapeutic approach aiming CB_2 receptor as target of interest. Thus we will focus more in detail on CB_2 recptor and its neuroprotective effects in neurodegenerative diseases.

Table 1. ECS targeted pharmacological compounds for treating ND.

Subjects	ECS based therapeutic approaches	Effects	References
Tg2576 mice (Alzheimer´s disease)	WIN55,212-2 JWH-133 (CB2 agonist)	↓cognitive impairments; ↓microglial activation; ↓COX-2 expression; ↓TNF-α release ↓Cortical Aβ deposition.	(Martin-Moreno et al., 2012)
LPS-lesioned rats (Parkinson´s disease)	HU-210 HU-308 (CB2 agonist)	↑neuroprotective effects; ↑neuroprotective effects; ↑TH^+ neurons in the substantia nigra	(Garcia et al., 2011)
APP/PS1mice	JWH-133	↑Cognitive performance ↓Microglial response to Aβ ↓Pro-inflammatory cytokines(IL-1β, IL-6,TNF-α, and IFN- γ) ↓Tau hyperphosphorylation around plaques ↓Oxidative stress damage around plaques	(Aso et al., 2013)
Acute experimental autoimmune encephalomyelitis	2-AG	↑Activation and rampification of microglia	(Lourbopoulos et al., 2011)
Alzheimer´s disease	MAGL KO	↓Gliosis and neuroinflammation ↓TNF- α, IL-1β, IL-6, AA, PGE2, PGD2, TXB2	(Piro et al., 2012)
Huntington's disease	DAGL inhibitor	↑Neuroprotection	(Valdeolivas et al., 2013)
Multiple sclerosis	MAGL inhibitor	↑Neuroprotection, ↓Inflammation	(Bernal-Chico et al., 2015)
Parkinson's disease	SR141716 (CB1 antagonist)	↑Neuroprotection	(Gonzalez et al., 2006)
Multiple sclerosis	WIN 55,212-2 (CB1/CB2 agonist)	↑Neuroprotection	(Baker et al., 2001)
Human microglia and THP-1 cells treated with LPS/IFN-γ	JWH015 (CB2 agonist)	↓Neurotoxicity	(Ehrhart et al., 2005)
Mouse microglia BV-2	THC	↓IL-1β, IFN-β and IL-6	(Kozela et al., 2010)

1.6 CB_2 receptor as a promising therapeutic target

Despite CNS considered to be relatively immune-privileged tissue, it implies an endogenous immune response against pathogens or damage by the resident glial cells mainly astrocytes and microglia which provides the innate immune response in brain parenchyma (Halliday and Stevens, 2011). A large number studies have been conducted showing the potential therapeutic properties targeting CB_2 receptor in many experimental animal and cellular models. The most extensively studied mechanism of neuroprotection of CB_2 receptor includes the anti-inflammatory effects caused by its activation linked to decreased inflammatory cell recruitment by inhibiting the pro-inflammatory mediators and cytokines and increased anti-inflammatory cytokine production.

One of the major limitations of compounds activating CB_1 receptors is unwanted psychotrophic effects mediated by them. These CB_1 mediated effects have severely lessened the development of CB_1 agonist in terms of both practical and administrative cases. In contrast, these psychotrophic effects were absent in CB2 receptor activation by its specific agonist. However, desirable actions via CB2 receptor were found in different preclinical models making CB_2 as a considerable target of interest. For instance, agonists targeting CB_2 receptors have been proposed as therapies for the treatment or management of a range of painful conditions, including acute pain, chronic inflammatory pain, and neuropathic pain (Ehrhart et al., 2005). As described above CB_2 receptors are mainly expressed in microglia and prevents the microglia mediated neurotoxicity by inhibiting the inflammatory responses and modulating the macrophage migration towards lesion sites (Amenta et al., 2012, Cabral and Griffin-Thomas, 2009). In addition CB_2 receptors shown to regulate the transformation of M1 and M2 phenotype after different insults (Mecha et al., 2015). Supporting evidences are provided by a number of preclinical and human studies showing the involvement of CB_2 receptor in pathology of many neurological disorders. Postmortem brain samples from patients with AD, HD, PD have shown upregulation of CB_2 receptors (Benito et al., 2003, Gomez-Galvez et al., 2016, Palazuelos et al., 2009, Ramirez et al., 2005). Apart many neurodegenerative experimental animal models also revealed higher CB_2 receptor levels (Aso et al., 2013, Palazuelos et al., 2009). Moreover, increased CB_2 receptor expression in peripheral blood has been suggested as a peripheral biomarker for early

diagnosis of AD (Grunblatt et al., 2009). Thus, this observed upregulation of CB_2 receptor was suggested as an endogenous adaptive response against the pathology making an attempt to counteract against the neurodegenerative process. Many *in-vitro* and *in-vivo* studies have conducted showing anti-inflammatory effects of CB_2 agonist in different animal models**.** In particular, beneficial effects of CB_2 were shown in both *in-vitro* and *in-vivo* by its stimulation counteracts the Aβ induced microglia activation (Aso et al., 2013, Milton, 2002). Ayemerich and the colleagues have showed that JZL184 (inhibitor of *Mgll*) prevents the cell death of neuron-like cells treated with 1-methyl-4-phenylpyridinium iodide and this effect was absent when cultures are treated with AM630, CB_2 receptor antagonist showing the involvement of CB_2 receptor against inflammation (Aymerich et al., 2016). Besides, $CB_2^{-/-}$ mice are much more sensitive to LPS insult and displayed more vulnerability to neurofilament degeneration and inflammation in EAE mice model (Garcia et al., 2011, Palazuelos et al., 2008). In the case of APP/PS1 mice lacking CB_2 receptors shows greater accumulation of Aβ in brain facilitating the hypothesis that CB_2 activation may induce the clearance of Aβ deposition (Aso et al., 2016).

1.7 Methylene blue, an old century drug: new application for neurodegnerative diseases

Although MB failed to meet the standards of the textile industry, its biological application was soon discovered. In 1891, the staining of MB for plasmodia and its effect on malaria were developed by Paul Guttmann and Paul Ehrlich which provided the foundation of modern chemotherapy (Parascandola, 1981). In 1890s, MB was administered in psychiatric patients to monitor their compliance, which led to the discovery its antipsychotic effects and the later discovery of chlorpromazine, the first synthetic antipsychotic drug, in 1951 (Ohlow and Moosmann, 2011, Schirmer et al., 2011). The first neuroprotective effects by MB were observed by Yu in 1992 using the model of ischemic stroke (Yu et., al 1992a).

Due to its unique redox properties, MB directly accepts electrons from NADH, NADPH, and $FADH_2$ and mediates the flow of electrons between the mitochondrial respiratory complexes and regulates mitochondrial respiration. Importantly, it has been

demonstrated that the MB-induces the increase of mitochondrial complex I and I-III activities and is insensitive to complex I and III inhibition. Furthermore, reduced form MB (MBH_2) found to be able to deliver the electrons to cytochrome c in the presence of oxygen in mitochondria in an alternate route despite the inhibition of complex I and III (Atamna et al., 2012, Wen et al., 2011). These properties together with the ability to cross BBB made MB as a good candidate for targeting mitochondria dysfunction and oxidative stress in many neurological disoders.

Low doses of MB have shown to be neuro-protective and improve spatial memory retention in a toxic model of brain damage in rats (Callaway et al., 2002). It shows to block the tau aggregation in a *C.elegans* model of tau pathology and in AD (Fatouros et al., 2012). Promising results were emerged in AD patients treated with MB over a course of year. Phase II clinical trial testing implies positives effects on the cognitive dysfunction in 332 probable AD patients. MB treatment significantly improved cognitive function with an 81% reduction in the rate of cognitive decline as compared with those receiving placebo (Oz et al., 2009). Following with these results, MB is currently in on global phase III trials for AD and fronto temporal dementia. In addition, MB treatment attenuates behavioral, neurochemical and pathological impairments in animal models of PD, AD and stroke (Oz et al., 2009, Wen et al., 2011). However, it is interesting to note that MB at low nanomoles exerts neuroprotective effect against oxidative stress in *in-vitro* studies while shows mitochondrial protection only at micromoles indicating a novel mechanism involved in its protection.

AIMS
&
OBJECTIVES

2 Aims and objectives

The main aim of this thesis is to unravel the contribution of glial cells in the progression of disease and to identify the new therapeutic targets for X-ALD. The study has been presented in thee different chapters by applying both *in-vitro* & *in-vivo* approaches to identify the molecular pathology of X-ALD.

Here are the specific objectives of each study of this thesis

1. To investigate the role of astrocytes and microglia in the physio-pathogenesis of X-ALD and to decipher the cell type responsible for the disease onset (chapter 1).

2. To explore the role of ECS (endocannabinoid system) in X-ALD mice and to target CB_2 receptor as a therapeutic tool for the treatment of X-ALD (chapter 2).

3. To evaluate the efficacy of the Methylene blue, to ameliorate the mitochondrial function and prevent axonal degeneration in X-ALD mice (chapter 3).

MATERIALS & METHODS

3 Materials and Methods

3.1 Reagents and antibodies

The following chemicals were used: Hexacosanoic acid (C26:0, Ref. H0388), Antimycin A (Ref. A8674), Laminin (Ref. L2020), Ara-C (Cytosine β-D-arabinofuranoside, Ref. C1768), Deoxyribonuclease (DNase Ref. D5025-150KU) from Sigma-Aldrich (Steinheim, Germany); DMEM:F12 (Dulbecco's Modified Eagle's Medium/Ham's Nutrient Mixture Ref. 31330-038) from GIBCO, H_2DCFDA (2′,7′-Dichlorodihydrofluorescein diacetate, Ref. C2938), DHE (Dihydroethidium, Ref. D23107), MitoSOX (Red mitochondrial superoxide indicator, Ref. M36008) from Molecular probes; Fungizone (Amphotericin B-Ref. 15290-026) from life technologies; FBS (Foetal bovine serum, Cultek, Ref. 91S1800; Madrid, Spain). Detail information about Taqman probes and antibodies are summarized in **Table 2 and Table 3** respectively.

3.2 Mice breeding and model

Mice used for experiments were of a pure C57BL/6J background and were all male. Animals were sacrificed, and tissues were recovered and conserved at –80 °C. All methods used in this study were in accordance with the Guide for the Care and Use of Laboratory Animals published by the US National Institutes of Health (NIH Publications No. 85–23, revised 1996) and European (2010/63/UE) and Spanish (RD 53/2013) legislation. Experimental protocol had been approved by IDIBELL, IACUC (Institutional Animal Care and Use Committee) and regional authority (3546 DMAH, Generalitat de Catalunya, Spain). IDIBELL animal facility has been accredited by The Association for Assessment and Accreditation of Laboratory Animal Care (AAALAC, Unit 1155). Animals were housed at 22 ºC on specific-pathogen free conditions, in a 12-hour light/dark cycle, and *ad libitum* access to food and water. Each Cage contained 3 to 5 animals.

Two X-ALD mouse models were used in this study. The first model, mouse *Abcd1*$^{-}$ at 12 months of age shows biochemical signs of pathology, including oxidative stress and alterations in energy homeostasis, although the first clinical signs of AMN (axonopathy

and locomotor impairment) appear at 20 months. The second model was mouse with double gene knockout of both the Abcd1 and Abcd2 transporters *(Abcd1^{-}/Abcd2$^{-/-}$).* The *Abcd1^{-}/Abcd2$^{-/-}$* mouse displays greater VLCFA accumulation in the spinal cord, higher levels of oxidative damage to proteins and a more severe AMN-like pathology with an earlier onset at 12 months of age. We assessed all the biochemical signs in single knockout (*Abcd1^{-}*) and the clinical signs in double knockout *(Abcd1^{-}/Abcd2$^{-/-}$).*

3.3 Treatment in mice

3.3.1 Treatment with CB_2 agonist (JWH 133)

The selective CB_2 agonist- JWH133 (Ki= 677 nM for CB_1 and 3.4 nM for CB_2 was supplied by Tocris Bioscience. JWH133 (0.2 mg/kg) was dissolved in ethanol and 90% saline and injected intraperitoneally (i.p).

For the characterization of biochemical signs on adult X-ALD mice, 11 months old animals were randomly assigned to one of the following dietary groups for 1 month. Group I: wild-type (WT) mice received one daily administration of corresponding vehicle (n=12); group II: *Abcd1^{-}* mice received one daily administration of corresponding vehicle (n=12); group III: *Abcd1^{-}* mice received one daily administration with JWH 133 (n=12). To evaluate the effect of CB_2 agonist on the clinical signs of AMN-like pathology, 15 months old animals were randomly assigned to one of the following dietary groups for 1 month. Group I: (WT) mice received one daily administration of corresponding vehicle (n=14); group II: *Abcd1^{-}/Abcd2$^{-/-}$* mice received one daily administration of corresponding vehicle (n=16); group III: *Abcd1^{-}/Abcd2$^{-/-}$* mice received one daily administration with JWH 133 (n=14).

3.3.2 Treatment with Methylene blue

MB (3, 7-bis (Dimethylamino) phenazathionium chloride, $C_{16}H_{18}C_lN_3S$) was received from Sigma-Aldrich (St Louis, MO, USA) and was supplemented in water with dose of 4 mg/kg. For the characterization of biochemical signs on adult X-ALD mice, 10 months old animals were randomly assigned to one of the following dietary groups for 2 months. Group I: wild-type (WT) mice were supplemented with normal water (n=12);

group II: *Abcd1*$^{-}$ mice were supplemented with normal water (n=12); group III: *Abcd1*$^{-}$ were supplemented with MB in water (n=12). To evaluate the effect of MB on the clinical signs of AMN-like pathology, 15 months old animals were randomly assigned to one of the following dietary groups for 1 month. Group I: (WT) mice received one daily administration of corresponding vehicle (n=14); group II: *Abcd1*$^{-}$*/Abcd2*$^{-/-}$ mice received one daily administration of corresponding vehicle (n=16); group III: *Abcd1*$^{-}$*/Abcd2*$^{-/-}$ mice received one daily administration with JWH 133 (n=14).

3.4 Behavioral Test

3.4.1 Treadmill test

Treadmill apparatus (Panlab, Barcelona, Spain) consists of a belt (50 cm long and 20 cm wide) varying in terms of speed (5–30 cm/s) and slope (0–25°) enclosed in a plexiglass chamber. An electrified grid is located to the rear of the belt on which foot shocks (0.2 mA) were administered whenever the mice fell down the belt. The mice were placed on the top of the belt in the opposite direction to the movement of the belt. Thus, to avoid the foot shocks, the mice had to move forward. The latency to falling off the belt (time of shocks in seconds) and the number of shocks received were measured. The mice were evaluated in five trials in a single-day session, always between 2 p.m. and 6 p.m. In the first trial, the belt speed was set at 20 cm/s and the inclination at 5º. In the second and third trial, the belt speed was 10 cm/s and the slope was increased to 10° and 20°, respectively. Then, for the fourth and the fifth trials, the slope was maintained at 20° and the belt speed was increased to 20 and 30 cm/s, respectively. For the thee first trials, mice ran for 1 min. For the fourth and fifth tests, times of the experiment were 3 minutes, and 7 minutes and 30 seconds, respectively. Intervals between each test were 1, 1, 5 and 20 minutes, respectively. When the mice were subjected to consecutive trials at increasing speeds of up to 20 cm/s and a 20° slope, no differences were detected from one session to another between the WT and *Abcd1*$^{-}$*/Abcd2*$^{-/-}$ mice. However, when the belt speed was increased up to 30 cm/s and the slope was 20°, differences were detected between the *Abcd1*$^{-}$*/Abcd2*$^{-/-}$ mice and the controls because this task requires greater coordination. These conditions were therefore chosen to assess the effects of the treatment or the genotype.

3.4.2 Bar cross test

Bar cross test uses a wooden bar of 100 cm in length and 2 cm in width (diameter). This bar is just wide enough for mice to stand on with their hind feet hanging over the edge such that any slight lateral misstep will result in a slip. The bar was elevated 50 cm from the bench surface, so that animals did not jump off, yet were not injured upon falling from the bar. The mice were put on one end of the bar and expected to cross to the other end. To eliminate the novelty of the task as a source of slips, all animals were given two trials on the bar the day before and at the beginning of the testing session. In the experimental session, the numbers of hind limbs lateral slips and the time to cross the bar were counted on thee consecutive trials. The researchers that performed this experiment were blinded for the genotype or treatment of the mice.

3.5 Cell cultures and treatments

3.5.1. Primary human fibroblasts

Primary human fibroblasts were prepared from skin biopsies collected from healthy individuals (n=5) and AMN patients (n=5) according to the IDIBELL guidelines for sampling, including informed consent from the persons involved or their representatives. The fibroblasts were grown in DMEM containing 10% FBS and 100 μg/ml Penicillin Streptomycin (Pen Strep; Gibco, Ref. 15140-122) and maintained at 37 °C in humidified 95% air / 5% CO_2 incubator.

3.5.2. Primary cortical mixed glia and microglia culture protocol

After decapitation of newborn pups (WT & *Abcd1*$^{-}$, P0–P1), the meninges were removed and the brains (cortex) were minced into small pieces using surgical scalpel. Brain pieces were washed with ice cold PBS and centrifuged at 250 g for 5 min. Then the pellet was digested with trypsin (2.0 ml/ brain) for 20 to 30 min at 37 °C with agitation. Digestion was stopped by adding DMEM:F12 media (supplemented with 10% FBS, 100 μg/ml penicillin and 100 μg/ml streptomycin) with DNase and the digested tissue were mixed several times (average 40-60 times) though a Pasteur pipette until the

mucus completely disintegrates. The cell suspension was centrifuged at 250 g for 8 min and then filtered by a tube-top cell strainer (pore size 100 μm). After resuspending the cell pellet in culture media (DMEM supplemented with 10% FBS, 100 U/ml penicillin, and 100 μg/ml streptomycin), cells were counted using the haemocytometer and finally plated into the culture flasks or plates at a density of 400,000 cells/ml and maintained at 37 °C in humidified 95% air / 5% CO_2 incubator. The medium was changed fully at days *in vitro* 5 (DIV5) and then every 3 to 4 days. Confluency was achieved after 10-12 DIV. Microglia cultures were obtained by mild trypsinisation. For mild trypsinisation, cultures between DIV15 and DIV20 were used for isolation of microglia. First conditioned media were collected and mixed cultures were washed with PBS once to eliminate the serum. Second mixed glia cultures were incubated (30 min-1 h) with trypsin 0.25 %: DMEM:F12 (w/o FBS) in 1:3 at 37 °C until the intact astrocyte layer got detached. Third DMEM:F12 media (supplemented with 10 % FBS, 100 μg/ml penicillin and 100 μg/ml streptomycin) was added for trypsin inactivation. Fourth, medium with detached cells were aspirated and replaced by the glia conditioned media for overnight. Possible contamination by astrocytes in the microglia cells preparations was estimated by staining for the marker proteins GFAP and tomato lectin respectively. All experiments were performed after 24 hours post- trypsinisation.

3.5.3. Primary cortical astrocyte culture

Mixed cortical glia cultures are prepared as described above on laminin-coated wells or flask (20 μg/ml). When astrocytes become confluent (generally 9-12 DIV), Ara-C at 10 μM was added to stop the growth of microglia and other cells. Astrocyte cultures were treated with Ara-C at least for 3 days (could be extended to 5 days) and the experiments were performed.

3.5.4. Treatments

The tested compounds or drugs were added with the following concentrations: 50 μM C26:0 (dissolved in ethanol), 500 nM CB_2 agonist JHW133 (dissolved in ethanol), 100 nM Cb2 antagonist AM630 (dissolved in ethanol) and 1 μM Methylene blue (diluted in water). All the above compounds were treated for 24 h and the experiments were

performed. Experiments with fibroblasts were performed at passage 10 to 20 with 80–90% cell confluence.

3.6 Evaluation of reactive oxygen species

Intracellular radical oxygen species levels were measured by using ROS sensitive H_2-DCFDA probe. Total superoxide and mitochondrial superoxide levels were measured by two specific probes DHE and MitoSox respectively. Cells were plated in 12-well (fibroblasts and astrocytes) or 6-well (microglia) tissue culture plates and were treated with interested compounds as indicated before. Treated cells were washed with pre-warmed PBS and incubated with the different probes with following concentration: H_2DCFDA-10 µM, DHE-5 µM and MitoSox-5 µM for 30 min at 37 °C. The complex III inhibitor Antimycin (200 µM - 1 h for astrocytes and fibrobalsts, 50 µM-15 min for microglia) was used as a positive control for all the probes used. Cells were detached from plate by using 1% triton with mild agitation. Cells were collected in a 96-black well plate and the fluorescence was measured with spectrofluorimeter (excitation wavelength 493 nm, emission wavelength 527 nm). Fluorescence values were corrected with protein content and results were expressed as fold change respect to controls or WT (untreated cells).

3.7 Inner mitochondrial membrane potential quantification

Inner mitochondrial membrane potential was measured by flow cytometry using the voltage-sensitive indicator, tetramethylrhodamine ethyl ester (TMRE) (Molecular Probes). This is a cell-permeant, cationic, red-orange fluorescent dye that is readily sequestered by active mitochondria. Disrupting or decreasing membrane potential results in a loss of dye from the mitochondria and a decrease in fluorescence intensity (Zhou et al., 2010). Cells (fibroblasts) were plated in 12-well (fibroblasts and astrocytes) or 6 well (microglia) tissue culture plates and were treated with interested compounds as indicated before. Treated cells were washed with PBS and incubated with 50 nM of TMRE in pre-warmed PBS for 30 min at 37°C. The uncoupler protonophore CCCP (200 µM- 1h) was used as positive control of membrane depolarization (Kasianowicz et al., 1984). Cells were trypsinised, centrifuged at 1000 g for 5 min and resuspended in pre-warmed PBS. All samples were captured in FACS Canto TM

recording 5000 cells for each condition and genotype tested. Percentage of depolarized cells was obtained after gating live cells. Data were analyzed with FlowJo Tree Star software.

3.8 ATP (Adenosine triphosphate) measurement

ATP levels were measured by a chemiluminescence system using ATPlite 1step (PerkinElmer, Inc., Waltham, MA, USA). Measurement of ATP was performed according to the manufacturer's instructions, and relative ATP levels were calculated by normalizing the luminescence obtained to the total protein concentration of the sample measured by BCA (bicinchoninic acid assay). The ATPlite 1step assay system is based on the production of light caused by the reaction of ATP with added luciferase and D-Luciferin, as depicted in the following reaction:

$$\text{ATP} + \text{D-Luciferin} + O_2 \xrightarrow[Mg^{2+}]{\textbf{Luciferase}} \text{Oxyluciferin} + \text{AMP} + \text{PPi} + CO_2 + \text{Light}$$

3.9 Quantitative reverse transcription polymerase chain reaction (qRT-PCR)

Total RNA was extracted from human brains, human fibroblasts, mouse tissues and primary mouse glial cultures using RNeasy Kit (Qiagen, Hilden, Germany). Total DNA was extracted from mouse tissues and primary mouse glial cultures using using Gentra Puregene Tissue Kit (Qiagen, Hilden, Germany). One μg to 300 ng of RNA was transcribed into cDNA using Superscript II reverse transcription reagents (Invitrogen, Thermo Fisher Scientific Inc.) in a final volume of 25 μl. Dilutions ranging from 1/50 to 1/5 dilution of cDNA or 100 ng of DNA were used to measure mRNA or mtDNA levels, respectively. The expression of the genes of interest was analyzed by Q-PCR using TaqMan® Gene Expression Assays (Thermo Fisher Scientific Inc.), standardized Taqman® probes (**Table 2**), SYBR Green Master Mix and standardized primers on a LightCycler® 480 Real-Time PCR System (Roche Diagnostics GmbH). Relative quantification was carried out using the 'Delta-Delta Ct' (ΔΔCt) method with m*Rplp0/hPLP0* as endogenous control. To quantify mouse mtDNA content, primers for

mouse cytochome b (*Cytb*) were designed (Custom TaqMan Gene Expression Assays; Thermo Fisher Scientific Inc.). The sequences for *Cytb* primers were: (forward) ATGACCCCAATACGCAAAATT, (reverse) GGAGGACATAGCCTATGAAGG and the FAM-labeled probe sequence was TTGCAACTATAGCAACAG. Quantification of mtDNA was referred to nuclear DNA (nDNA) as determined by the amplification of the intron-less mouse nuclear gene *Cebpα* (Morato et al., 2013). Transcript quantification was performed in triplicates for each sample.

Table 2 List of qPCR probes used in this thesis

Gene Name	Species	Taqman ref.
Arg1	Mouse	Mm00475991
Cebpα	Mouse	Mm00514283
Ccl2	Mouse	Mm00441242
Ccl5	Mouse	Mm01302427
Ccl7	Mouse	Mm00443113
Ccr1	Mouse	Mm01216147
Ccr6	Mouse	Mm99999114
Chil3	Mouse	Mm00657889
Cnr1	Mouse	Mm01212171
Cnr2	Mouse	Mm00438286
Cox2	Mouse	Mm00478374
Csf1	Mouse	Mm00432686
Cxcl5	Mouse	Mm00436451
Cxcl9	Mouse	Mm00434946
Cxcl10	Mouse	Mm00445235
Cxcl12	Mouse	Mm00457276
Cx3cr1	Mouse	Mm02620111
Cxcr4	Mouse	Mm01292123
Daglα	Mouse	Mm00813830
Daglβ	Mouse	Mm00523381
Faah1	Mouse	Mm00515684
Igf1	Mouse	Mm00439560
Il1α	Mouse	Mm00439620
Il1β	Mouse	Mm01336189
Il6	Mouse	Mm00446190
IL9ra	Mouse	Mm00434313
Il10	Mouse	Mm00439614
iNos	Mouse	Mm00440502
Napepld	Mouse	Mm00724596
Mgll	Mouse	Mm00449274
Mif	Mouse	Mm01611157
Mrc1	Mouse	Mm01329362
Nfκb2	Mouse	Mm00479807
Nrf1	Mouse	Mm00447996
Pgc-1α	Mouse	Mm00447183
Ppar-α	Mouse	Mm00440939
Pparγ	Mouse	Mm01184322
Retnlα	Mouse	Mm00445109
Sirt1	Mouse	Mm00490758
Tfam	Mouse	Mm00447485
Tgfβ1	Mouse	Mm01178820
Tnfα	Mouse	Mm00443258
Tnfrsf1a	Mouse	Mm01182929
Rplp0	Mouse	Mm01974474

Table 3 List of antibodies used in this thesis

Antibody	**Source**	**Reference**	**Dilution**
APP	AbD Serotec	AHP538	1:100
Cytochome C	BD Biosciences Pharmigen	55643	1:500
GFAP	Mako	Z0334	1:500
IBA1	Wako	019-19741	1:1000
MDA	-	Hall et al., 2007[1]	1:1000
Neurofilament H non-phosphorylated(SM132)	Covalence Antibody-Biolegend	801701	1:3000
Synaptophysin	Leica Biosystems	299-L-CE	1:500
Y-tubulin	Sigma-Aldrich	T6557	1:20000
DRP1 (4E11B11)	Cell Signaling Technology	146475	1:1000
P-DRP1 (S616)	Cell Signaling Technology	3455s	1:500

3.10 Immunoblot

Mouse spinal cord were homogenized in radioimmunoprecipitation assay (RIPA) buffer, then sonicated for 2 min with 10 sec interval and centrifuged for 10 min at max speed. Samples were heated for 10 min at 70 ºC with 4X NuPAGE® LDS Sample Buffer (Invitrogen, Thermo Fisher Scientific Inc.) before loading. Proteins at the concentration of 40 µg were loaded onto 8% Novex NuPAGE® SDS-PAGE gel system (Invitrogen, Thermo Fisher Scientific Inc.), and run for 60-90 min at 120 V in NuPAGE® MOPS SDS Running Buffer (Invitrogen, Thermo 85 Fisher Scientific Inc.) supplemented with 5 mM sodium bisulfite (Ref. 243973, Sigma-Aldrich). SeeBlue® Plus2 Pre-stained (Invitrogen, Thermo Fisher Scientific Inc.) was used as a ladder. Resolved proteins were transferred onto nitrocellulose membranes using iBlot® 2 Gel Transfer Device (Invitrogen, Thermo Fisher Scientific Inc.). After blocking in 5 % bovine serum albumin (BSA, Sigma-Aldrich) in 0.05% TBS-Tween (TBS-T) for 1 hour at room temperature, membranes were incubated with corresponding diluted primary antibodies (**Table 3**) in 5% BSA in 0.05% TBS-T overnight at 4 ºC. Following incubation with diluted secondary antibody in 0.05% TBS-T for 1 hour at room temperature, proteins were detected with ECL western blotting analysis system.

3.11 Immunofluorescence or Immunohistochemistry and imaging

Mice tissues

Mice were anaesthetized by intraperitoneal injection of Sodium Pentobarbital (Dolethal®; Vetoniquol, Alcobendas, Spain) diluted 1/10 in physiological serum (Braun, Rubí, Spain). Spinal cord was harvested after perfusing the mice with 4 % paraformaldehyde (PFA; Sigma-Aldrich, Ref. 441244) in 0.1 M phosphate buffer pH 7.4.

For studying axonal degeneration, spinal cord was embedded in paraffin and serial sections (4 µm thick) were cut in a transversal or longitudinal (1 cm long) plane with a

microtome (Microm HM 340E, Thermo Fisher Scientific). IHC studies were performed in WT; *Abcd1*$^{-}$*/Abcd2*$^{-/-}$; *Abcd1*$^{-}$*/Abcd2*$^{-/-}$+ CB_2 agonist or Methylene blue; mice were carried out with the avidin–biotin peroxidase method.

Slides with tissues undergo rehydration and then antigen retrieval using 10 mM citrate buffer pH 6.0. Endogenous peroxidases blocking was done using 3 % H_2O_2 (H1009, Sigma-Aldrich), then the rehydrated sections were stained with 3 % Sudan black (Ref. 199664, Sigma-Aldrich) or processed for IHC. After primary antibody incubation for overnight (**Table 3**), the sections were incubated with the Labelled Streptavidin-Biotin2 System (LSAB2, Ref. K0675, Dako). Staining was visualized after incubation with 3-3'-diaminobenzidine (DAB) substrate chomogen 91 (Ref. D5637, Sigma-Aldrich) which results in a brown-coloured precipitate at the antigen site. After dehydrating the sections, slides were mounted with DPX (Ref. 06522, Sigma-Aldrich).

Images were acquired using Olympus BX51 microscope (20x/N.A 0.50 Ph 1 UPlan FL N; Olympus Corporation, Tokyo, Japan) connected to an Olympus DP71 camera and Cell^B software (Olympus Corporation). The researcher was blinded to both the genotype and the treatment of the sample when analyzing the results.

Cells

Cells were seeded on glass cover slips in 12-well tissue culture plates with semi confluence and treated accordingly. Then cells were fixed with 4 % paraformaldehyde for 15 min at RT and blocked with filtered blocking buffer (1 % bovine serum albumin (BSA), 0.2% powdered milk, 2% FBS, 0.1 M glycine, 0.1 % Triton-X-100) for half an hour. Following incubation with primary antibody for overnight, the cells were incubated with respective secondary antibody for 1 hour at RT in dark. Finally cells were stained with DAPI and mounted with Fluoromount.

Confocal images were collected using a Leica TCS SP5 confocal microscope (Leica Biosystems), and processed with ImageJ v1.50i (U. S. National Institutes of Health, Bethesda, MD, USA).

3.12 High resolution respirometry

O_2 consumption was measured in sets of five permeabilized lumbar spinal cord slices (LSCS) (n=5 mice per genotype) at 37 °C in MiR05 medium pH 7.4 by high-resolution respirometry using an Oxygraph-2k (Oroboros Instruments, Innsbruck, Austria) as previously described (Lopez-Erauskin et al., 2013).

In detail, fresh spinal cords were rinsed in ice-cold normal saline and cut into slices with a tissue chopper adjusted to a cut width of 300 μM. O_2 consumption was measured in sets of 5 LSCS at 37 °C with high-resolution respirometry in permeabilized conditions (including substrates and inhibitors of specific respiratory complexes) using an Oxygraph-2k (Oroboros Instruments, Innsbruck, Austria) with chamber volumes set at 2 ml. Spinal cord permeabilization was a modification of a previously published method (Safiulina et al., 2004). About 12-15 slices of the lumbar region were collected and transferred quickly into an individual well of a 6-well tissue culture plate with 2 ml of ice-cold permeabilization medium (7.23 mM potassium ethylene glycol-bis{baminoethyl ether}N,N,N',N'-tetraacetate [K_2-EGTA]; 2.77 mM CaK_2-EGTA; 60 mM N,N-bis{2-hydroxyethyl}-2-aminoethanesulfonic acid [BES]; 5.69 mM MgATP, 20 mM taurine; 3 mM K_2HPO_4; 0.5 mM dithiotheitol [DTT] and 81 mM potassium methanesulfonate, pH 7.1 at 25ºC), rinsed and immediately transferred into another well with the same medium containing 20 μl of saponin stock solution (5 mg/ml; final concentration 50 μg/ml). LSCS were then shaken by gentle agitation at 4ºC for 30 min. Afterwards, all samples were quickly transferred from the saponin permeabilization medium into 2 mL of respiration medium (7.23 mM K2-EGTA; 2.77 mM CaK_2-EGTA; 100 mM potassium salt of 2-{N-morpholino}ethanesulfonic acid [K-MES], 1.38 mM $MgCl_2$; 20 mM taurine; 3 mM K_2HPO4; 0.5 mM DTT; 20 mM imidazole and 5 mg/mL BSA, pH 7.1 at 25 ºC), then shaken by gentle agitation for 10 min in the cold room (on ice) before performing respirometry.

In order to avoid tissue disaggregation, LSCS required setting a slow bar stirring speed (150 rpm), but not too low to compromise homogeneity of substrate and oxygen concentrations in the measuring chambers, and, therefore, signal stability. DatLab software (Oroboros Instruments, Innsbruck, Austria) was used for data acquisition (2 s 88 time intervals) and analysis, which includes calculation of the time derivative of oxygen concentration and correction for instrumental background oxygen flux (Gnaiger, 2001). Respiration of LSCS required tissue or cell permeabilization before placing the

sample in the measurement chamber. Initially, we measured endogenous respiration in the absence of additional substrates. For evaluation of relative contributions of mitochondrial complexes to oxygen consumption, several specific mitochondrial inhibitors and substrates were added sequentially and calculated as steady-state respiratory flux in the time interval between 5 and 10 min after their addition. First, we added glutamate (10 mM) and malate (5 mM) to increase NADH levels in order to measure the complex I non-phosphorylative activity, or state 2. ADP (10 mM) was added to quantify the complex I-dependent phosphorylative activity, or state 3. Immediately afterwards, we added succinate (10mM), which is the substrate for complex II. At this point, the level of oxygen consumption corresponded to complex I- and II-dependent phosphorylative activity. The addition of rotenone (0.5 µM; Sigma-Aldrich) inhibits complex I; therefore, oxygen consumption measured after the addition of rotenone only reflects complex II-dependent phosphorylative activity (in the absence of electron back flux to complex I). Then, complex III activity was inhibited with antimycin A (2.5 µM; Sigma-Aldrich) to obtain residual oxygen consumption. In order to avoid oxygen limitations, all the experiments were performed above 50% oxygen saturation. Oxygen consumption was normalized for actual protein content in the respirometer chambers.

3.13 Evaluation of oxidative lesions

AASA, CML, CEL and MDAL concentrations in total proteins from spinal cord homogenates were measured with GC/MS, as reported (Fourcade et al., 2008). The amounts of products were expressed as the ratio of micromole of AASA, CML, CEL, or MDAL per mol of lysine.

3.14 Statistical Analysis

All data are presented as mean ± standard deviation (SD). Statistical significance was assessed using Student's *t*-test when two groups were compared. When comparing multiple groups, significant differences were determined by one-way ANOVA followed by Tukey's post hoc test after verifying normality. All *P* values were two tailed, and a *P*

value of less than 0.05 was considered statistically significant (*P < 0.05; **P < 0.01; ***P < 0.001). Statistical analyses were performed using SPSS.

RESULTS

4 RESULTS

4.1 Chapter 1: Study of inflammation in X-ALD pathophysiology: noxious effects of C26:0 in glial cells

4.1.1 X-ALD mice spinal cord displays a mixed inflammatory profile at pre symptomatic stage

With the existing reports from our laboratory about the inflammatory mechanism in X-ALD, we observed subtle chonic inflammatory imbalance in spinal cord of X-ALD mice associated with astrocytosis and microgliosis. Moreover, by functional genomics approach we unraveled the non-canonical *Nfkb2* mediated inflammatory pathway activation and increased levels of pro-inflammatory cytokines and chemokines in *Abcd1*$^{-}$ mice spinal cord at 12 months of age (Schluter et al., 2012). However, the knowledge of anti-inflammatory profile in our mouse model was lacking. Thus, here we sought to further investigate in deep the role of inflammation in *Abcd1*$^{-}$ mice spinal cord at 12 months of age and we analyzed an list of pro and anti-inflammatory mediators, cytokines and chemokines. Almost all the pro-inflammatory markers including *Tnfα, Ilα, Ilβ, Ccl2, Ccl5, Cxcl10, Ccr1, Ccr6, Cxcr4* and *Cxcl9* were found to be up-regulated with some exception like *Il6* an important pro-inflammatory cytokine found to be down-regulated (**Fig. 6a**). Interestingly, some of the neuroprotective factors and anti-inflammatory markers like *Igf1, Il10, Tgfβ1, Chil3* and *Il5* were found to be increased suggesting an endogenous response by X-ALD mice against the disease pathogenesis by the maintainence of pro and anti-inflammatory balance **(Fig. 6b)**.

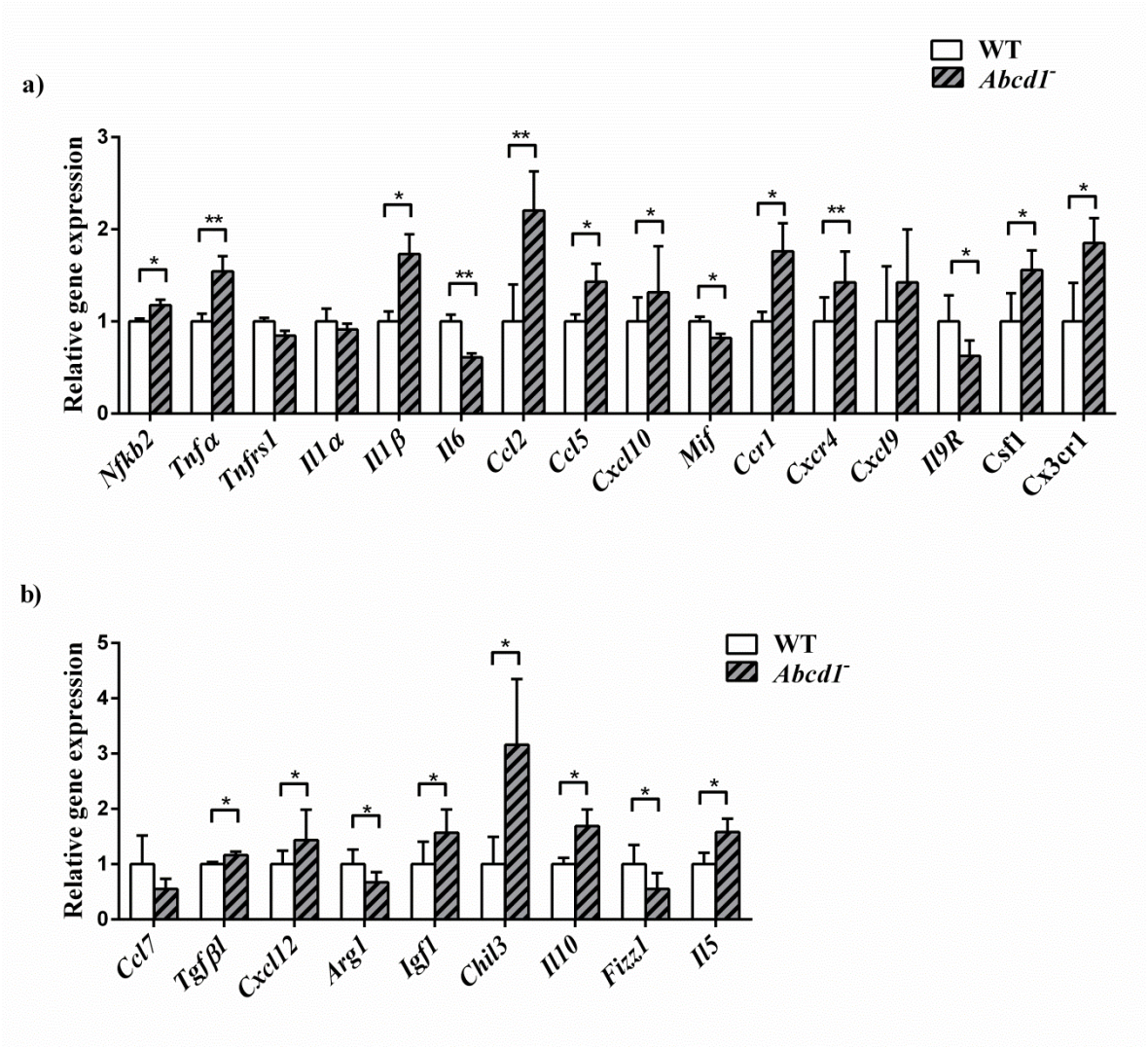

Figure 6. *Abcd1*⁻ mice spinal cord displays inflammatory imbalance at pre-symptomatic stage

(a) Pro-inflammatory cytokines and chemokines (*Nflβ2, Tnfα, Tnfrs1, Il1α, Il1β, Il6, Ccl2, Ccl5, Ccr1, Cxcl10, Mif, Cxcr4, Cxcl9, Il9r, Csf1 & Cx3cr1).* **(b)** anti-inflammatory cytokines and chemokines (Ccl7, *Tgfβ1 , Arg1,Igf Chil3 , Il10, Fizz1*and *Il10r* were measured in *Abcd1*⁻ mice spinal cord at 12 months of age. Gene expression levels were measured by quantitative RT-PCR and normalized relative to mouse *Rplp0.* Quantification is represented as fold change to WT. Values are expressed as mean ± SD. * $p<0.05$, ** $p<0.01$, *** $p<0.001$ after one way ANOVA test followed by Tukey's post-hoc test.

4.1.2 X-ALD mice microglia shows an inflammatory imbalance, high ROS at baseline and more severe pattern after C26:0 insult.

With the above findings regarding the M1 and M2 inflammatory pattern observed in X-ALD mice spinal cord. It is tempting to speculate whether these inflammatory responses

are mainly produced by microglia, as microglia had been thought to play a vital role in X-ALD pathogenesis (Cartier and Aubourg, 2008) described briefly in the introduction part of neuroinflammation. Therefore, in the present work we took the advantage of primary astroglia and microglia cultures from both WT and *Abcd1*$^{-}$ mice to investigate their role in physio-pathogenesis of disease and to reveal whether exogenous insult of C26:0, the main VLCFA accumulated in X-ALD patients on astrocytes and microglia could have an impact on various parameters like inflammation, redox homeostasis that are altered in our mouse model.

We first checked the inflammatory profile in these cultures at baseline and upon C26:0 treatment. At baseline, *Abcd1*$^{-}$ microglia represents a mild inflammatory profile denoted by up-regulation of some cytotoxic factors like *Il1β, Tnfα, Ccl5* and *Cxcl10* and neuroptotective factors like *Il10*, *Arg1* (**Fig. 7a**). Moreover, excess of C26:0 further modulates the inflammatory profile in microglia from WT and *Abcd1*$^{-}$ mice. Thus, these cultures showed a mixed inflammatory pattern characterized by an up-regulation of the pro-inflammatory cytokines and chemokines including *Cd86, iNOS, Cox2, Il1α, Tnfα, Ccl2, Cxcl10, Ccr1* and *Csf1* (**Fig. 7a)** and anti-inflammatory including *Arg, Igf1, Tgfβ1, Mif* and *Ccl7* (**Fig. 7b**). Interestingly, the two important cytotoxic factors *Cox2* and *iNOS* were found to be increased only in *Abcd1*$^{-}$ microglia after C26:0 insult at a dosage of 50 uM indicating these cultures were more sensitive to VLCFA (**Fig. 7c**). Also, *Il10* an important anti-inflammatory cytokine was found to be decreased with C26:0 in both genotypes indicating the involvement of VLCFA in inducing inflammation in primary mice microglia cultures (**Fig. 7b)**. We then analyzed the total free radicals in microglia cultures at baseline and after the C26:0 treatment. ROS levels were increased in both WT and *Abcd1*$^{-}$ mice microglia upon C26:0 insult at 50 µM (**Fig. 7c**). Moreover, at baseline we found a slight increase in ROS level in *Abcd1*$^{-}$ microglia compared to WT. The origin of ROS induced by C26:0 in X-ALD human fibroblasts was found to be mainly from mitochondria (Lopez-Erauskin et al., 2013b). Here we sought to investigate whether mitochondria from microglia represent the same source after C26:0 treatment. We used two fluorescent probes DHE (dihydroethidium) and MitoSOX (DHE covalently bonded to hexyl triphenylphosphonium cation), which measure intracellular and intramitochondrial superoxide levels respectively. We noted that the levels of superoxide measured by either DHE or MitoSOX were similar, which

indicates mitochondria as the major source of ROS in *Abcd1*$^{-}$ microglia when cultures are loaded with C26:0 (**Fig. 7d**).

In conclusion, X-ALD mouse adopts a dual phenotype expressing the factors that are hypothesized to be cytotoxic (M1) and neuroprotective (M2) mimicking the inflammatory environment of X-ALD mouse spinal cord. Moreover, X-ALD microglia represents more severe inflammatory pattern and produces mitochondrial ROS under the treatment of C26:0 suggesting microglia as a good *in-vitro* model for deep mechanistic studies.

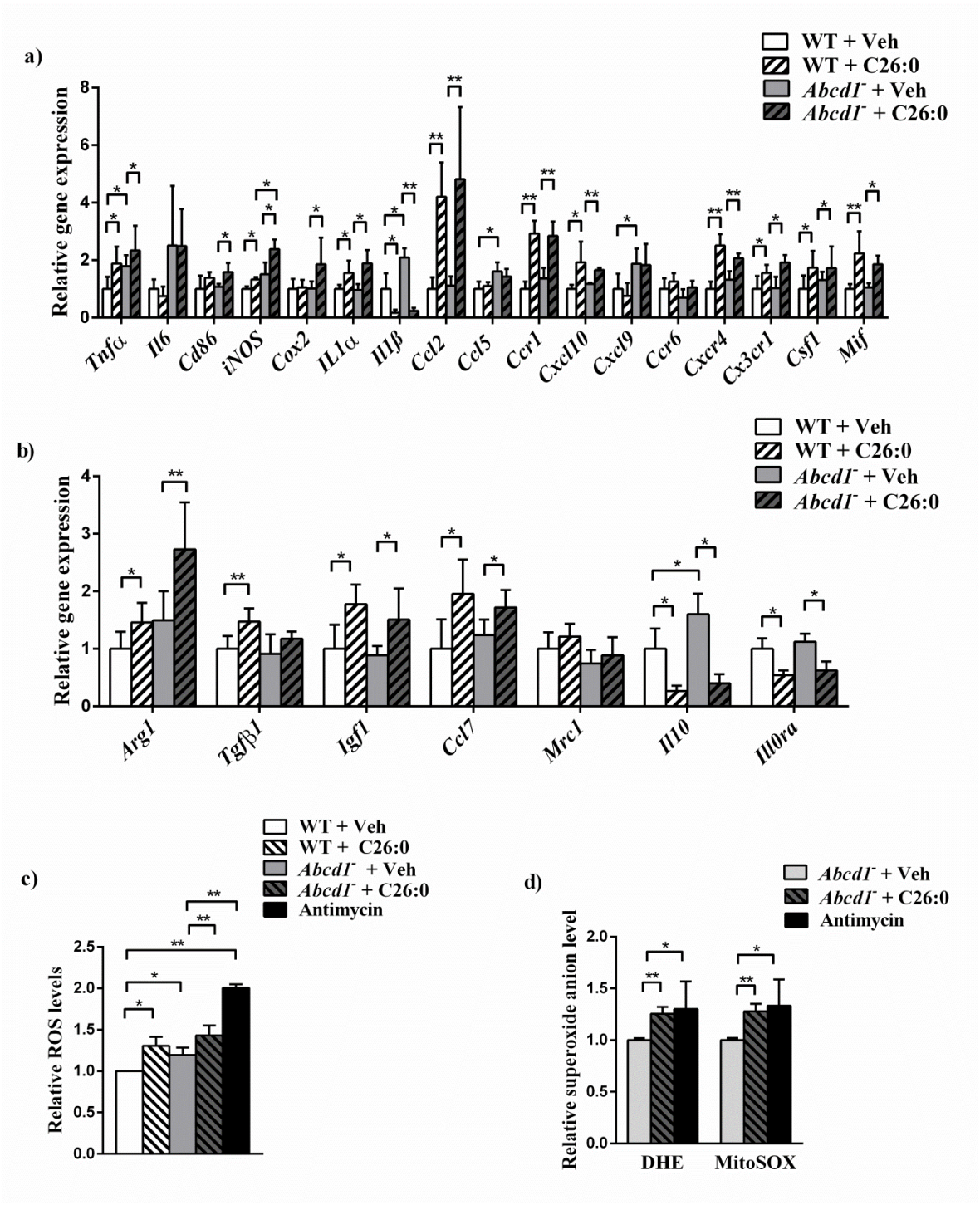

Figure 7. *Abcd1*⁻ primary mice microglia displays inflammatory imbalance and VLCFA induced ROS production and inflammation

(a) Pro-inflammatory cytokines and chemokines (*Tnfα, Il6, Cd86, iNOS, Cox2, Il1α, Il1β, Ccl2, Ccl5, Ccr1, Cxcl10, Cxcl9, Ccr6, Cxcr4,Cx3Cr1, Csf1* and *Mif* (**b)** anti-inflammatory cytokines and chemokines (*Arg1,Tgfβ1,Igf1, Ccl7, Mrc1, Il1 0*and *Il10ra* were measured in primary WT (n=4 per condition) and *Abcd1*⁻(n=4 per condition) mice microglia after 24 h upon C26:0 (50 µM) insult and at baseline. Gene expression levels were measured by quantitative RT-PCR and normalized relative to mouse *Rplp0*. Quantification is represented as fold change to respective WT vehicle (Veh). **(c)** Total ROS

levels in both primary WT (n=4 per condition) and *Abcd1*⁻(n=4 per condition) mice microglia and **(d)** total superoxide and mitochondrial superoxide levels in *Abcd1*⁻(n=4 per condition) mice microglia were measured upon C26:0 (50 µM) insult after 24 h. The complex III inhibitor, antimycin was used as a positive control. Quantification is represented as fold change to WT vehicle (Veh). Values are expressed as mean ± SD. * $p<0.05$, ** $p<0.01$, *** $p<0.001$ after one way ANOVA test followed by Tukey's post-hoc test.

4.1.3 C26:0 causes severe inflammation and increases the generation of ROS in primary mice astrocytes

We further investigated the role of C26:0 in astrocyte cultures to know whether the effect of C26:0 is cell dependent. We checked some inflammation markers and measured the levels of total ROS after C26:0 insult. Both the WT and *Abcd1*⁻ mice astrocytes showed severe inflammation (**Fig. 8a and b**) and elevated ROS levels (**Fig. 8b)** after the addition of C26:0. Inflammation was characterized by huge elevation of some classical inflammatory cytokines and chemokines *like Il6, Ccl2, Ccl5, INOS, Cox2, Cxcl0, Cxcl9* and *Cxcl5* (**Fig 8a**). Many of the anti-inflammatory makers like *Igf1, Tgfb1* remain unchanged with exceptional elevation of *Ccl7* found after C26:0 insult (**Fig 8b)**. It is worth to note that there was no amplification in some of anti-inflammatory markers like *Arg1* and *Il10,* as they are very low expressed in these cultures. Moreover, at baseline no changes were observed in both parameters in astrocytes.

Overall, the above data revealed *Abcd1*⁻ mice astrocytes shows no inflammation and ROS production unlike microglia at basal level. However, C26:0 induces high ROS production and inflammation in both WT and *Abcd1*⁻ mice astrocytes.

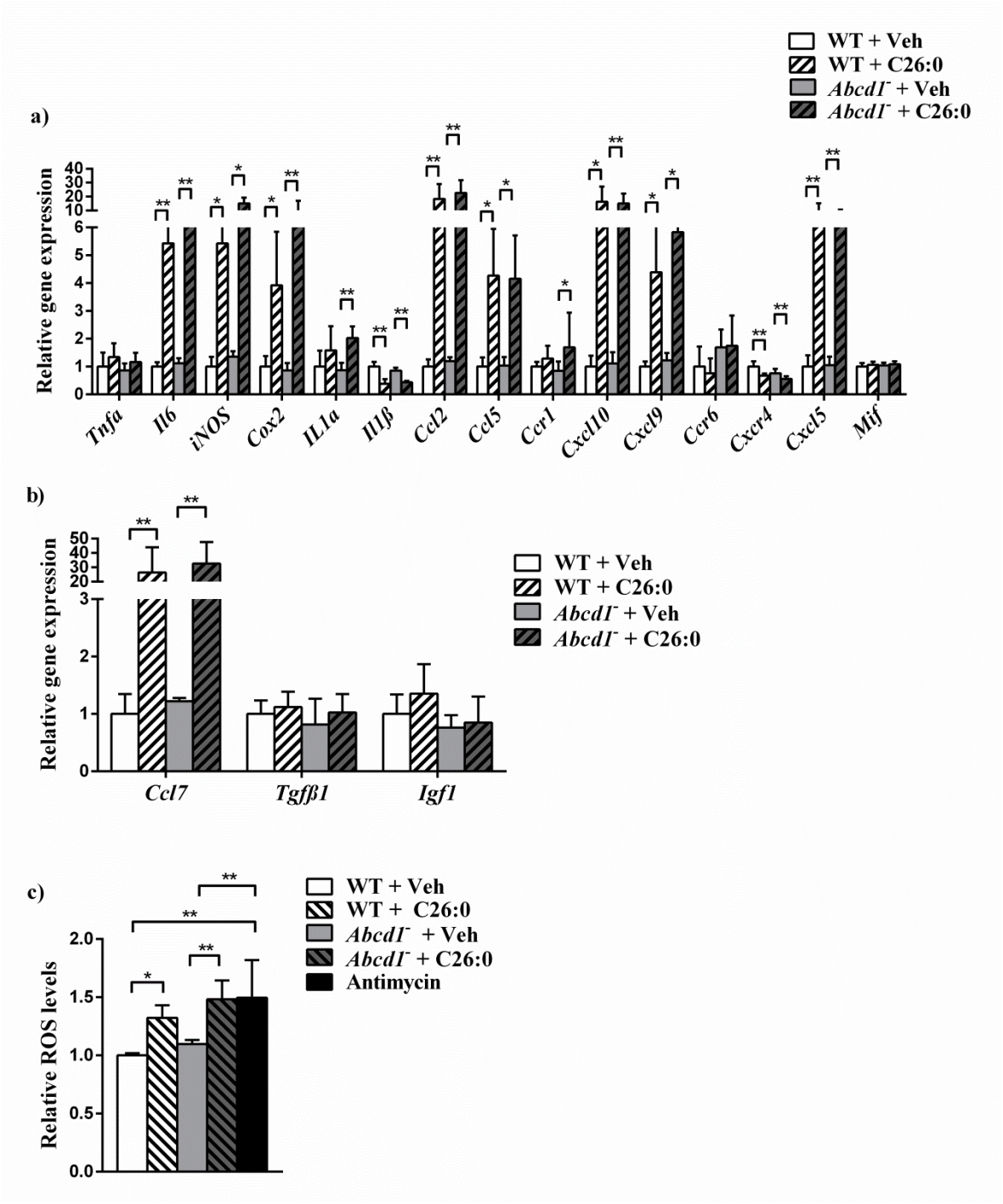

Figure 8. Excess VLCFA induces inflammation and ROS production in primary X-ALD mice astrocytes

Inflammatory profile in primary WT (n=4) and *Abcd1*⁻ (n=4) mice astrocytes. Pro-inflammatory (*Tnfα, Il6, iNOS, Cox2, Il1α, Il1β, Ccl2, Ccl5, Ccr1, Cxcl10, Cxcl9, Ccr6, Cxcr4, Cxcl5* & *Mif*) **(a)** and anti-inflammatory (*Ccl7, Igf1*& *Tgfβ*) **(b)** cytokines, chemokines and other inflammatory related markers were measured after C26:0 (50uM) treattment for 24 h by quantitative RT-PCR in both primary WT (n=4 per condition) and *Abcd1*⁻ (n=4 per condition) mice astrocytes. Gene expression levels were normalized relative to *Rplp0*. Quantification is represented as fold change to WT vehicle. **(c)** Total ROS levels were

measured upon C26:0 (50 µM) insult after 24 h in both primary WT (n=4 per condition) and *Abcd1*⁻ (n=4 per condition) mice astrocytes. The complex III inhibitor, antimycin was used as a positive control. Quantification is represented as fold change to WT vehicle (Veh).Values are expressed as mean ± SD. * $p<0.05$, ** $p<0.01$, *** $p<0.001$ after unpaired Student's t test and one way ANOVA test followed by Tukey's post-hoc test.

4.2 Chapter 2: Neuroptotective role of CB_2 receptor in a mouse model of X-ALD

4.2.1 Endogenous cannabinoid system (ECS) is altered in X-ALD mouse spinal cord and in primary microglia

ECS has been shown to play a pro-homeostatic role facilitated by the production and degradation of endocannabinoids on demand and activate the targets when needed. As a consequence, these endocannabinoid levels altered under pathological conditions in nearly all chonic neurodegenerative diseases either as an adaptive or non-adaptive response against the diseases progression. Here we deliberate its role in X-ALD mouse spinal cord by measuring the followings: 1) Receptors level (*Cnr1*&*Cnr2*); 2) endogenous cannabinoid levels (2-arachidonoyl glicerol (2-AG), 2- linoleoyl glicerol (2-LG), 2-oleoyl glicerol (2-OG), N-arachidonoyl ethanolamine (AEA o anandamide), N-docosatetraenoyl ethanolamine (DEA), N-docosahexaenoyl ethanolamine (DHEA), N-linolenoyl ethanolamine (LEA), N-olenoyl ethanolamine (OEA), N-palmitoyl ethanolamine (PEA), N-palmitolenoyl ethanolamine (POEA) and N-stearoyl ethanolamine (SEA); 3) enzymes involved in bio-sysnthesis (*Napepld, Daglα& Daglβ*) and degradation (*Magl & Faah*) of endocannabinoids.

Levels of some endocannabinoids like N-palmitoyl ethanolamine (PEA), N-palmitolenoyl ethanolamine (POEA) and N-stearoyl ethanolamine (SEA) were found to be decreased showing an altered endogenous cannabinoid system in *Abcd1*⁻ mice spinal cord (**Fig. 9a**). Further X-ALD mice spinal cord revealed increased levels of CB_2 receptor and endocannabinoid metabolic enzymes like *Daglα, Daglβ* and *Magl* at mRNA level at 12 months of age (**Fig. 9b**). However, no change had been found in CB_1 receptor level indicating the endogenous response via CB_2 receptor in X-ALD mice (**Fig. 9b)**.

Moreover, we measured the receptor and enzymes at mRNA level in both primary microglia and astrocyte primary cultures to know whether these alterations in spinal cord were cell specific and whether C26:0 treatment could modulate the endogenous cannabinoid enzymes and receptors in these cultures. *Magl* levels were found to be increased in microglia at baseline and it was raised by C26:0 treatment (**Fig. 9c**). Moreover, *Cnr2* (CB_2) levels were induced in microglia at baseline and with C26:0 in WT cultures representing physiological response of CB_2 receptor in *Abcd1*$^{-}$ mice microglia (**Fig. 9c**). No change was observed in *Cnr1* (CB_1) level (**Fig. 9c**). Apparently in case of astrocytes, all ECS enzymes and *Cnr1* level were found to be unchanged at baseline and upon C26:0 insult in both WT and *Abcd1*$^{-}$ mice (**Fig. 9d**). Moreover, *Cnr2* levels were almost undetectable as their expression found to be very low or absent in our cultures.

Thus these data indicate that endocannabinoid system is dysregulated in X-ALD mice spinal cord and in primary mice microglia.

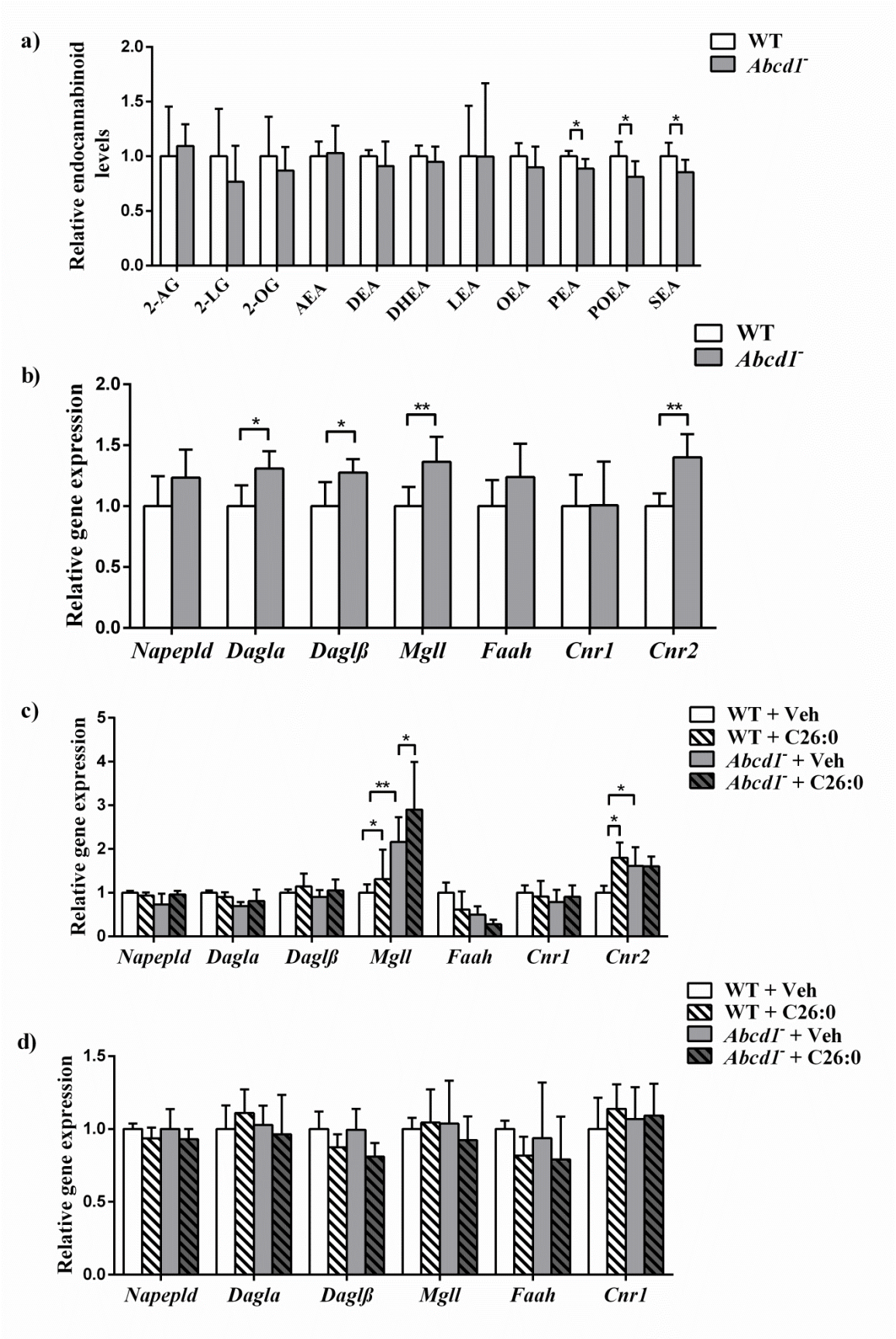

Figure 9. Endocannabinoid system is altered in spinal cord and in primary microglia of X-ALD mice

(a) Endocannabinoid ((2-AG, 2-LG, 2-OG, AEA, DEA, DHEA, LEA, OEA, PEA, POEA, and SEA) levels were measured in WT (n=7) and *Abcd1*⁻ (n=7) spinal cord at 12 months of age. (**b)** Biosynthetic (*Napepld, Daglα*and *Daglβ),*catabolic enzymes (*Mgll* and *Faah*) and cannabinoid receptors (Cnr1 & Cnr2) were measured at 12 months of age in spinal cord at mRNA level by quantitative RT-PCR. Gene expression levels were normalized relative to *Rplp0* and quantification is represented as fold change respect to WT mice. *Napepld, Daglα, Daglβ, Mgll, Faah, Cnr1* & *Cnr2* at mRNA level were measured in both WT (n=4 per condition) and *Abcd1*⁻(n=4 per condition) **(c)** microgliaand **(d)** astrocytes under basal conditions and upon C26:0 insult after 24 h. Gene expression levels were measured by quantitative RT-PCR and normalized relative to *RPLP0.* Quantification is represented as fold change to WT vehicle (Veh). Values are expressed as mean ± SD. * $p<0.05$, ** $p<0.01$, *** $p<0.001$ after unpaired Student's t test (or) one-way ANOVA test followed by Tukey's post-hoc test.

4.2.2 Activation of CB_2 prevents inflammation in X-ALD mice

There is enough accumulated evidence indicating that cannabinoids (CBs) might serve as a promising tool to modify the outcome of inflammation. Many *in-vivo* (Ehrhart et al., 2005, Maresz et al., 2007, Martin-Moreno et al., 2011) and *in-vitro* models of inflammation (Mecha et al., 2015, Ortega-Gutierrez et al., 2005) have been proved the beneficial effects of CBs in diverse pathological states. As described above, a low grade inflammation with generic imbalance between pro and anti-inflammatory profile and upregulated CB_2 levels as an endogenous response have been observed in X-ALD mice. With these described studies in literature linking the inflammation with ECS made us to evaluate that the activation of CB_2 receptor could be an effective strategy to halt the disease progression by preventing the inflammation. Therefore, we treated the mice with CB_2 specific agonist JWH133 and analyzed the whole inflammatory profile in X-ALD spinal cord. We found almost all the pro-inflammatory cytokines and chemokines like *Nfkb2, Tnfα, Tnfrsf1a, Ccl5, Ccl2, Cxcl10, Il1β, Ccr1* and *Cxcr4* production were averted after agonist treatment (**Fig. 10a**). Few anti-inflammatory markers like *Il10* and *Chil3* remain increased like mutant (*Abcd1*⁻) thus maintain the anti-inflammatory environment for further reparative process (**Fig. 10b)**.

Thus, overall these data reveal that activation of CB_2 receptor in X-ALD mice provokes neurotrophic factors and normalized the levels of pro-inflammatory mediators suggesting the protective role of CB_2 in neuroinflammation.

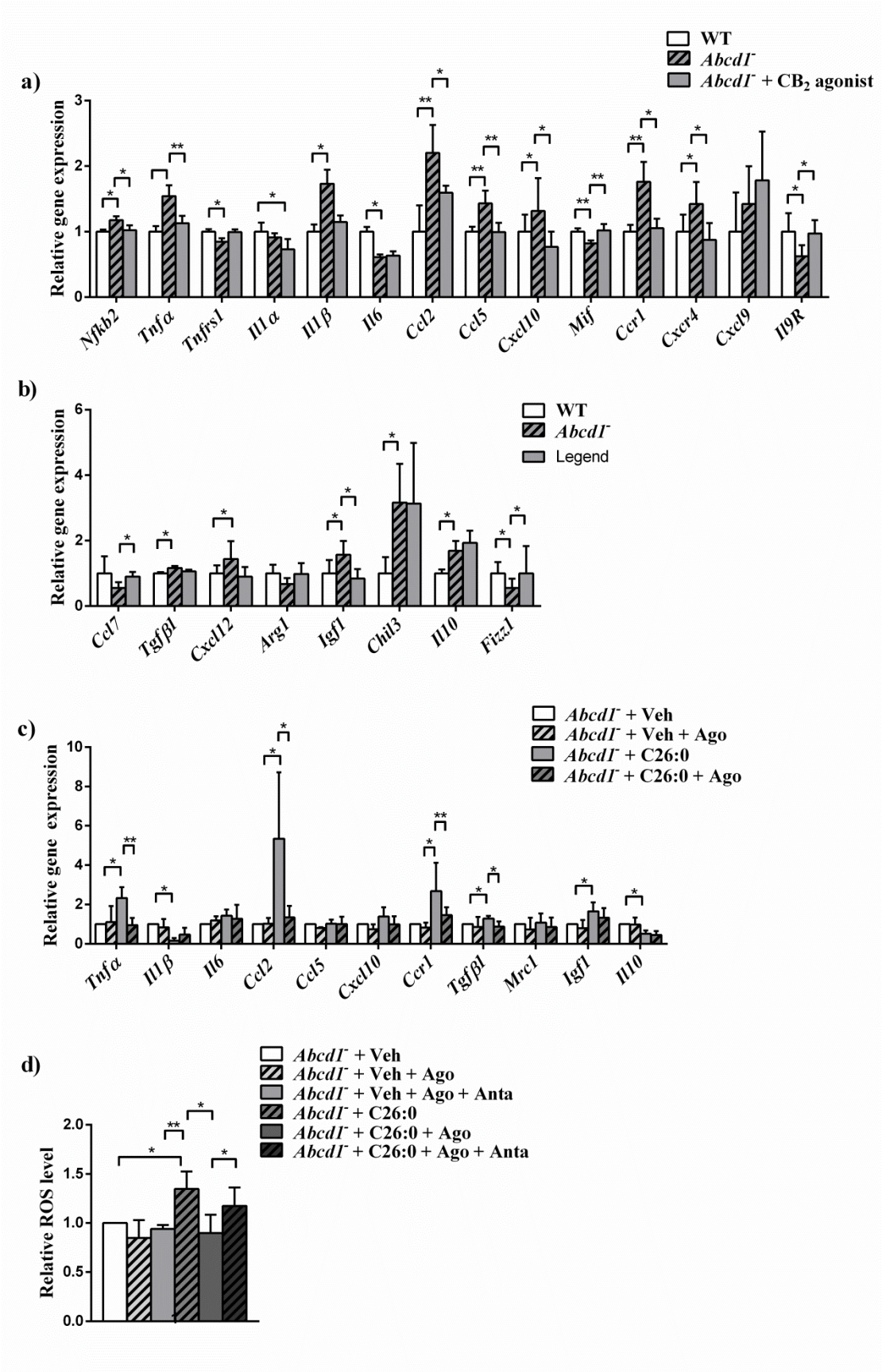

Figure 10. CB_2 activation prevents inflammation in X-ALD mouse spinal cord and inhibits the C26:0 mediated ROS production and inflammation in *Abcd1*-primary mice microglia

Inflammatory profile in WT (n=8), *Abcd1*⁻ (n=8) and *Abcd1*⁻ + CB_2 agonist (JWH133) (n=8) mice spinal cord at 12 months of age. **(a)** Pro-inflammatory markers (*Nfkb2, Tnfα,Tnfrs1, Il1α, Il1β, Il6, Ccl2, Ccl5,Cxcl10, Mif, Ccr1, Cxcr4, Cxcl9* and *Il9r*) and **(b)** anti-inflammatory markers (*Ccl7, Tgfβ1, Cxcl12, Arg1, Igf1, Chil3, Il10*and *Fizz1*) were measured at mRNA level by quantitative RT-PCR. Gene expression levels were normalized relative to *Rplp0*. Data is represented as fold change respect to WT mice. **(c)** Inflammatory profile in primary *Abcd1*⁻ (n=4 per condition) microglia after C26:0 insult and treatment with CB_2 agonist (100nM) for 24 h. Inflammatory markers (*Tnfα,Il1β, Il6, Ccl2, Ccl5,Cxcl10,Ccr1, Tgfβ1, Mrc1, Igf1* and*Il10*) were measured at mRNA level by quantitative RT-PCR and normalized relative to mouse *Rplp0.* Quantification is represented as fold change to *Abcd1*⁻vehicle (Veh).**(d)** ROS levels were measured upon treatment with C26:0 in the presence and absence of CB_2 agonist (JWH133-100nM) and antagonist (AM630-100nM) after 24 h in primary *Abcd1*⁻(n=4 per condition) microglia.Quantification is represented as fold change to the respective *Abcd1*⁻vehicle (Veh).Values are expressed as mean ± SD * $p<0.05$; ** $p<0.01$; *** $p<0.001$ after one-way ANOVA test followed by Tukey's post-hoc test.

4.2.3 CB2 activation by specific agonist reduces C26:0 driven inflammation and ROS production in primary microglia

Microglia expresses a functional endocannabinoid system (Stella, 2010) and its activation associated neuropathology can be modulated by CB_2 receptor and endocannabinoids (Mecha et al., 2015). Giving the importance to the role of CB_2 receptor in microglia, we treated the primary microglia cultures with its specific agonist for 24 h and validate its effect on C26:0 induced inflammation and redox status. Similarly, CB_2 activation decreased the levels of pro-inflammatory cytokines like *Tnfα, Ccl5, Ccl2,* and *Cxcl10* produced by C26:0 in primary *Abcd1*⁻ mice microglia (**Fig 10c**). Further, to evaluate the effect of agonist on ROS, we treated the *Abcd1*⁻ mice microglia with CB_2 agonist alone and together with CB_2 antagonist after C26:0 treatment. We demonstrated that activation of CB_2 in microglia diminished the elevated ROS levels produced by C26:0 in *Abcd1*⁻ mice microglia (**Fig. 10d)**. In addition, a partial normalization in ROS levels was found when cultures were treated with both agonist and antagonist indicating a partial involvement of CB_2 receptor (**Fig. 10d)**.

Therefore, the above data indicate that activation of CB_2 receptor arrested the C26:0 induced ROS and inflammation in primary *Abcd1*⁻ mice microglia.

4.2.4 Activation of CB_2 promotes mitochondrial function in X-ALD mice

Previous studies from our laboratory showed mitochondria dysfunction as one of the key factor for disease progression in X-ALD mice characterized by decrease in mitochondria copy number and its target genes, reduced mitochondria respiration and impaired energy homeostasis in *Abcd1*$^{-}$ mice spinal cord at 12 months of age. We therefore treated the X-ALD mice with CB_2 agonist and checked first mitochondrial DNA levels (**Fig. 11a**) and the biogenesis genes (**Fig. 11b)** in *Abcd1*$^{-}$mice after the treatment. The agonist normalized the mtDNA levels and promotes mitochondria biogenesis characterized by increased levels of target genes (*Pgc-1α, Nrf1* and *Tfam).*
We then sought to investigate the effects of agonist in preserving mitochondrial function in X-ALD mice. By using the high resolution respirometry (Oroboros) analysis in freshly sectioned spinal cord slices, we revealed that activation of CB_2 prevented the impaired mitochondria oxidative phosphorylation in *Abcd1*$^{-}$ mice (**Fig. 11c).** Previously, it has been reported by our laboratory that *Abcd1*$^{-}$ mice shows decreased levels of ATP (Galino et al., 2011) suggesting an energetic failure occurred during the pathology of the disease. Treatment with agonist normalized the ATP levels (**Fig. 11d)** to WT maintaining the energy homeostasis of *Abcd1*$^{-}$ mice.

In summary, activation of CB_2 restores the mitochondria copy number and functions, and prevented the energetic failure in *Abcd1*$^{-}$ mice spinal cord.

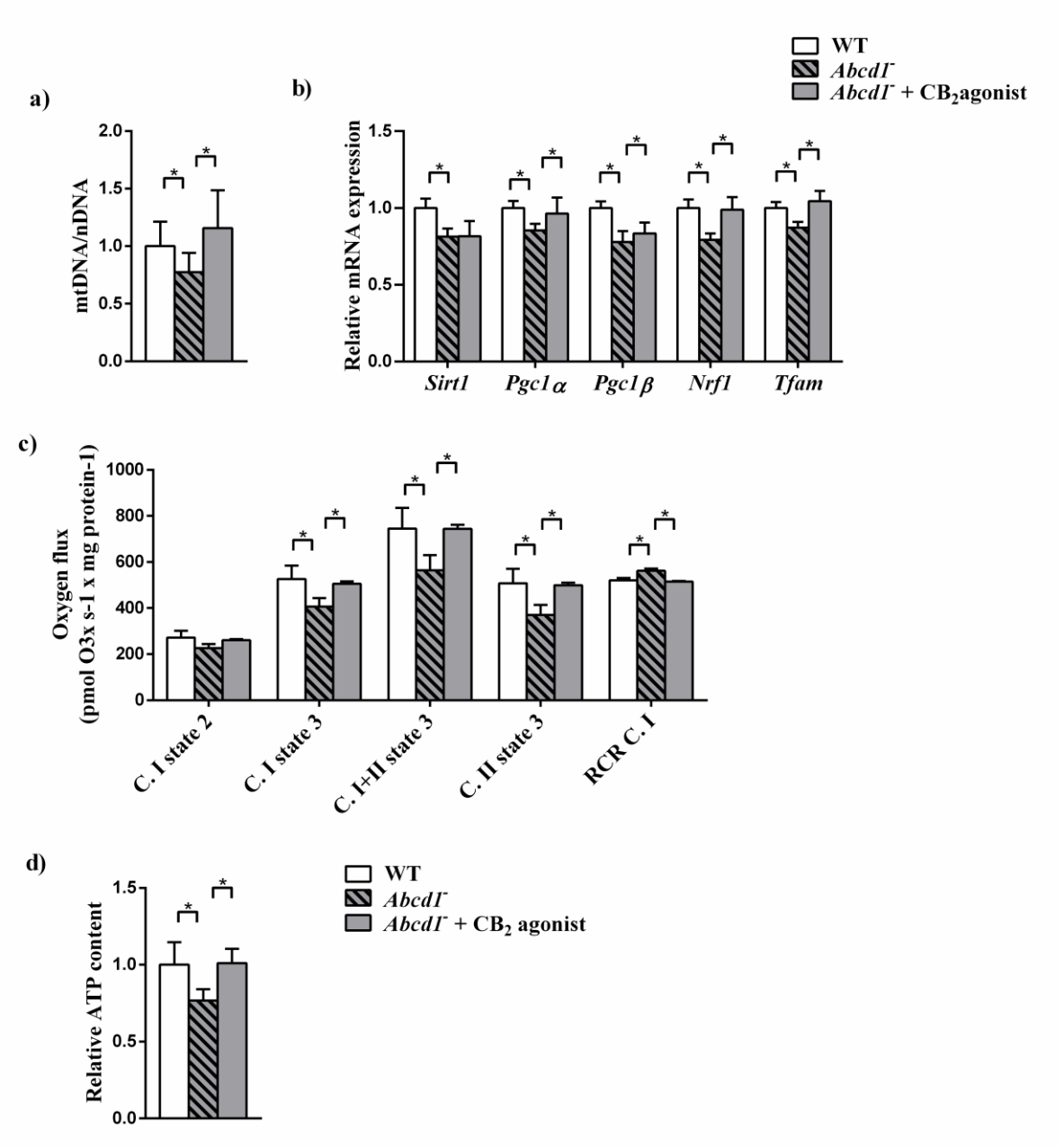

Figure 11. CB_2 activation by its specific agonist restores mitochondrial copy number and function as well as normalizes the ATP levels in X-ALD mouse spinal cord

(a) mtDNA levels in WT (n=8), *Abcd1*$^{-}$(n=8) and *Abcd1*$^{-}$ + CB_2 agonist (JWH133) (n=8) mice spinal cord at 12 months of age. mtDNA content was analyzed by quantitative RT-PCR and expressed as the ratio of mtDNA to nuclear DNA (*CytB* levels/ *Cebpα*levels). Data is shown as fold change respect to WT mice. **(b)** *Sirt1, Pgc-1α, Pgc1-β, Nrf1 and Tfam* mRNA levels were measured by quantitative RT-PCR in WT (n=8), *Abcd1*$^{-}$ + agonist (n=8) mice spinal cord at 12 months of age. Gene expression levels were normalized relative to *Rplp0*. Data is shown as fold change respect to WT mice. **(c)** *Ex vivo* mitochondrial respiration analysis performed on permeabilized sections of 12-months-old spinal cord from WT (n=5), *Abcd1*$^{-}$(n=5), *Abcd1*$^{-}$+ agonist (n=5) mice. (C.I = complex I. C.II = complex II). **(d)** ATP levels were quantified in 12-months-old spinal cord from WT (n=8), *Abcd1*$^{-}$ (n=6), and *Abcd1*$^{-}$+ agonist mice. Data is

shown as fold change respect to WT mice. Values are expressed as mean ± SD * p<0.05; ** p<0.01; *** p<0.001 after one-way ANOVA test followed by Tukey's post-hoc test.

4.2.5 CB_2 agonist treatment reverses locomotor deficits in X-ALD mice

We next examined the effects of CB_2 activation in axonopathy and associated locomotor deficits presented by X-ALD mice. We used double mutants mice *Abcd1*$^{-}$*/Abcd2*$^{-/-}$ as they exhibit more severe AMN like phenotype with earlier axonal degeneration at 12 months of age (Fourcade et al., 2008). Animal were challenged with two different behavior tests: Bar cross and Treadmill. We showed that DKO (*Abcd1*$^{-}$*/Abcd2*$^{-/-}$) mice at 15 months of age needed longer time to reach the other side of the bar and tend to slipped off more frequently while crossing the bar. In treadmill test, we observed an increase in time length of shocks and number of shocks in DKO mice compared to WT. Thus we wanted to know whether activation of CB_2 can modulate these locomotor deficits in DKO mice. For that we had given the CB_2 specific agonist to DKO mice at the age of 15 months intraperitoneally for one months and challenged with the different behavior tests at 16 months of age. After agonist treatment, DKO mice behaved normally similar to WT mice in both the task performed (**Fig. 12a & b)** indicating that the agonist treatment had stopped the progression of locomotor deficits in X-ALD mice. Very interestingly, the effect of drug persists even after two months without treatment when behavioral tests were performed again at 18 months of age (**Fig. 12c & d)**.

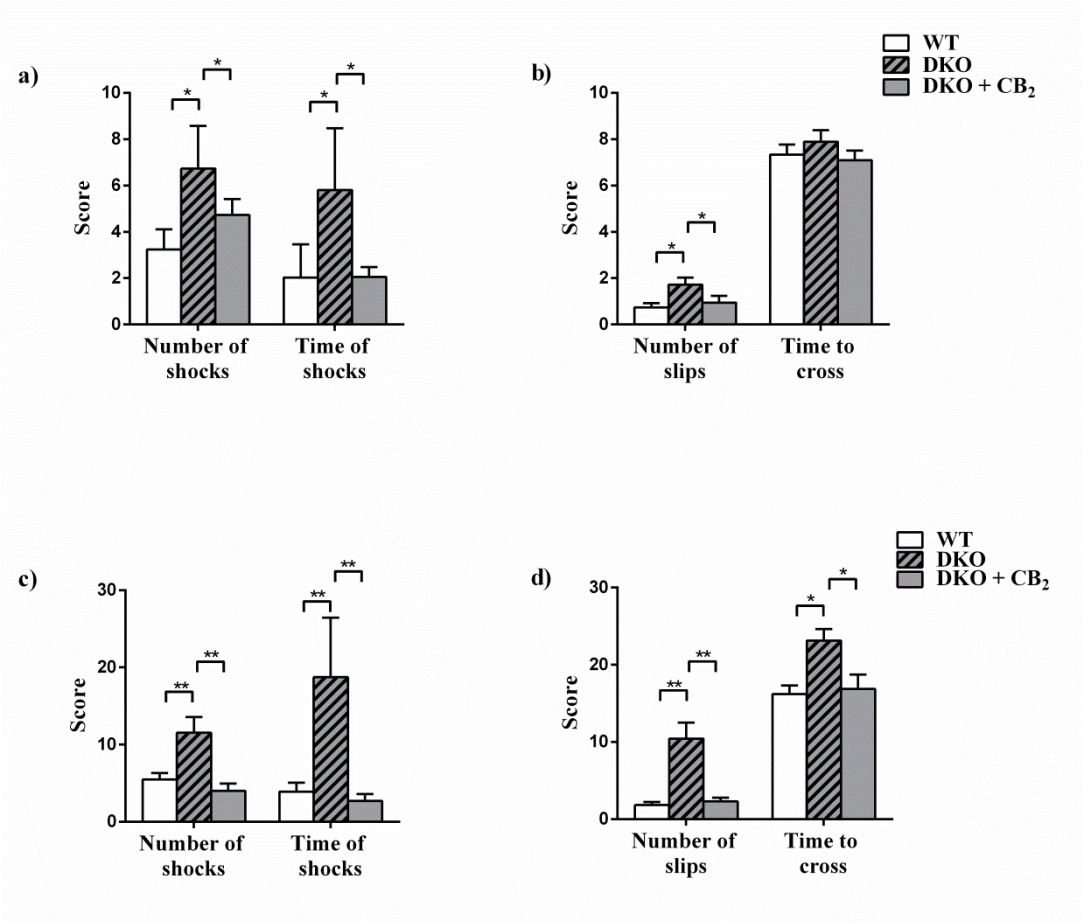

Figure 12. CB_2 activation reverses locomotor defecits in X-ALD mice

(a) Bar-cross and **(b)** treadmill tests performed on 16 months-old WT (n=14), *Abcd1⁻/Abcd2⁻/⁻* (DKO) (n=16) and *Abcd1⁻/Abcd2⁻/⁻* mice treated with CB_2 agonist (JWH133) (n= 14). **(c)** Bar-cross and **(d)** treadmill tests performed on 18 months-old WT (n=14), *Abcd1⁻/Abcd2⁻/⁻* (DKO) (n=16) and *Abcd1⁻/Abcd2⁻/⁻* mice treated with CB_2agonist (JWH133) (n= 14). The number of slips and time (seconds) spent to cross the bar were quantified in the bar cross test, as described in Methods. In the treadmill test, the latency to falling off the belt (timeofshocks) and then number of shocks received were computed after 7 min, as described in Methods. Values are expressed as mean ± SD * $p<0.05$; ** $p<0.01$; *** $p<0.001$ after one-way ANOVA test followed by Tukey's post-hoc test.

4.2.6 CB_2 agonist treatment prevents axonal degeneration in X-ALD mice

We finally assess the correlation of improved locomotor disability with axonal degeneration by checking the immune-histochemical signs of neuropathology in DKO mice. DKO mice at 18 months of age displays an overt neuropathological phenotype characterized by i) axonal damage seen by the accumulation of amyloid precursor protein (APP) and synaptophysin in axonal swellings; (ii) scattered myelin debris by Sudan Black staining ; (iii) astrocytosis and microgliosis by GFAP and Iba1 staining

respectively; (iv) reduced staining of SMI-32 in motor neurons indicating as unhealthy motor neurons. SMI-32 is an antibody that labels a non-phosphorylated epitope of neurofilament proteins and (v) decreased mitochondrial content observed by low staining of cytochome c (Cyt C) in motor neurons (Morato et al., 2013, Pujol et al., 2002).

CB_2 agonist treatment suppressed microgliosis but not the astrocytosis, prevented the accumulation of APP and synaptophysin in axons and induced the clearance of myelin debris along the spinal cord (**Fig. 13a-o**). Moreover CB_2 agonist normalized the mitochondrial content and improved the motor neuron health (**Fig. 13p-u)**.

Thus, these data reveal that CB_2 receptor activation prevents microglia activation and thus halts axonal degeneration in X-ALD mice.

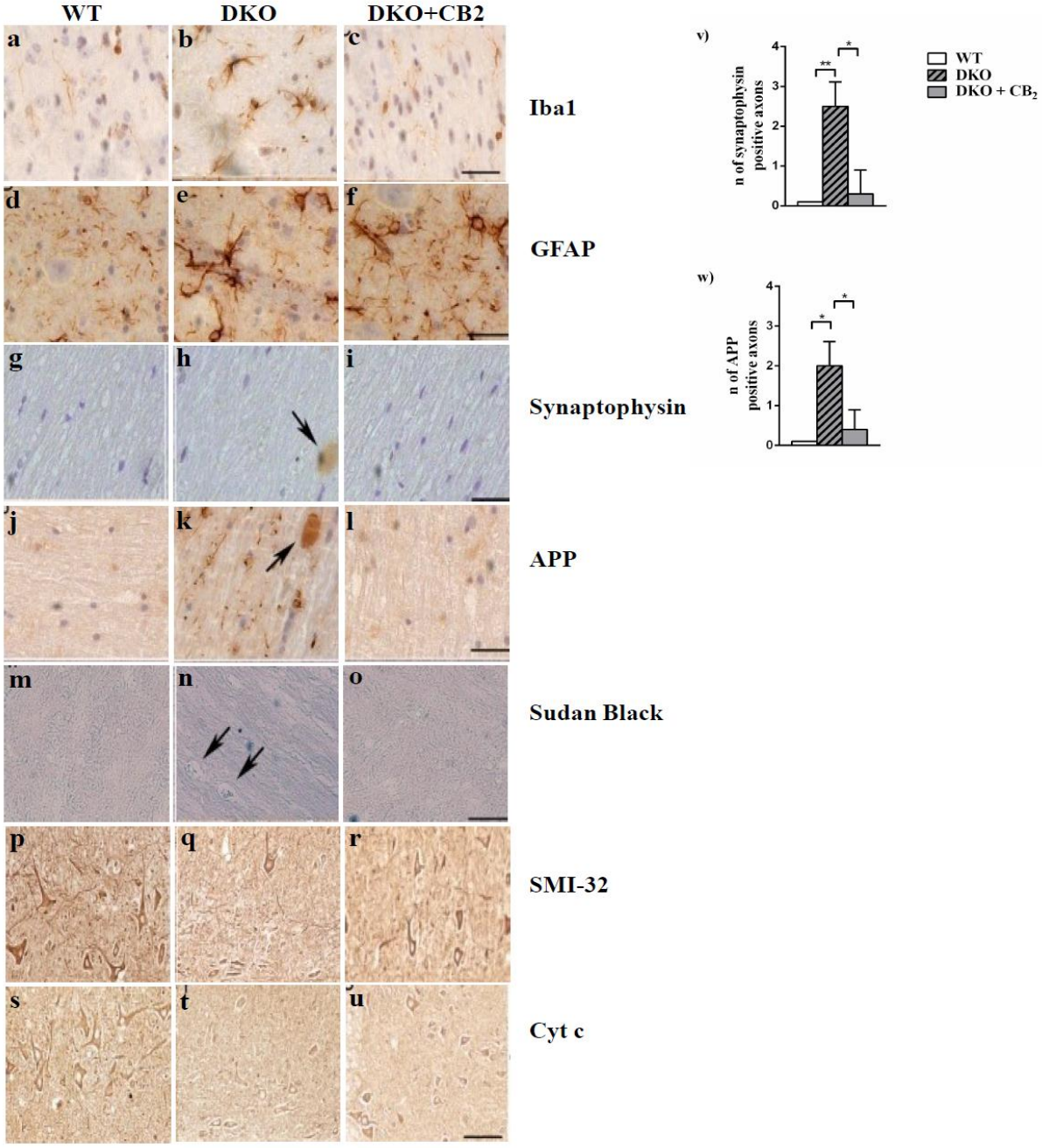

Figure 13. Activation of CB2 normalizes axonal degeneration in X-ALD mice

Immunohistological analysis of axonal pathologies performed in 18-months-old WT, *Abcd1⁻/Abcd2⁻/⁻*(DKO) and *Abcd1⁻/Abcd2⁻/⁻* mice treated with CB_2 agonist (JWH133) (n= 5 per genotype) **(a-u).** Spinal cord sections were processed for **(a-c)** Iba1, **(d-f)** GFAP, **(g-i)** Synaptophysin, **(j-l)** APP, **(m-o)** Sudan black, **(p-r)** SMI32 and **(s-u)** Cyt C immunostaining. Representative images for WT (**a, d, g, j, m, p, s**), *Abcd1⁻/Abcd2⁻/⁻* **(b, e, h, k, n, q, t),** *Abcd1⁻/Abcd2⁻/⁻*mice treated with CB_2agonist (JWH133) **(c, f, i, l, o, r, u)** are shown. Quantification of **(v)** synaptophysin and **(w)** APP accumulations in axons. Values are expressed as mean ± SD * $p<0.05$; ** $p<0.01$; *** $p<0.001$ after one-way ANOVA test followed by Tukey's post hoc test.

4.3 Chapter 3: Neuroprotective role of Methylene blue in mouse model of X-ALD

4.3.1 Methylene blue (MB) normalizes mitochondria function and bio-energetic failure in X-ALD mice

With the known knowledge of modulating mitochondria function by MB (Wen et al., 2011), we investigated the effect of MB on mitochondrial impairment displayed by our X-ALD mouse model (Lopez-Erauskin et al., 2013b, Morato et al., 2013). We found that MB increases the mitochondria DNA levels (**Fig. 14a**) and their target genes (*Sirt1*, *Pgc-1α, Nrf1 Tfam) (***Fig. 14b**) supporting the positive role of MB on mitochondria biogenesis. Moreover, we measured oxidative phosphorylation (OXPHOS) activity by high-resolution respirometry using Oroboros technology and ATP levels in X-ALD mice. MB treatment retrieves the respiratory control ratio as well as the oxygen consumption thereby recovered the energetic failure with normalized ATP levels (**Fig. 14c & d**).

Thus above findings illustrates that MB recovers all the observed mitochondrial defects in *Abcd1*$^{-}$ mice spinal cord.

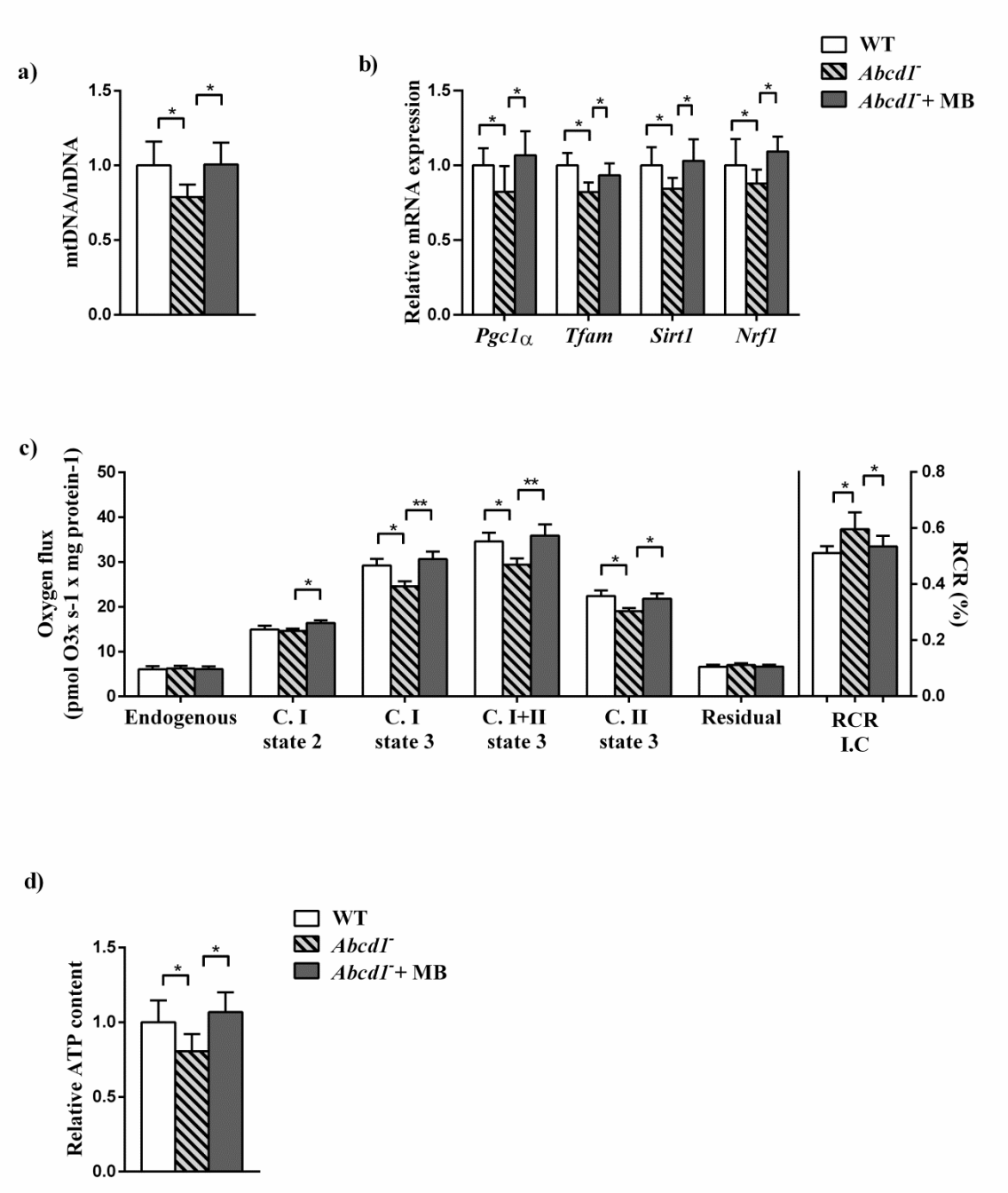

Figure 14. MB improves mitochondria function and prevents bio-energetic failure in X-ALD mice

(a) mtDNA levels in WT (n=8), *Abcd1*⁻(n=8) and *Abcd1*⁻+ MB (n=8) mice spinal cord at 12 months of age. mtDNA content was analyzed by quantitative RT-PCR and expressed as the ratio of mtDNA to nuclear DNA (*CytB* levels/ *Cebpα*levels). Data is shown as fold change respect to WT mice**. (b)** *Pgc-1α*, *Tfam*, *Sirt1*and *Nrf1* mRNA levels were measured by quantitative RT-PCR in WT (n=8), *Abcd1*⁻+ MB (n=8) mice spinal cord at 12 months of age. Gene expression levels were normalized relative to *Rplp0*. Data is shown as fold change respect to WT mice. **(c)** *Ex vivo* mitochondrial respiration analysis performed on permeabilized sections of 12-months-old spinal cord from WT (n=5), *Abcd1*⁻(n=5),*Abcd1*⁻+ MB (n=5) mice. (C.I = complex I. C.II = complex II). **(d)** ATP levels were quantified in 12-months-old spinal cord from WT (n=8), *Abcd1*⁻ (n=6), and *Abcd1*⁻+ MB (n=7) mice.

Data is shown as fold change respect to WT mice. Values are expressed as mean ± SD * $p<0.05$; ** $p<0.01$; *** $p<0.001$ after one-way ANOVA test followed by Tukey's post-hoc test.

4.3.2 Methylene blue prevents VLCFA forced ROS production and recovered oxidative stress induced mitochondria fission in X-ALD patient´s fibroblasts

Based on the antioxidant properties of MB and its ability to interact with electron transport chain (Rojas et al., 2012, Stack et al., 2014), we evaluated its effect on oxidative stress and altered mitochondria dynamics observed in X-ALD mice. Recently we have demonstrated that X-ALD fibroblasts shows an activation of Drp1 characterized by increased levels of activated form of *Drp1* (pS616) which further mediates mitochondrial fragmentation (Patrizia thesis: Impairment of mitochondrial dynamics in X-linked adrenoleukodystrophy). Therefore we first treated the control and X-ALD fibroblasts with MB upon C26:0 treatment and measured the ROS levels followed by mitochondria network and then the localization of *Drp1*. MB completely abolished the increased ROS levels with C26:0 in both control and X-ALD fibroblasts (**Fig. 15a**). Moreover it prevented the C26:0 induced recruitment of *Drp1* to mitochondria thus arrested the mitochondrial fission (**Fig. 15b & c**).

These above data finally reveal that MB attenuates the C26:0 driven ROS production and inhibit the mitochondrial fission there by restoring the mitochondria network integrity in X-ALD fibroblasts.

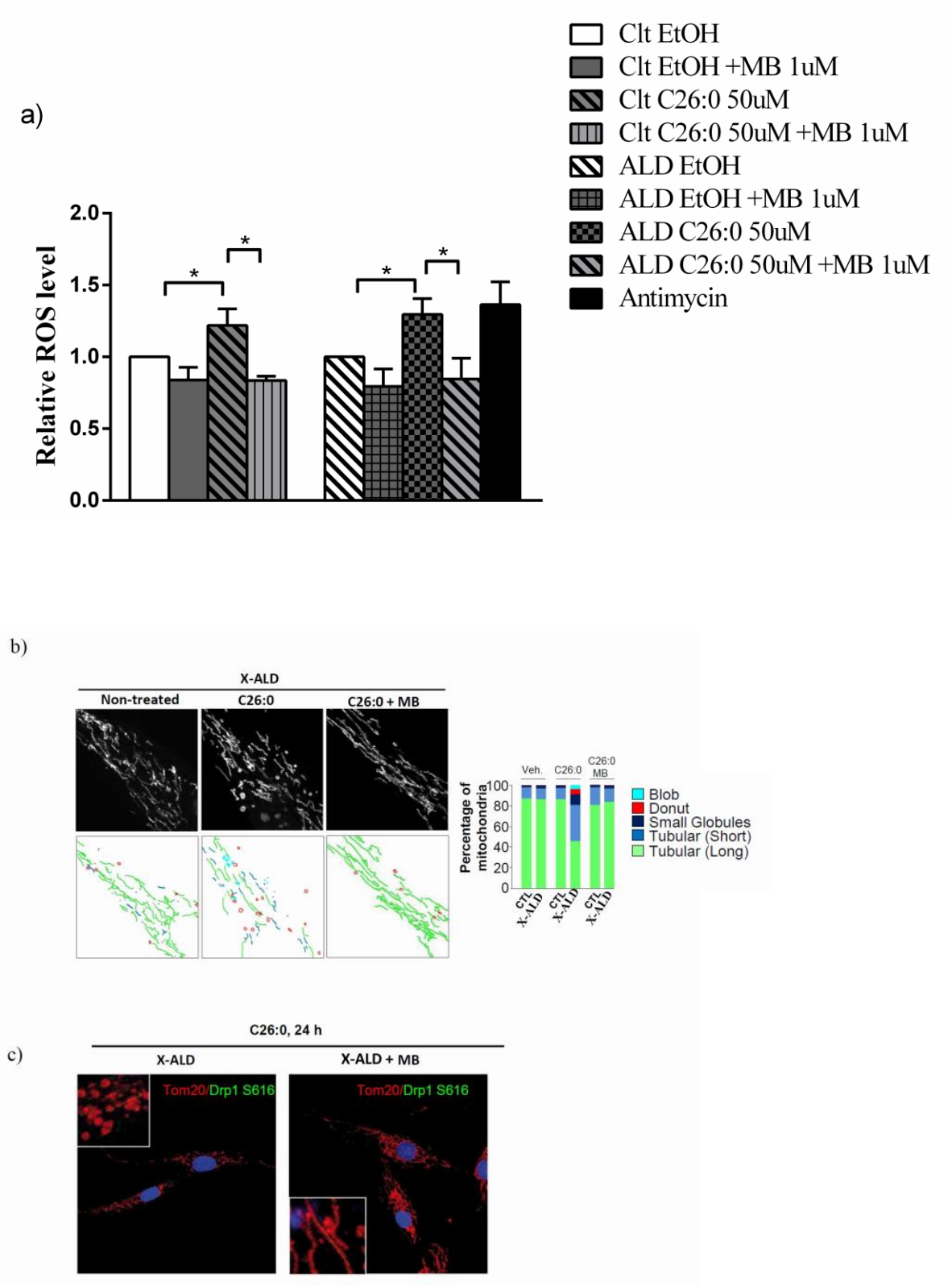

Figure 15. MB prevents ROS production and mitochondria fission in X-ALD patient´s fibroblasts

(a) ROS levels were measured after treatment with MB (1 uM) in Clt (n=3 per condition) and X-ALD (n=4 per condition) patient fibroblasts upon C26:0 for 24 h. Quantification is depicted as fold change to vehicle-treated (EtOH) fibroblasts. **(b)** Representative confocal images of co-immunofluorescence against

TOM20 (red) in human X-ALD patient fibroblasts upon C26:0 with and without MB treatment. Scale bar = 10 µm. **(c)** Fluorescence intensity of DRP1 puncta over the mitochondria were quantified in X-ALD patient fibroblasts. At least 15 cells per condition and genotype were analyzed. Quantification is depicted as fold change to vehicle-treated (EtOH) fibroblasts. Values are expressed as mean ± SD. Statistical analysis were done by ANOVA test followed by Tukey post hoc, * p<0.05; ** p<0.01; *** p<0.001).

4.3.3 Methylene blue prevents oxidative stress and mitochondria fission in X-ALD mice spinal cord

To corroborate the *in-vitro* studies of mitochondrial fission in *Abcd1*⁻ mice spinal cord, we measured the levels of DRP1 and oxidative stressmarkers like direct carbonylation of proteins (AASA), glycoxidation (CEL), lipoxidation (CML) and protein lipoxidation (MDAL) previously reported in our mouse model (Fourcade et al., 2008). We revealed normalization of all the oxidative damage markers (**Fig. 16a**) after the treatment of MB. Besides, treatment reduced the activated DRP1 (pS616) levels in *Abcd1*⁻ mice spinal cord correlating the *in-vitro* results seen in X-ALD patient´s fibroblasts (**Fig. 16b).**

In brief, MB prevents oxidative stress and reduced the DRP1 levels thus preventing the mitochondrial fission in X-ALD mice.

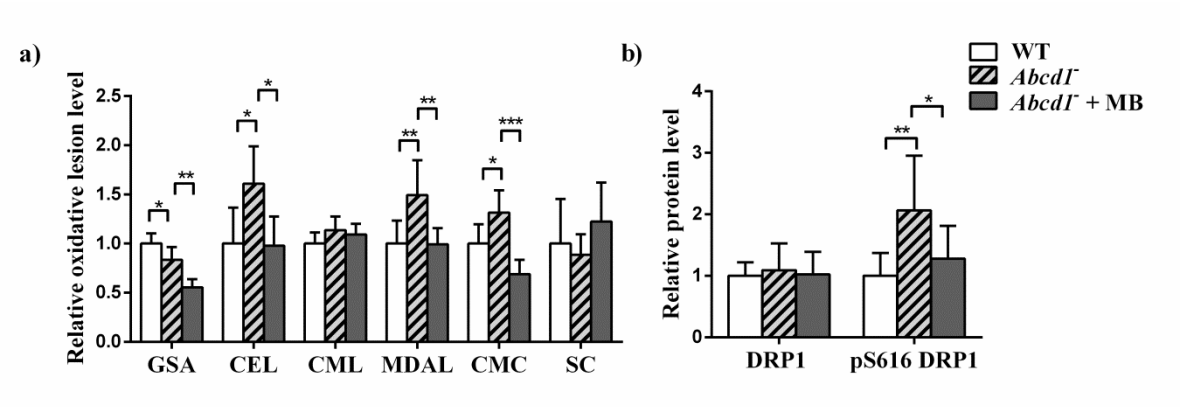

Figure 16. MB prevents oxidative stress and mitochondria fission in X-ALD mice spinal cord

(a) Oxidative lesion levels-GSA, CEL, CML, MDAL, CMC & SC in 12months old WT (N=5), *Abcd1*⁻ (n=6) and *Abcd1*⁻+ MB (n=4) spinal cord**. (b)** DRP1 total and pS616 protein levels were measured in WT (N=7), *Abcd1*⁻(n=7) and *Abcd1*⁻+ MB (n=5) spinal cord at 12months of age. Protein levels were normalized relative to γ-tubulin or non-phosphorylated protein and represented as fold change relative WT**.**Values are expressed as mean ± SD. Statistical analysis were done by ANOVA test followed by Tukey post hoc, * p<0.05; ** p<0.01; *** p<0.001).

4.3.4 Methylene bue treatment controls the inflammation in X-ALD mice

We next examined the effect of MB on inflammatory imbalance observed in *Abcd1*$^{-}$ mice spinal cord at 12 months of age as we have mentioned in brief before. MB treatment retrieved the inflammatory pattern by normalizing almost all the observed alterations in expression of genes like *Cox2*, *iNOS*, *Tnfα, Il1β, Ccl5, Ccl2, and Cxcl10* (**Fig. 17a & b**). However no effect was observed in expression of *Il6* and *Ccr1*. Besides, we found a further elevation of anti-inflammatory genes like *Chil3* and *Cxc12* (**Fig. 17c)**.

Thus, these data revealed that MB prevented the inflammatory imbalance in X-ALD mice.

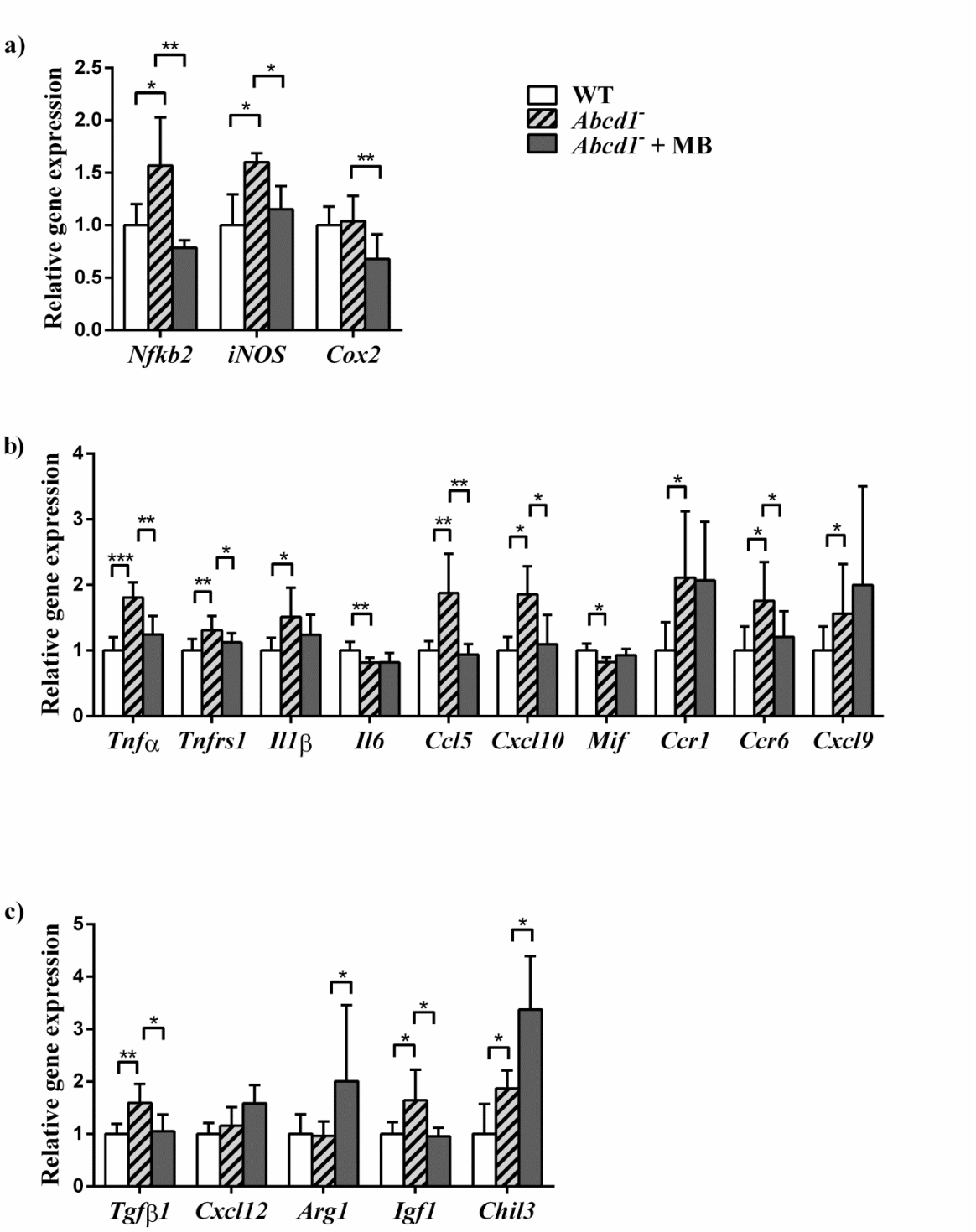

Figure 17. MB treatment halts the inflammation in X-ALD mice

Inflammatory profile in WT (n=8), *Abcd1*$^{-}$(n=8) and*Abcd1*$^{-}$ + MB (n=8) mice spinal cord at 12 months of age. **(a)** Inflammatory mediators (*Nfkb2, iNOS* and *Cox2*) **(b)** pro-inflammatory cytokines & chemokines (, *Tnfα,Tnfrs1, Il1β, Il6, Ccl5,Cxcl10, Mif, Ccr1, Ccr6* and *Cxcl9*) and **(c)** anti-inflammatory markers (*Tgfβ1, Cxcl12, Arg1, Igf1* and *Chil3*)were measured by quantitative RT-PCR. Gene expression levels were normalized relative to *Rplp0*. Data is represented as fold change respect to WT mice. Values are

expressed as mean ± SD * p<0.05; ** p<0.01; *** p<0.001 after one-way ANOVA test followed by Tukey's post-hoc test.

4.3.5 Methylene blue halts axonal degeneration and normalized locomotor deficits in X-ALD mice

Finally we assessed the effect of MB in axonopathy and locomotor disability exhibited in X-ALD mice. We assessed the histochemical signs of neuropathology in DKO mice characterized by microgliosis and astrocytosis, accumulation of APP and synaptophysin, scattered myelin debris, low staining of SMI-32 & cytochome C and increased staining of MDA. MB treatment efficiently suppressed the activation of microglia and astrocytes **(Fig. 17a-f)**. The mice after the treatment present healthy neurons by higher staining of SMI-32, reduced signs of lipoxidation and the normalized mitochondria content (**Fig. 17g-o**). Moreover, accumulations of APP, synaptophysisn and myelin debris were cleared after the treatment, thus preventing axonal degeneration (**Fig. 17p-x)**. We performed the two behavioural tests: Bar-cross and treadmill as described in detail above. In bar cross test, after the MB treatment the DKO (*Abcd1*$^{-}$*/Abcd2*$^{-/-}$) mice tend to slip less and took less time to cross the bar. Also DKO mice improved the performance in treadmill test up to the level of WT (**Fig. 18a´ & b´**). Thus overall, these above results indicate that Methylene blue treatment halted axonal degeneration and the progression of locomotor deficits in *Abcd1*$^{-}$*/Abcd2*$^{-/-}$ mice.

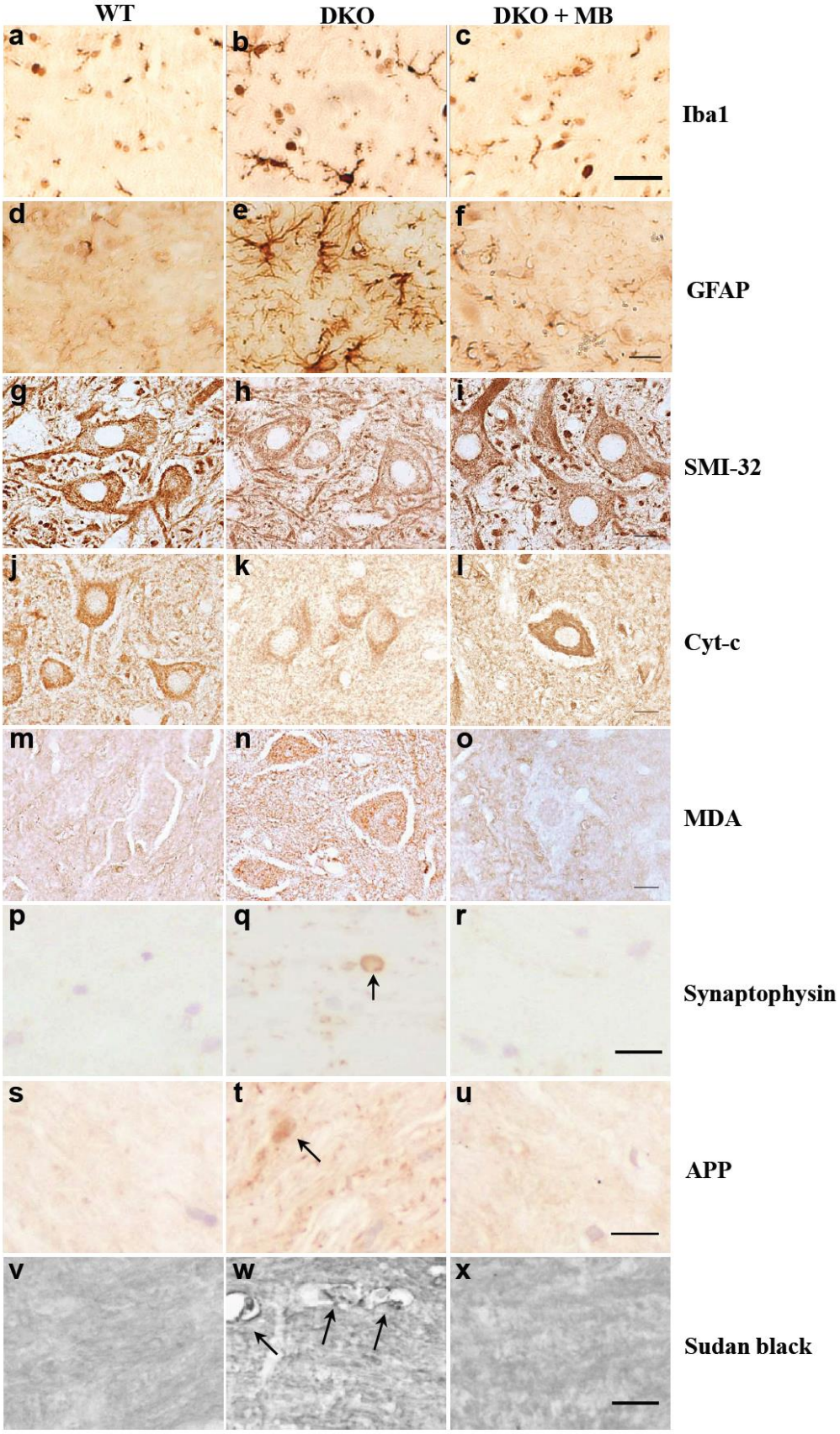
WT
DKO
DKO + MB
a
b
c
Iba1
d
e
f
GFAP
g
h
i
SMI-32
j
k
l
Cyt-c
m
n
o
MDA
p
q
r
Synaptophysin
s
t
u
APP
v
w
x
Sudan black

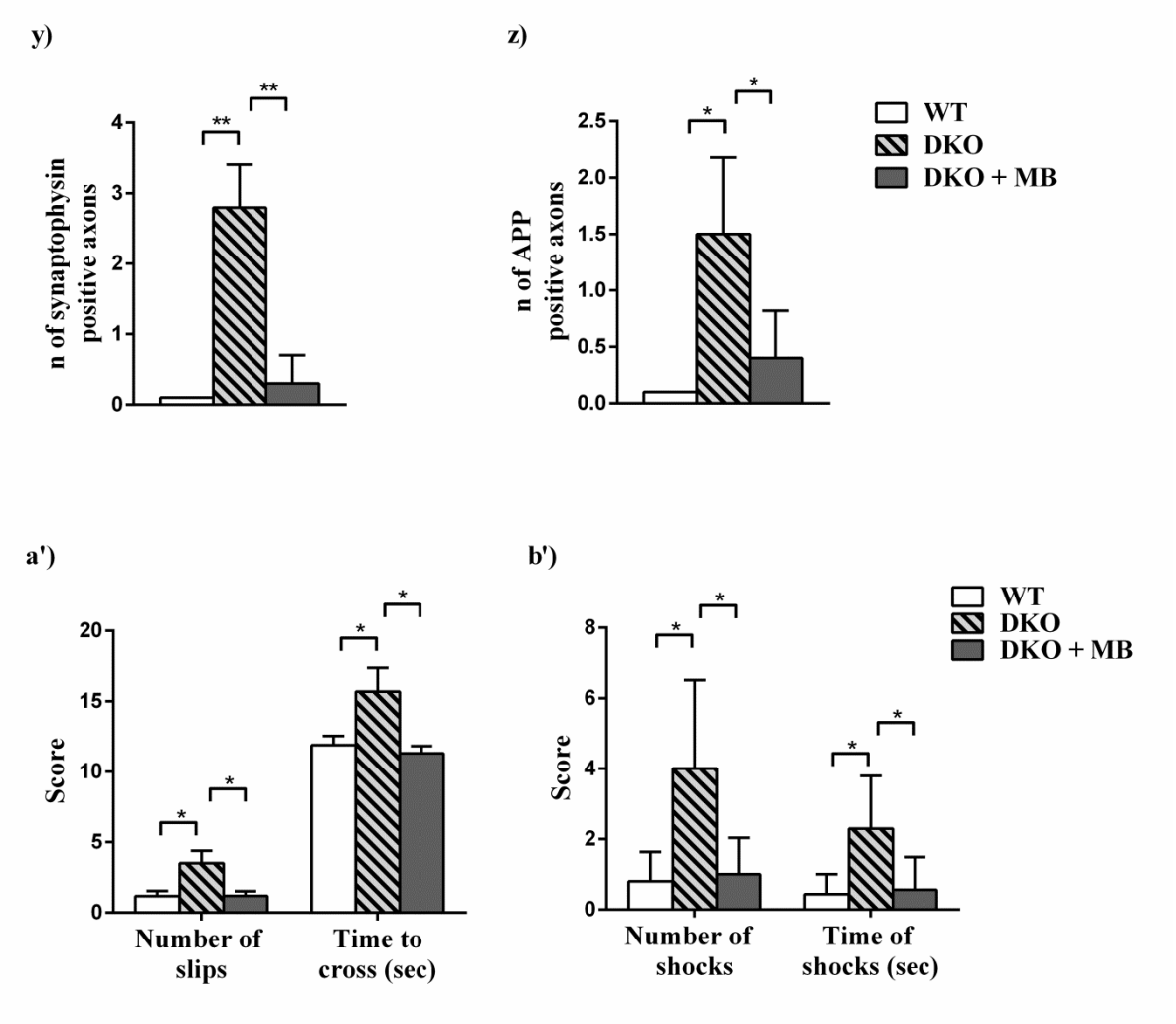

Figure 18. MB normalized locomotor deficits and halts axonal degeneration in X-ALD mice

Immunohistological analysis of axonal pathologies performed in 18-months-old WT, *Abcd1⁻/Abcd2⁻/⁻*(DKO) and *Abcd1⁻/Abcd2⁻/⁻* mice treated with MB (n= 5 per genotype) (a-u). Spinal cord sections were processed for (**a-c**) Iba1, (**d-f**) GFAP, (**g-i**) SMI32, (**j-l**) Cyt c, (**m-o**) MDA, (**p-r**) Synaptophysin, (**s-u**) APP and (**v-x)** Sudan black immunostaining. Representative images for WT (**a, d, g, j, m, p, s, v**), *Abcd1⁻/Abcd2⁻/⁻* (**b, e, h, k, n, q, t, w**), *Abcd1⁻/Abcd2⁻/⁻* mice treated with MB (**c, f, i, l, o, r, u, x**) are shown. Scale bars = 25 µm (a-t) and 125 µM (u-f).Quantification of (**y**) synaptophysin and (**z)** APP accumulations in axons. **(a')** Bar-cross and **(b')** treadmill tests were performed on 21-months-old WT (n=14), *Abcd1⁻/Abcd2⁻/⁻* (DKO) (n=16) and *Abcd1⁻/Abcd2⁻/⁻*mice treated with MB (n= 14). The number of slips and time (seconds) spent to cross the bar were quantified in the bar cross test, as described in Methods. In the treadmill test, the latency to falling off the belt (timeofshocks) and then number of shocks received were computed after 7 min, as described in Methods. Data represent mean ± SD.Statistical analysis were carried by ANOVA test followed by Tukey post hoc, * $p<0.05$; ** $p<0.01$; *** $p<0.001$).

DISCUSSION

5.0 Discussion

Chapter I

Neuroinflammation is a prominent feature shared by many neurodegenerative diseases including PD, AD and ALS (Glass et al., 2010, Minghetti, 2005). The principal component of neuroinflammation in CNS is microglia activation which provides the first line of defense when the disease occurs (Glass et al., 2010). Due to the heterogeneous nature of microglia within the CNS milieu, it displays diverse functional phenotypes ranging from pro-inflammatory M1 to anti- inflammatory M2 (Colton, 2009). The depicted M1/M2 paradigm under neuropathological conditions shed the light on the research of microglia activation states in CNS. The imbalance between these phenotypes or prolonged toxic M1 inflammatory responses often leads to degeneration of neurons. Here we analyzed the two inflammatory profile in X-ALD mouse model by meausring the markers and cytokines responsible of causing these phenotypes. A mixed inflammatory profile characterized by elevated levels of both neurotoxic (M1) and neuroprotective factors (M2) was found in X-ALD mice spinal cord. These results agree with previous studies from our laboratory showing induction of both anti and pro-inflammatory cytokines in AMN patients, thus counterbalance the sustained pro-inflammatory environment ocuuring in the CNS.

Microglia were thought to be the major contributor in the pathogenesis of X-ALD supported by the piece of evidence from (Aubourg et al., 1990, Cartier and Aubourg, 2010) showing the arrest of demyelination in ccALD patients using hematopoietic stem cell therapy. Moreover, prolonged activation of microglia and astrocytes together with axonal degeneration has been main one of the main clinical signs exerted by X-ALD mice. These sustained gliosis with inflammatory responses is not limited to X-ALD, also being reported by other neurodegenerative diseases including FTD, HD and ALS (Brettschneider et al., 2012, Cagnin et al., 2004, Singhrao et al., 1999). In addition, a low grade inflammatory responses was found in AMN patients with the induction of both pro and anti-inflammatory genes (Ruiz et al., 2015). Furthermore, VLCFA triggers inflammatory response mainly by abnormal activation of microglia and apoptosis in mice injected with C24:0-LPC (Eichler et al., 2008).

It is tempting to speculate whether these observed inflammatory environment in spinal cord was dominated either by astrocytes or microglia, we took the advantage of primary microglia and astrocyte cultures from WT and *Abcd1*$^{-}$ mice and performed different studies in the presence and absence of C26:0, the main VLCFA accumulated in X-ALD patients. As most of the *in-vitro* studies related in X-ALD had been made with X-ALD patient´s fibroblasts or *Abcd1*$^{-}$ astrocytes or oligodentrocytes (Fourcade et al., 2014, Hein et al., 2008, Kruska et al., 2015). Here for the first time we addressed the role of VLCFA using *in-vitro* approaches in *Abcd1*$^{-}$ microglia. Our studies report elevated ROS levels and inflammatory imbalance when both WT and *Abcd1*$^{-}$ primary microglia were insulted with exogenous C26:0. Moreover, C26:0 was able to induce cytotoxic mediators like *iNOS* and *Cox2* associated with elevated levels of pro-inflammatory cytokines and chemokines like *Tnfα, Ccl2, Il1α* and *Cxcl10* and also growth factors and anti-inflammatory markers like *Igf1, Tgfb1, Arg1, Csf1* and *Mif* in primary microglia. Indeed, *Il10* an very important anti-inflammatory cytokine and its receptor *Il10ra* were found to be decreased after the C26:0 treatment, indicating noxious effect of C26:0 driven cytotoxic environment. It is worth to note that microglia from *Abcd1*$^{-}$ mice presents a mild inflammation mediated by up-regulation of *Tnfα, Il1β, Ccl5, Cxcl0, Cxcl9* and *Arg1* and was more sensitive to C26:0 insult for some mediators like *iNOS* and *Cox2* supporting with the previous findings showing a direct link of inflammation and VLCFA accumulation in astrocytes (Singh et al., 2009). In addition, a very recent study had shown correlation between inflammation and VLCFA (Marchetti et al., 2017) and therefore measuring C26:0 levels in *Abcd1*$^{-}$ microglia cultures would be highly beneficial to correlate the observed inflammation at baseline with VLCFA accumulation. Thus to our knowledge the results disclosed here is the first evidence that primary microglia from WT & *Abcd1*$^{-}$ mice showed a mixed inflammatory profile upon exogenous C26:0 insult characterized by elevated levels of both neurotoxic (M1) and neuroprotective factors (M2) that differs from LPS activated microglia which shows predominated M1 profile with low M2 gene induction. Thus WT & *Abcd1*$^{-}$ mice microglia insulted with C26:0 represent a double edge sword (Chiu et al., 2013).

Of note as already indicated in our previous study that mitochondria were the major source of ROS production in X-ALD patient´s fibroblasts after loaded with C26:0 (Lopez-Erauskin et al., 2013b). Here we further explore the findings by analyzing the source of ROS after C26:0 insult in primary microglia cultures. We found that

application of C26:0 at supra-physiological concentrations caused elevated mitochondrial ROS after the chonic exposure to WT and *Abcd1*$^{-}$ mice microglia. Moreover, we were interested to know whether the VLCFA induced inflammation and oxidative stress was cell specific, we applied the same strategy to astrocytes. Apparently, elevated inflammation and ROS levels were observed in both the genotype after C26:0 insult. An exceptional difference in some M1 markers like *iNOS, Cd86* and *Cox2* induced by C26:0 was found only in case of *Abcd1*$^{-}$ mice microglia. However, there was a lack of differences in both genotypes in ROS levels. A contradictory study had shown that *Abcd1*$^{-}$ astrocytes respond more sensitively than WT when treated with different VLCFA (Kruska et al., 2015). However, we should take into consideration that culture and experimental conditions were different in both cases. Although no baseline difference was observed by both laboratories. Thus, these above studies suggest that primary microglia could be an *in-vitro* model as it is mimicking the X-ALD spinal cord inflammatory environment to study the deep molecular mechanisms underlying the physio-pathogenesis of X-ALD and further for drug testing analysis.

Chapter II

There is a general agreement about the important role of endogenous cannabinoids and their receptors against the inflammatory events occurred in neurodegenerative diseases and the possible strategies to manipulate their function pharmacologically or genetically. With this regard, thee main strategies have been studied to modulate their functions that could exert protective effects in these disorders: 1) increasing the levels of endocannabinoids by using 2-AG or AEA hydrolysis inhibitors, 2) the administration of exogenous endocannabinoids or synthetic cannabinoids, 3) Pharmacological or genetic modulation of CB receptors. As the X-ALD mouse model shows axonal degeneration associated with microgliosis and neuroinflammation. With the given knowledge of endocannabinoid system as a therapeutic target, current study shows that in contrast to CB1 receptor, CB2 receptors were induced in X-ALD mice and administration of CB_2 specific agonist prevents microgliosis but not astrocytosis and thus halts axonal degeneration indicating the vital role of microglia activation as a therapeutic target in the patho-physiology of X-ALD. Indeed, we showed an impaired endocannabinoid system in X-ALD mice spinal cord and in primary mice microglia.

Microglia activation is considered to be one of the major contributors for neuroinflammation and has been implicated in the pathogenesis of many neurodegenerative diseases. Many evidences have been proved that activation of microglia is neurotoxic while others have shown that actually inflammation is beneficial under some circumstances for stimulating myelin repair, removing debris and cytotoxic aggregated proteins to stop the further injury of healthy neurons (Glezer et al., 2006). From the known information of other neurodegenerative disorders that one possibility underlying the neuroprotective effects obtained by activation of CB_2 receptor could be the reduction of pro-inflammatory mediators generated by the environment of gliosis and that destroy the neuronal homeostasis. Activation of CB_2 receptor shown to dampens the neurotoxic factors like *iNOS*, *Tnfα*, and *Il1β* (Oh et al., 2010) in many neurological disorders including PD (Gomez-Galvez et al., 2016), HD (Bouchard et al., 2012). However, reduced microglia activation with associated neurodegeneration after CB2 activation were observed in X-ALD mice which were in agreement with reduced neutric plaques in AD brains and reduced neurodegeneration by regulating microglia activation by CB_2 receptor in AD and PD (Marques et al., 2012, Palazuelos et al., 2009). The described up-regulation of CB_2 receptor in X-ALD mouse model is also evident in many neurodegenerative disease models and patients suggesting an endogenous protective response.

Moreover, a study has indicated that the mice lacking CB_2 receptor were much more vulnerable to LPS insult together with loss of nigral TH neurons (Garcia et al., 2011). Also the genetic deletion CB_2 receptor in R6/2 mouse model of HD exacerbates disease progression and is more sensitive to striatal neurodegeneration after excitotoxicity and presents a more severe glial activation pattern supporting the pharmacological possibilities of activation of these receptors (Palazuelos et al., 2009). Here we analyzed the dysregulated inflammatory profile observed in our mouse model after the agonist treatment. Activation of CB_2 receptor prevents pro-inflammatory response in *Abcd1*$^{-}$ mice spinal cord and also in primary *Abcd1*$^{-}$ mice microglia after exogenous C26:0 treatment by controlling the release of pro-inflammatory cytokines and chemokines. These findings support the earlier observations that modulation of CB_2 signalling prevents neuroinflammation and thus might be an important target of further preclinical investigation. Although these studies lack to validate the protective effect of CB_2 agonist on inflammation was due to involvement of CB_2 receptor. We therefore posit to

exploit its role in ROS production induced by C26:0 in primary microglia using CB_2 antagonist and agonist. Activation of CB_2 receptor in *Abcd1*$^{-}$ microglia primary cultures completely abolished the C26:0 induced ROS production. However these inhibitory effects were not clearly observed when cells were treated with both agonist and antagonist suggesting a partial involvement of CB_2 receptor in maintaining the redox homeostasis. Similar findings have shown that inhibitory effect of WIN55, 212-2, a non selective cannabinoid agonist on Tnfα production from LPS stimulated microglia is not altered by CB_2 or CB_1 receptor antagonists (Facchinetti et al., 2003). Moreover, WIN55, 212-2 inhibited the iNOS and NO production and prevent the release of chemokines like *Ccl2, Cxcl10, Ccl5* and *Tnfα* from *Il1β* activated human fetal astrocytes whereas these effects were partially blocked by CB_1 and CB_2 specific antagonist which suggests the involvement of both receptors (Sheng et al., 2005).

One of the striking findings in this study was the protective role of CB_2 receptor on mitochondrial function in X-ALD mice. Very few indirect studies have been conducted relating CB_2 receptor with mitochondria function. For instance, Latini and her colleagues proved that activation of CB_2 receptor by specific agonist delayed rubrospinal mitochondrial dependent neurodegeneration by reducing cytochome C release (Latini et al., 2014). Similarly, another study had shown that activation of CB_2 receptor inhibit the loss of mitochondrial membrane potential and prevents the release of cytochome c to cytosol and thus promoting anti-apoptotic effect in ischemic rat (Li et al., 2013). However, studies relating CB_2 receptor with mitochondrial biogenesis and its function via OXPHOS system were limited which made us to check whether its activation could exerts any protective effect on mitochondrial impairment observed in our mouse model. Interestingly, we found that activation of CB_2 receptor by specific agonist induces mitochondrial biogenesis characterized by upregulation of mitochondria target genes like *Tfam, Pgc1α* and *Nrf1*, mitochondrial respiration by regulating the OXPHOS system and finally preventing the energy depletion. These positive results from *in-vitro* studies from microglia abolishing mitochondria ROS via CB_2 and from *in-vivo* data from spinal cord made us to give a plausible hypothesis, that these positive effects could be due to the presence of mitochondrial CB_2 receptors which were activated by its specific agonist. These hypothesis may have an agreement with the studies showing the presence of CB_1 receptors in mitochondria. Moreover, activation of

mtCB1 receptors showed to induce protective effects on neurons and mitochondria functions (Ma et al., 2015).

Increasing evidence underscore the significance of endocannbinoid system in most of the physiological and pathological perturbances of the cell steady state facilitated by the fact that endocannabinoids as local mediators can be synthesized and released on demand and activate their targets when and where needed, thus playing an important role in maintaining the cell homeostasis. Apparently, endocannabinoid levels fluctuate in many inflammatory conditions notably brain injury, cerebral ischemia, Huntington disease, Multiple sclerosis as an adaptive response aimed at restoring the homeostasis or as maladaptive response contributing to the symptoms or progress of the disease. Thus we sought to investigate whether X-ALD mice shows any dysregulation in ECS. Decreased levels of PEA, POEA and SEA were found in *Abcd1*$^{-}$ mice spinal cord at 12 months with elevated mRNA levels of synthesizing and degrading enzymes like *Daglα, Daglβ* and *Mgll* respectively. Of note, no differences were observed in AEA and 2-AG levels, the most two important and studied endocannabinoid. Therefore, it is likely that there is a generic balance between the synthesis and degradation of these enzymes that could leads to slight alteration in the physiological levels of endocannabinoids with increased CB_2 levels suggesting these changes could be an endogenous adaptive response towards the disease progression. Thus, as described above pharmacological or genetic manipulation of ECS exert beneficial effects on neurodegenerative animal models indicating ECS as a useful therapeutic target in many neurological disorders.

In conclusion, our data provides the compelling evidence that VLCFA mediates toxicity in both WT and *Abcd1*$^{-}$ primary microglia associated with induced mitochondrial ROS production and inflammation. Moreover, we showed that *Abcd1*$^{-}$ primary microglia exerts a mild inflammation at baseline like in X-ALD mice spinal cord and do not display a significant bias toward either M1 or M2 phenotypes rather shows a mixed inflammatory profile in primary microglia characterized by elevated levels of both neurotoxic (M1) and neuroprotective factors (M2) after the C26:0 insult representing as a double edge sword. Finally, CB_2 cannabinoid agonist JWH133 is able to ameliorate the behavior deficits and halts axonal degeneration in experimental mouse model of X-ALD by preventing the activation of microglia, reducing the inflammation and promoting the mitochondrial biogenesis and function. These findings emphasize the

hypothesis that the activation of CB_2 receptor halts the disease mainly by blocking the overt activation of microglia and not astrocytes, suggesting a non-cell autonomous mechanism via microglia behind the disease progression in X-ALD. As CB_2 are mainly expressed in microglia in CNS under physiological conditions and can be induced under external insult or injury. Therefore, aiming microglia activity via CB_2 receptor could be considered as a novel therapeutic strategy against X-ALD pathogenesis.

Chapter III

Neurodegenerative diseases are heterogeneous group of disorders mainly characterized by selective loss of neuronal system that includes AD, PD, Multiple sclerosis, HD and ALS. Despite of its heterogeneity existence, the involvement of mitochondria is likely to be an important common theme in these diseases. Mitochondria are crucial regulators of cell death and survival and have found to interact with many proteins implicated with genetic forms of these neuronal disorders. Mitochondria contain multiple electron carriers capable of producing ROS, as well as an extensive network of antioxidant defenses. Different insults, including oxidative damage itself, can cause an imbalance between ROS production and removal, resulting in net ROS production. Thus, oxidative stress and mitochondria dysfunction are cross-linked and considered to be the primary contributing factors of pathology in many neurodegenerative diseases. Previously we had reported mitochondria as the primary source of ROS at least in human X-ALD fibroblasts (Lopez-Erauskin et al., 2013b) and the impaired mitochondria respiration and biogenesis underlies the axonal degeneration in X-ALD mice spinal cord (Morato et al., 2015). Moreover, an altered *Nrf2* antioxidant pathway was noticed in X-ALD mice spinal cord and in human X-ALD patient fibroblast upon different insults. Thus, boosting the endogenous antioxidant or anti-inflammatory system could be an effective approach to deal with the pathogenesis of X-ALD (Pablo thesis: NRF2 and RIP140 as new therapeutic targets for X-ALD: Control of redox/metabolic homesotasis and inflammation).

With the accumulating reports about the neuroprotective effects of MB and its ability to readily cross the blood brain barrier (BBB), in the present study we evaluated its effect on all the altered parameters observed in X-ALD mice. Methylene blue has known for

its redox chemistry and exerts numerous hormetic effects in which lower or intermediate doses are usually beneficial. The capability of MB as an electron carrier has been long recognized. MB directly accepts the electron from NADH, NADPH, and $FADH_2$ and is able to mediate the transfer of electron from certain enzymes to cytochome c thus provides an alternative electron transport route and induces the mitochondria oxidative phoshorylation. Furthermore, these unique redox property of MB not only increases mitochondria respiration also attenuates superoxides and ROS production under complex I & III inhibited conditions (Atamna and Kumar, 2010, Wen et al., 2011). Here we demonstrated that MB up-regulates the mitochondria target genes like *Pgc1-α, Tfam,* and *Nrf1* and thereby normalizes the mitochondria copy number in X-ALD mice spinal cord. Besides, treatment also increases mitochondrial respiration and restores ATP level which were supported with the existing findings showing MB induced mitochondria biogenesis via *Pgc1-α* and increased mitochondria copy number (Stack et al., 2014).

Based on its ability to act as a regenerable antioxidant and its distinct redox properties (Poteet et al., 2012), we analyzed the effect of MB on C26:0 induced increased ROS production in X-ALD human fibroblasts. Complete normalization was found in both cultures suggesting two possible mechanisms; either by inducing the endogenous anti-oxidant system via *Nrf2 (Poteet et al., 2012, Stack et al., 2014)* or via direct scavenging of superoxide components. Besides, reduced levels of oxidative lesion markers were found in *Abcd1*$^{-}$ mice spinal cord after treatment. Moreover an *Nrf2* dependent protective effects of MB was shown in tau mice model (Stack et al., 2014). Thus the protective action of MB described here was dependent or independent of Nrf2/ARE signaling pathway deserves further studies.

Previous studies from our laboratory showed oxidative stress mediated mitochondria fission in X-ALD patient fibroblasts and mice spinal cord (Patrizia thesis: Impairment of mitochondrial dynamics in X-linked adrenoleukodystrophy). We found that excess of C26:0 promotes the translocation of DRP1 to mitochondria and induces mitochondria fragmentation in redox dependent manner in X-ALD patient fibroblasts. Moreover, increased DRP1 protein levels were found at 12 months of age in *Abcd1*$^{-}$ mice spinal cord suggesting a shift towards mitochondrial fission causing an imbalance in mitochondria dynamics mechanism. This induction occurs just before the disease onset

around 12 months of age with no changes at 3 months. No reports so far had been studied the effects of MB on mitochondria fission and fusion mechanism, here we demonstrated that MB arrests the translocation of DRP1 to mitochondria there by prevents the mitochondria fragmentation and restoring the integrity of the mitochondria network. These results were consistent with *in-vivo* studies showing the down-regulation of DRP1 after MB treatment in *Abcd1*$^{-}$ mice spinal cord at 12 months of age. Thus, to our knowledge it is the first report indicating the role of MB in the modulation of DRP1.

Chonic inflammation has been allied with many neurodegenerative diseases that leads to neuronal damage and death are usually controlled by resident macrophages, microglia in the innate immune system. Microglia gets activated in response to toxic insults or injury as a self defense mechanism by releasing super-oxides and inflammatory factors to remove cell debris and pathogens. Chonic activation of these cells will leads to excessive and uncontrolled inflammatory responses thus causes exacerbated oxidative stress environment in turn ends with self perpetuating neurodegeneration. Despite of dietary antioxidant or anti-inflammatory compounds combat against oxidative stress and inflammation, these strategies were so far not very successful. In an attempt to counterbalance the inflammation, we analyzed the inflammatory mediators and oxidative lesion markers in *Abcd1*$^{-}$ mice spinal after the MB treatment. Here we normalized almost all the inflammatory mediators and the associated pro-inflammatory cytokines and chemokines after the treatment. Indeed, activation of microglia and astrocytes were ceased after MB treatment in X-ALD mice leading to prevention of axonal degeneration. Nitric oxide is an important signaling molecule increases the conversion of guanidine triphosphate to cyclic guanidine monophosphate (cGMP), acting as an early chemoattractant and microglial activator. Low cGMP immunoreactivity with less microglia accumulation at lesion sites was found after MB treatment (Duan et al., 2003) which could support the neuroprotective action of MB in X-ALD mice together with lower levels of iNOS found after the treatment. Direct binding of MB to peroxinitrites and inhibiting the activity of NOS could be another possible explanation of inhibition of microgliosis (Gibbs and Truman, 1998). In contrast, no alteration in the microglia activity was noticed in SOD1^{G93A} transgenic mice model for ALS after MB treatment. Although a direct observed positive effect on neuronal survival was found suggesting that the effect is not a consequence of inhibiting

microglia activity in this model (Dibaj et al., 2012). Apart from the model and experimental design differences, the systematic administration of MB could explain the contradictory results.

Our present results, therefore demonstrate that MB improves behavioral impairment and halts axonal degeneration mediated by increased mitochondria biogenesis and respiration, reduced mitochondrial fission, inflammation and oxidative damage in X-ALD mice spinal cord. Nevertheless, these studies provide enough evidence that favor the idea that MB can be an attractive drug for treating X-ALD and other neurodegenerative disorders that shares mitochondria dysfunction and inflammation as common feature.

After the explanation of the results and its correspondent discussion and possible future works derived from them, the final conclusions of this thesis are stated in the next section.

CONCLUSIONS

6.0 Conclusions

1. *Abcd1*$^{-}$ mice spinal cord adopts a dual phenotype expressing the factors that are cytotoxic (M1) and neuroprotective (M2).
2. Lack of *ABCD1* (ALD protein) causes inflammation and ROS production in primary microglia.
3. Microglia from WT and *Abcd1*$^{-}$ mice coexpresses cytotoxic (M1) and neuroprotective (M2) factors upon C26:0 insult and do not display a significant bias towards either M1 or M2 phenotypes, unveiling a possible role of C26:0 mediated inflammation in X-ALD mice spinal cord. Excess of C26:0 induces mitochondria ROS in primary *Abcd1*$^{-}$ microglia.
4. Excess of C26:0 induces severe inflammation and ROS production in both WT and *Abcd1*$^{-}$ primary mice astrocytes.
5. *Abcd1*$^{-}$ mice spinal cord presents an altered ECS characterized by low levels of some endogenous cannabinoids together with upregulation of metabolic enzymes of endocannbinoids revealing a plausible molecular therapeutic target for X-ALD.
6. Upregulated CB_2 receptor levels were found in *Abcd1*$^{-}$ mice spinal cord and primary mice microglia.
7. Activation of CB_2 receptor by the specific agonist, JWH133 neuroprotective by arresting the microglial activation, inflammation, mitochondrial dysfunction and halts axonal degeneration and locomotor disability in X-ALD mice.
8. Activation of CB_2 receptor prevents C26:0 driven inflammation and ROS production in primary *Abcd1*$^{-}$ mice microglia.
9. MB treatment induces mitochondria biogenesis and respiration in X-ALD mice spinal cord. MB modulates the DRP1 activity and prevents the altered mitochondria fission mechanism in X-ALD mice spinal cord and in human patient fibroblasts upon C26:0 insult.
10. MB averts inflammation by blocking the pro-inflammatory mediators and halts axonal degeneration and improves locomotor disability in X-ALD mice.

REFERENCES

7.0 References

ALBET, S., CAUSERET, C., BENTEJAC, M., MANDEL, J. L., AUBOURG, P. & MAURICE, B. 1997. Fenofibrate differently alters expression of genes encoding ATP-binding transporter proteins of the peroxisomal membrane. *FEBS Lett,* 405**,** 394-7.

ALDSKOGIUS, H., LIU, L. & SVENSSON, M. 1999. Glial responses to synaptic damage and plasticity. *J Neurosci Res,* 58**,** 33-41.

ALVAREZ, J. I., KATAYAMA, T. & PRAT, A. 2013. Glial influence on the blood brain barrier. *Glia,* 61**,** 1939-58.

AMBROSINI, E., COLUMBA-CABEZAS, S., SERAFINI, B., MUSCELLA, A. & ALOISI, F. 2003. Astrocytes are the major intracerebral source of macrophage inflammatory protein-3alpha/CCL20 in relapsing experimental autoimmune encephalomyelitis and in vitro. *Glia,* 41**,** 290-300.

AMENTA, P. S., JALLO, J. I., TUMA, R. F. & ELLIOTT, M. B. 2012. A cannabinoid type 2 receptor agonist attenuates blood-brain barrier damage and neurodegeneration in a murine model of traumatic brain injury. *J Neurosci Res,* 90**,** 2293-305.

ASO, E., ANDRES-BENITO, P., CARMONA, M., MALDONADO, R. & FERRER, I. 2016. Cannabinoid Receptor 2 Participates in Amyloid-beta Processing in a Mouse Model of Alzheimer's Disease but Plays a Minor Role in the Therapeutic Properties of a Cannabis-Based Medicine. *J Alzheimers Dis,* 51**,** 489-500.

ASO, E., JUVES, S., MALDONADO, R. & FERRER, I. 2013. CB2 cannabinoid receptor agonist ameliorates Alzheimer-like phenotype in AbetaPP/PS1 mice. *J Alzheimers Dis,* 35**,** 847-58.

ATAMNA, H. & KUMAR, R. 2010. Protective role of methylene blue in Alzheimer's disease via mitochondria and cytochrome c oxidase. *J Alzheimers Dis,* 20 Suppl 2**,** S439-52.

ATAMNA, H., MACKEY, J. & DHAHBI, J. M. 2012. Mitochondrial pharmacology: electron transport chain bypass as strategies to treat mitochondrial dysfunction. *Biofactors,* 38**,** 158-66.

AUBOURG, P., ADAMSBAUM, C., LAVALLARD-ROUSSEAU, M. C., ROCCHICCIOLI, F., CARTIER, N., JAMBAQUE, I., JAKOBEZAK, C., LEMAITRE, A., BOUREAU, F., WOLF, C. & ET AL. 1993. A two-year trial of oleic and erucic acids ("Lorenzo's oil") as treatment for adrenomyeloneuropathy. *N Engl J Med,* 329**,** 745-52.

AUBOURG, P., BLANCHE, S., JAMBAQUE, I., ROCCHICCIOLI, F., KALIFA, G., NAUD-SAUDREAU, C., ROLLAND, M. O., DEBRE, M., CHAUSSAIN, J. L., GRISCELLI, C. & ET AL. 1990. Reversal of early neurologic and

neuroradiologic manifestations of X-linked adrenoleukodystrophy by bone marrow transplantation. *N Engl J Med,* 322**,** 1860-6.

AYMERICH, M. S., ROJO-BUSTAMANTE, E., MOLINA, C., CELORRIO, M., SANCHEZ-ARIAS, J. A. & FRANCO, R. 2016. Neuroprotective Effect of JZL184 in MPP(+)-Treated SH-SY5Y Cells Through CB2 Receptors. *Mol Neurobiol,* 53**,** 2312-9.

BAARINE, M., BEESON, C., SINGH, A. & SINGH, I. 2015. ABCD1 deletion-induced mitochondrial dysfunction is corrected by SAHA: implication for adrenoleukodystrophy. *J Neurochem,* 133**,** 380-96.

BAKER, D., PRYCE, G., CROXFORD, J. L., BROWN, P., PERTWEE, R. G., MAKRIYANNIS, A., KHANOLKAR, A., LAYWARD, L., FEZZA, F., BISOGNO, T. & DI MARZO, V. 2001. Endocannabinoids control spasticity in a multiple sclerosis model. *FASEB J,* 15**,** 300-2.

BENITO, C., NUNEZ, E., TOLON, R. M., CARRIER, E. J., RABANO, A., HILLARD, C. J. & ROMERO, J. 2003. Cannabinoid CB2 receptors and fatty acid amide hydrolase are selectively overexpressed in neuritic plaque-associated glia in Alzheimer's disease brains. *J Neurosci,* 23**,** 11136-41.

BERGER, J., FORSS-PETTER, S. & EICHLER, F. S. 2014. Pathophysiology of X-linked adrenoleukodystrophy. *Biochimie,* 98**,** 135-42.

BERNAL-CHICO, A., CANEDO, M., MANTEROLA, A., VICTORIA SANCHEZ-GOMEZ, M., PEREZ-SAMARTIN, A., RODRIGUEZ-PUERTAS, R., MATUTE, C. & MATO, S. 2015. Blockade of monoacylglycerol lipase inhibits oligodendrocyte excitotoxicity and prevents demyelination in vivo. *Glia,* 63**,** 163-76.

BISOGNO, T., HOWELL, F., WILLIAMS, G., MINASSI, A., CASCIO, M. G., LIGRESTI, A., MATIAS, I., SCHIANO-MORIELLO, A., PAUL, P., WILLIAMS, E. J., GANGADHARAN, U., HOBBS, C., DI MARZO, V. & DOHERTY, P. 2003. Cloning of the first sn1-DAG lipases points to the spatial and temporal regulation of endocannabinoid signaling in the brain. *J Cell Biol,* 163**,** 463-8.

BIZZOZERO, O. A., ZUNIGA, G. & LEES, M. B. 1991. Fatty acid composition of human myelin proteolipid protein in peroxisomal disorders. *J Neurochem,* 56**,** 872-8.

BOUCHARD, J., TRUONG, J., BOUCHARD, K., DUNKELBERGER, D., DESRAYAUD, S., MOUSSAOUI, S., TABRIZI, S. J., STELLA, N. & MUCHOWSKI, P. J. 2012. Cannabinoid receptor 2 signaling in peripheral immune cells modulates disease onset and severity in mouse models of Huntington's disease. *J Neurosci,* 32**,** 18259-68.

BRAITERMAN, L. T., ZHENG, S., WATKINS, P. A., GERAGHTY, M. T., JOHNSON, G., MCGUINNESS, M. C., MOSER, A. B. & SMITH, K. D. 1998.

Suppression of peroxisomal membrane protein defects by peroxisomal ATP binding cassette (ABC) proteins. *Hum Mol Genet,* 7**,** 239-47.

BRAMBILLA, R., PERSAUD, T., HU, X., KARMALLY, S., SHESTOPALOV, V. I., DVORIANTCHIKOVA, G., IVANOV, D., NATHANSON, L., BARNUM, S. R. & BETHEA, J. R. 2009. Transgenic inhibition of astroglial NF-kappa B improves functional outcome in experimental autoimmune encephalomyelitis by suppressing chronic central nervous system inflammation. *J Immunol,* 182**,** 2628-40.

BRETTSCHNEIDER, J., TOLEDO, J. B., VAN DEERLIN, V. M., ELMAN, L., MCCLUSKEY, L., LEE, V. M. & TROJANOWSKI, J. Q. 2012. Microglial activation correlates with disease progression and upper motor neuron clinical symptoms in amyotrophic lateral sclerosis. *PLoS One,* 7**,** e39216.

CABRAL, G. A. & GRIFFIN-THOMAS, L. 2009. Emerging role of the cannabinoid receptor CB2 in immune regulation: therapeutic prospects for neuroinflammation. *Expert Rev Mol Med,* 11**,** e3.

CAGNIN, A., ROSSOR, M., SAMPSON, E. L., MACKINNON, T. & BANATI, R. B. 2004. In vivo detection of microglial activation in frontotemporal dementia. *Ann Neurol,* 56**,** 894-7.

CALLAWAY, N. L., RIHA, P. D., WRUBEL, K. M., MCCOLLUM, D. & GONZALEZ-LIMA, F. 2002. Methylene blue restores spatial memory retention impaired by an inhibitor of cytochrome oxidase in rats. *Neurosci Lett,* 332**,** 83-6.

CAPPA, M., BERTINI, E., DEL BALZO, P., CAMBIASO, P., DI BIASE, A. & SALVATI, S. 1994. High dose immunoglobulin IV treatment in adrenoleukodystrophy. *J Neurol Neurosurg Psychiatry,* 57 Suppl**,** 69-70; discussion 71.

CARTIER, N. & AUBOURG, P. 2008. Hematopoietic stem cell gene therapy in Hurler syndrome, globoid cell leukodystrophy, metachromatic leukodystrophy and X-adrenoleukodystrophy. *Curr Opin Mol Ther,* 10**,** 471-8.

CARTIER, N. & AUBOURG, P. 2010. Hematopoietic stem cell transplantation and hematopoietic stem cell gene therapy in X-linked adrenoleukodystrophy. *Brain Pathol,* 20**,** 857-62.

CARTIER, N., HACEIN-BEY-ABINA, S., BARTHOLOMAE, C. C., VERES, G., SCHMIDT, M., KUTSCHERA, I., VIDAUD, M., ABEL, U., DAL-CORTIVO, L., CACCAVELLI, L., MAHLAOUI, N., KIERMER, V., MITTELSTAEDT, D., BELLESME, C., LAHLOU, N., LEFRERE, F., BLANCHE, S., AUDIT, M., PAYEN, E., LEBOULCH, P., L'HOMME, B., BOUGNERES, P., VON KALLE, C., FISCHER, A., CAVAZZANA-CALVO, M. & AUBOURG, P. 2009. Hematopoietic stem cell gene therapy with a lentiviral vector in X-linked adrenoleukodystrophy. *Science,* 326**,** 818-23.

CARTIER, N., LOPEZ, J., MOULLIER, P., ROCCHICCIOLI, F., ROLLAND, M. O., JORGE, P., MOSSER, J., MANDEL, J. L., BOUGNERES, P. F., DANOS, O. & ET AL. 1995. Retroviral-mediated gene transfer corrects very-long-chain fatty acid metabolism in adrenoleukodystrophy fibroblasts. *Proc Natl Acad Sci U S A,* 92**,** 1674-8.

CHIU, I. M., MORIMOTO, E. T., GOODARZI, H., LIAO, J. T., O'KEEFFE, S., PHATNANI, H. P., MURATET, M., CARROLL, M. C., LEVY, S., TAVAZOIE, S., MYERS, R. M. & MANIATIS, T. 2013. A neurodegeneration-specific gene-expression signature of acutely isolated microglia from an amyotrophic lateral sclerosis mouse model. *Cell Rep,* 4**,** 385-401.

COELHO, D., KIM, J. C., MIOUSSE, I. R., FUNG, S., DU MOULIN, M., BUERS, I., SUORMALA, T., BURDA, P., FRAPOLLI, M., STUCKI, M., NURNBERG, P., THIELE, H., ROBENEK, H., HOHNE, W., LONGO, N., PASQUALI, M., MENGEL, E., WATKINS, D., SHOUBRIDGE, E. A., MAJEWSKI, J., ROSENBLATT, D. S., FOWLER, B., RUTSCH, F. & BAUMGARTNER, M. R. 2012. Mutations in ABCD4 cause a new inborn error of vitamin B12 metabolism. *Nat Genet,* 44**,** 1152-5.

COLTON, C. & WILCOCK, D. M. 2010. Assessing activation states in microglia. *CNS Neurol Disord Drug Targets,* 9**,** 174-91.

COLTON, C. A. 2009. Heterogeneity of microglial activation in the innate immune response in the brain. *J Neuroimmune Pharmacol,* 4**,** 399-418.

DE BEER, M., ENGELEN, M. & VAN GEEL, B. M. 2014. Frequent occurrence of cerebral demyelination in adrenomyeloneuropathy. *Neurology,* 83**,** 2227-31.

DEAN, M. & ALLIKMETS, R. 2001. Complete characterization of the human ABC gene family. *J Bioenerg Biomembr,* 33**,** 475-9.

DI MARZO, V. 2011. Endocannabinoid signaling in the brain: biosynthetic mechanisms in the limelight. *Nat Neurosci,* 14**,** 9-15.

DIBAJ, P., ZSCHUNTZSCH, J., STEFFENS, H., SCHEFFEL, J., GORICKE, B., WEISHAUPT, J. H., LE MEUR, K., KIRCHHOFF, F., HANISCH, U. K., SCHOMBURG, E. D. & NEUSCH, C. 2012. Influence of methylene blue on microglia-induced inflammation and motor neuron degeneration in the SOD1(G93A) model for ALS. *PLoS One,* 7**,** e43963.

DICARLO, G., WILCOCK, D., HENDERSON, D., GORDON, M. & MORGAN, D. 2001. Intrahippocampal LPS injections reduce Abeta load in APP+PS1 transgenic mice. *Neurobiol Aging,* 22**,** 1007-12.

DUAN, Y., HAUGABOOK, S. J., SAHLEY, C. L. & MULLER, K. J. 2003. Methylene blue blocks cGMP production and disrupts directed migration of microglia to nerve lesions in the leech CNS. *J Neurobiol,* 57**,** 183-92.

EGLITIS, M. A. & MEZEY, E. 1997. Hematopoietic cells differentiate into both microglia and macroglia in the brains of adult mice. *Proc Natl Acad Sci U S A,* 94**,** 4080-5.

EHRHART, J., OBREGON, D., MORI, T., HOU, H., SUN, N., BAI, Y., KLEIN, T., FERNANDEZ, F., TAN, J. & SHYTLE, R. D. 2005. Stimulation of cannabinoid receptor 2 (CB2) suppresses microglial activation. *J Neuroinflammation,* 2**,** 29.

EICHLER, F. S., REN, J. Q., COSSOY, M., RIETSCH, A. M., NAGPAL, S., MOSER, A. B., FROSCH, M. P. & RANSOHOFF, R. M. 2008. Is microglial apoptosis an early pathogenic change in cerebral X-linked adrenoleukodystrophy? *Ann Neurol,* 63**,** 729-42.

ENGELEN, M., OFMAN, R., DIJKGRAAF, M. G., HIJZEN, M., VAN DER WARDT, L. A., VAN GEEL, B. M., DE VISSER, M., WANDERS, R. J., POLL-THE, B. T. & KEMP, S. 2010. Lovastatin in X-linked adrenoleukodystrophy. *N Engl J Med,* 362**,** 276-7.

ENGELEN, M., SCHACKMANN, M. J., OFMAN, R., SANDERS, R. J., DIJKSTRA, I. M., HOUTEN, S. M., FOURCADE, S., PUJOL, A., POLL-THE, B. T., WANDERS, R. J. & KEMP, S. 2012a. Bezafibrate lowers very long-chain fatty acids in X-linked adrenoleukodystrophy fibroblasts by inhibiting fatty acid elongation. *J Inherit Metab Dis,* 35**,** 1137-45.

ENGELEN, M., TRAN, L., OFMAN, R., BRENNECKE, J., MOSER, A. B., DIJKSTRA, I. M., WANDERS, R. J., POLL-THE, B. T. & KEMP, S. 2012b. Bezafibrate for X-linked adrenoleukodystrophy. *PLoS One,* 7**,** e41013.

FACCHINETTI, F., DEL GIUDICE, E., FUREGATO, S., PASSAROTTO, M. & LEON, A. 2003. Cannabinoids ablate release of TNFalpha in rat microglial cells stimulated with lypopolysaccharide. *Glia,* 41**,** 161-8.

FATOUROS, C., PIR, G. J., BIERNAT, J., KOUSHIKA, S. P., MANDELKOW, E., MANDELKOW, E. M., SCHMIDT, E. & BAUMEISTER, R. 2012. Inhibition of tau aggregation in a novel Caenorhabditis elegans model of tauopathy mitigates proteotoxicity. *Hum Mol Genet,* 21**,** 3587-603.

FERRER, I., KAPFHAMMER, J. P., HINDELANG, C., KEMP, S., TROFFER-CHARLIER, N., BROCCOLI, V., CALLYZOT, N., MOOYER, P., SELHORST, J., VREKEN, P., WANDERS, R. J., MANDEL, J. L. & PUJOL, A. 2005. Inactivation of the peroxisomal ABCD2 transporter in the mouse leads to late-onset ataxia involving mitochondria, Golgi and endoplasmic reticulum damage. *Hum Mol Genet,* 14**,** 3565-77.

FLAVIGNY, E., SANHAJ, A., AUBOURG, P. & CARTIER, N. 1999. Retroviral-mediated adrenoleukodystrophy-related gene transfer corrects very long chain fatty acid metabolism in adrenoleukodystrophy fibroblasts: implications for therapy. *FEBS Lett,* 448**,** 261-4.

FORSS-PETTER, S., WERNER, H., BERGER, J., LASSMANN, H., MOLZER, B., SCHWAB, M. H., BERNHEIMER, H., ZIMMERMANN, F. & NAVE, K. A. 1997. Targeted inactivation of the X-linked adrenoleukodystrophy gene in mice. *J.Neurosci.Res.,* 50**,** 829-843.

FOURCADE, S., LOPEZ-ERAUSKIN, J., GALINO, J., DUVAL, C., NAUDI, A., JOVE, M., KEMP, S., VILLARROYA, F., FERRER, I., PAMPLONA, R., PORTERO-OTIN, M. & PUJOL, A. 2008. Early oxidative damage underlying neurodegeneration in X-adrenoleukodystrophy. *Hum Mol Genet,* 17**,** 1762-73.

FOURCADE, S., LOPEZ-ERAUSKIN, J., RUIZ, M., FERRER, I. & PUJOL, A. 2014. Mitochondrial dysfunction and oxidative damage cooperatively fuel axonal degeneration in X-linked adrenoleukodystrophy. *Biochimie,* 98**,** 143-9.

FOURCADE, S., RUIZ, M., CAMPS, C., SCHLUTER, A., HOUTEN, S. M., MOOYER, P. A., PAMPOLS, T., DACREMONT, G., WANDERS, R. J., GIROS, M. & PUJOL, A. 2009. A key role for the peroxisomal ABCD2 transporter in fatty acid homeostasis. *Am J Physiol Endocrinol Metab,* 296**,** E211-21.

FOURCADE, S., RUIZ, M., GUILERA, C., HAHNEN, E., BRICHTA, L., NAUDI, A., PORTERO-OTIN, M., DACREMONT, G., CARTIER, N., WANDERS, R., KEMP, S., MANDEL, J. L., WIRTH, B., PAMPLONA, R., AUBOURG, P. & PUJOL, A. 2010. Valproic acid induces antioxidant effects in X-linked adrenoleukodystrophy. *Hum Mol Genet,* 19**,** 2005-14.

FOURCADE, S., SAVARY, S., ALBET, S., GAUTHE, D., GONDCAILLE, C., PINEAU, T., BELLENGER, J., BENTEJAC, M., HOLZINGER, A., BERGER, J. & BUGAUT, M. 2001. Fibrate induction of the adrenoleukodystrophy-related gene (ABCD2): promoter analysis and role of the peroxisome proliferator-activated receptor PPARalpha. *Eur J Biochem,* 268**,** 3490-500.

GALINO, J., RUIZ, M., FOURCADE, S., SCHLUTER, A., LOPEZ-ERAUSKIN, J., GUILERA, C., JOVE, M., NAUDI, A., GARCIA-ARUMI, E., ANDREU, A. L., STARKOV, A. A., PAMPLONA, R., FERRER, I., PORTERO-OTIN, M. & PUJOL, A. 2011. Oxidative damage compromises energy metabolism in the axonal degeneration mouse model of x-adrenoleukodystrophy. *Antioxid Redox Signal,* 15**,** 2095-107.

GARCIA, C., PALOMO-GARO, C., GARCIA-ARENCIBIA, M., RAMOS, J., PERTWEE, R. & FERNANDEZ-RUIZ, J. 2011. Symptom-relieving and neuroprotective effects of the phytocannabinoid Delta(9)-THCV in animal models of Parkinson's disease. *Br J Pharmacol,* 163**,** 1495-506.

GEILLON, F., GONDCAILLE, C., RAAS, Q., DIAS, A. M., PECQUEUR, D., TRUNTZER, C., LUCCHI, G., DUCOROY, P., FALSON, P., SAVARY, S. & TROMPIER, D. 2017. Peroxisomal ATP-binding cassette transporters form mainly tetramers. *J Biol Chem*.

GIBBS, S. M. & TRUMAN, J. W. 1998. Nitric oxide and cyclic GMP regulate retinal patterning in the optic lobe of Drosophila. *Neuron,* 20**,** 83-93.

GLASS, C. K., SAIJO, K., WINNER, B., MARCHETTO, M. C. & GAGE, F. H. 2010. Mechanisms underlying inflammation in neurodegeneration. *Cell,* 140**,** 918-34.

GLEZER, I., LAPOINTE, A. & RIVEST, S. 2006. Innate immunity triggers oligodendrocyte progenitor reactivity and confines damages to brain injuries. *Faseb J,* 20**,** 750-2.

GOMEZ-GALVEZ, Y., PALOMO-GARO, C., FERNANDEZ-RUIZ, J. & GARCIA, C. 2016. Potential of the cannabinoid CB(2) receptor as a pharmacological target against inflammation in Parkinson's disease. *Prog Neuropsychopharmacol Biol Psychiatry,* 64**,** 200-8.

GONZALEZ, S., SCORTICATI, C., GARCIA-ARENCIBIA, M., DE MIGUEL, R., RAMOS, J. A. & FERNANDEZ-RUIZ, J. 2006. Effects of rimonabant, a selective cannabinoid CB1 receptor antagonist, in a rat model of Parkinson's disease. *Brain Res,* 1073-1074**,** 209-19.

GRUNBLATT, E., BARTL, J., ZEHETMAYER, S., RINGEL, T. M., BAUER, P., RIEDERER, P. & JACOB, C. P. 2009. Gene expression as peripheral biomarkers for sporadic Alzheimer's disease. *J Alzheimers Dis,* 16**,** 627-34.

HALLIDAY, G. M. & STEVENS, C. H. 2011. Glia: initiators and progressors of pathology in Parkinson's disease. *Mov Disord,* 26**,** 6-17.

HASHIOKA, S., MCGEER, E. G., MIYAOKA, T., WAKE, R., HORIGUCHI, J. & MCGEER, P. L. 2015. Interferon-gamma-induced neurotoxicity of human astrocytes. *CNS Neurol Disord Drug Targets,* 14**,** 251-6.

HEIN, S., SCHONFELD, P., KAHLERT, S. & REISER, G. 2008. Toxic effects of X-linked adrenoleukodystrophy-associated, very long chain fatty acids on glial cells and neurons from rat hippocampus in culture. *Hum Mol Genet,* 17**,** 1750-61.

HENEKA, M. T., CARSON, M. J., EL KHOURY, J., LANDRETH, G. E., BROSSERON, F., FEINSTEIN, D. L., JACOBS, A. H., WYSS-CORAY, T., VITORICA, J., RANSOHOFF, R. M., HERRUP, K., FRAUTSCHY, S. A., FINSEN, B., BROWN, G. C., VERKHRATSKY, A., YAMANAKA, K., KOISTINAHO, J., LATZ, E., HALLE, A., PETZOLD, G. C., TOWN, T., MORGAN, D., SHINOHARA, M. L., PERRY, V. H., HOLMES, C., BAZAN, N. G., BROOKS, D. J., HUNOT, S., JOSEPH, B., DEIGENDESCH, N., GARASCHUK, O., BODDEKE, E., DINARELLO, C. A., BREITNER, J. C., COLE, G. M., GOLENBOCK, D. T. & KUMMER, M. P. 2015. Neuroinflammation in Alzheimer's disease. *Lancet Neurol,* 14**,** 388-405.

HERRERA, A. J., ESPINOSA-OLIVA, A. M., CARRILLO-JIMENEZ, A., OLIVA-MARTIN, M. J., GARCIA-REVILLA, J., GARCIA-QUINTANILLA, A., DE

PABLOS, R. M. & VENERO, J. L. 2015. Relevance of chronic stress and the two faces of microglia in Parkinson's disease. *Front Cell Neurosci,* 9**,** 312.

HETTEMA, E. H., VAN ROERMUND, C. W., DISTEL, B., VAN DEN BERG, M., VILELA, C., RODRIGUES-POUSADA, C., WANDERS, R. J. & TABAK, H. F. 1996. The ABC transporter proteins Pat1 and Pat2 are required for import of long-chain fatty acids into peroxisomes of Saccharomyces cerevisiae. *Embo J,* 15**,** 3813-22.

HOWLETT, A. C., BARTH, F., BONNER, T. I., CABRAL, G., CASELLAS, P., DEVANE, W. A., FELDER, C. C., HERKENHAM, M., MACKIE, K., MARTIN, B. R., MECHOULAM, R. & PERTWEE, R. G. 2002. International Union of Pharmacology. XXVII. Classification of cannabinoid receptors. *Pharmacol Rev,* 54**,** 161-202.

HSIAO, H. Y., CHEN, Y. C., CHEN, H. M., TU, P. H. & CHERN, Y. 2013. A critical role of astrocyte-mediated nuclear factor-kappaB-dependent inflammation in Huntington's disease. *Hum Mol Genet,* 22**,** 1826-42.

IGARASHI, M., SCHAUMBURG, H. H., POWERS, J., KISHMOTO, Y., KOLODNY, E. & SUZUKI, K. 1976. Fatty acid abnormality in adrenoleukodystrophy. *J Neurochem,* 26**,** 851-60.

ISHIHARA, N., JOFUKU, A., EURA, Y. & MIHARA, K. 2003. Regulation of mitochondrial morphology by membrane potential, and DRP1-dependent division and FZO1-dependent fusion reaction in mammalian cells. *Biochem Biophys Res Commun,* 301**,** 891-8.

JIMENEZ, S., BAGLIETTO-VARGAS, D., CABALLERO, C., MORENO-GONZALEZ, I., TORRES, M., SANCHEZ-VARO, R., RUANO, D., VIZUETE, M., GUTIERREZ, A. & VITORICA, J. 2008. Inflammatory response in the hippocampus of PS1M146L/APP751SL mouse model of Alzheimer's disease: age-dependent switch in the microglial phenotype from alternative to classic. *J Neurosci,* 28**,** 11650-61.

KAMIJO, K., TAKETANI, S., YOKOTA, S., OSUMI, T. & HASHIMOTO, T. 1990. The 70-kDa peroxisomal membrane protein is a member of the Mdr (P-glycoprotein)-related ATP-binding protein superfamily. *J Biol Chem,* 265**,** 4534-40.

KANG, S. S., KEASEY, M. P., CAI, J. & HAGG, T. 2012. Loss of neuron-astroglial interaction rapidly induces protective CNTF expression after stroke in mice. *J Neurosci,* 32**,** 9277-87.

KEMP, S. & WANDERS, R. J. 2010. Biochemical aspects of X-adrenoleukodystrophy. *Brain Pathol***,** in press.

KEMP, S., WEI, H. M., LU, J. F., BRAITERMAN, L. T., MCGUINNESS, M. C., MOSER, A. B., WATKINS, P. A. & SMITH, K. D. 1998. Gene redundancy and

pharmacological gene therapy: implications for X-linked adrenoleukodystrophy. *Nat.Med.,* 4**,** 1261-1268.

KIGERL, K. A., GENSEL, J. C., ANKENY, D. P., ALEXANDER, J. K., DONNELLY, D. J. & POPOVICH, P. G. 2009. Identification of two distinct macrophage subsets with divergent effects causing either neurotoxicity or regeneration in the injured mouse spinal cord. *J Neurosci,* 29**,** 13435-44.

KOBAYASHI, T., SHINNOH, N., KONDO, A. & YAMADA, T. 1997. Adrenoleukodystrophy protein-deficient mice represent abnormality of very long chain fatty acid metabolism. *Biochem.Biophys.Res.Commun.,* 232**,** 631-636.

KORENKE, G. C., CHRISTEN, H. J., KRUSE, B., HUNNEMAN, D. H. & HANEFELD, F. 1997. Progression of X-linked adrenoleukodystrophy under interferon-beta therapy. *J Inherit Metab Dis,* 20**,** 59-66.

KOZELA, E., PIETR, M., JUKNAT, A., RIMMERMAN, N., LEVY, R. & VOGEL, Z. 2010. Cannabinoids Delta(9)-tetrahydrocannabinol and cannabidiol differentially inhibit the lipopolysaccharide-activated NF-kappaB and interferon-beta/STAT proinflammatory pathways in BV-2 microglial cells. *J Biol Chem,* 285**,** 1616-26.

KRUSKA, N., SCHONFELD, P., PUJOL, A. & REISER, G. 2015. Astrocytes and mitochondria from adrenoleukodystrophy protein (ABCD1)-deficient mice reveal that the adrenoleukodystrophy-associated very long-chain fatty acids target several cellular energy-dependent functions. *Biochim Biophys Acta,* 1852**,** 925-36.

LATINI, L., BISICCHIA, E., SASSO, V., CHIURCHIU, V., CAVALLUCCI, V., MOLINARI, M., MACCARRONE, M. & VISCOMI, M. T. 2014. Cannabinoid CB2 receptor (CB2R) stimulation delays rubrospinal mitochondrial-dependent degeneration and improves functional recovery after spinal cord hemisection by ERK1/2 inactivation. *Cell Death Dis,* 5**,** e1404.

LAUNAY, N., AGUADO, C., FOURCADE, S., RUIZ, M., GRAU, L., RIERA, J., GUILERA, C., GIROS, M., FERRER, I., KNECHT, E. & PUJOL, A. 2015. Autophagy induction halts axonal degeneration in a mouse model of X-adrenoleukodystrophy. *Acta Neuropathol,* 129**,** 399-415.

LAUNAY, N., RUIZ, M., FOURCADE, S., SCHLUTER, A., GUILERA, C., FERRER, I., KNECHT, E. & PUJOL, A. 2013. Oxidative stress regulates the ubiquitin-proteasome system and immunoproteasome functioning in a mouse model of X-adrenoleukodystrophy. *Brain,* 136**,** 891-904.

LAUNAY, N., RUIZ, M., GRAU, L., ORTEGA, F. J., ILIEVA, E. V., MARTINEZ, J. J., GALEA, E., FERRER, I., KNECHT, E., PUJOL, A. & FOURCADE, S. 2017. Tauroursodeoxycholic bile acid arrests axonal degeneration by inhibiting the unfolded protein response in X-linked adrenoleukodystrophy. *Acta Neuropathol,* 133**,** 283-301.

LECOMTE, M. D., SHIMADA, I. S., SHERWIN, C. & SPEES, J. L. 2015. Notch1-STAT3-ETBR signaling axis controls reactive astrocyte proliferation after brain injury. *Proc Natl Acad Sci U S A,* 112**,** 8726-31.

LI, Q., WANG, F., ZHANG, Y. M., ZHOU, J. J. & ZHANG, Y. 2013. Activation of cannabinoid type 2 receptor by JWH133 protects heart against ischemia/reperfusion-induced apoptosis. *Cell Physiol Biochem,* 31**,** 693-702.

LINDNER, M., THUMMLER, K., ARTHUR, A., BRUNNER, S., ELLIOTT, C., MCELROY, D., MOHAN, H., WILLIAMS, A., EDGAR, J. M., SCHUH, C., STADELMANN, C., BARNETT, S. C., LASSMANN, H., MUCKLISCH, S., MUDALIAR, M., SCHAEREN-WIEMERS, N., MEINL, E. & LININGTON, C. 2015. Fibroblast growth factor signalling in multiple sclerosis: inhibition of myelination and induction of pro-inflammatory environment by FGF9. *Brain,* 138**,** 1875-93.

LOES, D. J., FATEMI, A., MELHEM, E. R., GUPTE, N., BEZMAN, L., MOSER, H. W. & RAYMOND, G. V. 2003. Analysis of MRI patterns aids prediction of progression in X-linked adrenoleukodystrophy. *Neurology,* 61**,** 369-74.

LOPEZ-ERAUSKIN, J., FERRER, I., GALEA, E. & PUJOL, A. 2013a. Cyclophilin D as a potential target for antioxidants in neurodegeneration: the X-ALD case. *Biol Chem*.

LOPEZ-ERAUSKIN, J., FOURCADE, S., GALINO, J., RUIZ, M., SCHLUTER, A., NAUDI, A., JOVE, M., PORTERO-OTIN, M., PAMPLONA, R., FERRER, I. & PUJOL, A. 2011. Antioxidants halt axonal degeneration in a mouse model of X-adrenoleukodystrophy. *Ann Neurol,* 70**,** 84-92.

LOPEZ-ERAUSKIN, J., GALINO, J., BIANCHI, P., FOURCADE, S., ANDREU, A. L., FERRER, I., MUNOZ-PINEDO, C. & PUJOL, A. 2012. Oxidative stress modulates mitochondrial failure and cyclophilin D function in X-linked adrenoleukodystrophy. *Brain,* 135**,** 3584-98.

LOPEZ-ERAUSKIN, J., GALINO, J., RUIZ, M., CUEZVA, J. M., FABREGAT, I., CACABELOS, D., BOADA, J., MARTINEZ, J., FERRER, I., PAMPLONA, R., VILLARROYA, F., PORTERO-OTIN, M., FOURCADE, S. & PUJOL, A. 2013b. Impaired mitochondrial oxidative phosphorylation in the peroxisomal disease X-linked adrenoleukodystrophy. *Hum Mol Genet,* 22**,** 3296-305.

LOURBOPOULOS, A., GRIGORIADIS, N., LAGOUDAKI, R., TOULOUMI, O., POLYZOIDOU, E., MAVROMATIS, I., TASCOS, N., BREUER, A., OVADIA, H., KARUSSIS, D., SHOHAMI, E., MECHOULAM, R. & SIMEONIDOU, C. 2011. Administration of 2-arachidonoylglycerol ameliorates both acute and chronic experimental autoimmune encephalomyelitis. *Brain Res,* 1390**,** 126-41.

LU, J. F., LAWLER, A. M., WATKINS, P. A., POWERS, J. M., MOSER, A. B., MOSER, H. W. & SMITH, K. D. 1997. A mouse model for X-linked adrenoleukodystrophy. *Proc.Natl.Acad.Sci.U.S.A,* 94**,** 9366-9371.

MAHMOOD, A., RAYMOND, G. V., DUBEY, P., PETERS, C. & MOSER, H. W. 2007. Survival analysis of haematopoietic cell transplantation for childhood cerebral X-linked adrenoleukodystrophy: a comparison study. *Lancet Neurol,* 6**,** 687-92.

MALDONADO, R., BERRENDERO, F., OZAITA, A. & ROBLEDO, P. 2011. Neurochemical basis of cannabis addiction. *Neuroscience,* 181**,** 1-17.

MARCHETTI, D. P., DONIDA, B., JACQUES, C. E., DEON, M., HAUSCHILD, T. C., KOEHLER-SANTOS, P., DE MOURA COELHO, D., COITINHO, A. S., JARDIM, L. B. & VARGAS, C. R. 2017. Inflammatory profile in X-linked adrenoleukodystrophy patients: Understanding disease progression. *J Cell Biochem*.

MARESZ, K., PRYCE, G., PONOMAREV, E. D., MARSICANO, G., CROXFORD, J. L., SHRIVER, L. P., LEDENT, C., CHENG, X., CARRIER, E. J., MANN, M. K., GIOVANNONI, G., PERTWEE, R. G., YAMAMURA, T., BUCKLEY, N. E., HILLARD, C. J., LUTZ, B., BAKER, D. & DITTEL, B. N. 2007. Direct suppression of CNS autoimmune inflammation via the cannabinoid receptor CB1 on neurons and CB2 on autoreactive T cells. *Nat Med,* 13**,** 492-7.

MARQUES, J. M., RIAL, A., MUNOZ, N., PELLAY, F. X., VAN MAELE, L., LEGER, H., CAMOU, T., SIRARD, J. C., BENECKE, A. & CHABALGOITY, J. A. 2012. Protection against Streptococcus pneumoniae serotype 1 acute infection shows a signature of Th17- and IFN-gamma-mediated immunity. *Immunobiology,* 217**,** 420-9.

MARTIN-MORENO, A. M., BRERA, B., SPUCH, C., CARRO, E., GARCIA-GARCIA, L., DELGADO, M., POZO, M. A., INNAMORATO, N. G., CUADRADO, A. & DE CEBALLOS, M. L. 2012. Prolonged oral cannabinoid administration prevents neuroinflammation, lowers beta-amyloid levels and improves cognitive performance in Tg APP 2576 mice. *J Neuroinflammation,* 9**,** 8.

MARTIN-MORENO, A. M., REIGADA, D., RAMIREZ, B. G., MECHOULAM, R., INNAMORATO, N., CUADRADO, A. & DE CEBALLOS, M. L. 2011. Cannabidiol and other cannabinoids reduce microglial activation in vitro and in vivo: relevance to Alzheimer's disease. *Mol Pharmacol,* 79**,** 964-73.

MAYO, L., TRAUGER, S. A., BLAIN, M., NADEAU, M., PATEL, B., ALVAREZ, J. I., MASCANFRONI, I. D., YESTE, A., KIVISAKK, P., KALLAS, K., ELLEZAM, B., BAKSHI, R., PRAT, A., ANTEL, J. P., WEINER, H. L. & QUINTANA, F. J. 2014. Regulation of astrocyte activation by glycolipids drives chronic CNS inflammation. *Nat Med,* 20**,** 1147-56.

MCGUINNESS, M. C., LU, J. F., ZHANG, H. P., DONG, G. X., HEINZER, A. K., WATKINS, P. A., POWERS, J. & SMITH, K. D. 2003. Role of ALDP (ABCD1) and mitochondria in X-linked adrenoleukodystrophy. *Mol Cell Biol,* 23**,** 744-53.

MCGUINNESS, M. C., ZHANG, H. P. & SMITH, K. D. 2001. Evaluation of pharmacological induction of fatty acid beta-oxidation in X-linked adrenoleukodystrophy. *Mol Genet Metab,* 74**,** 256-63.

MECHA, M., CARRILLO-SALINAS, F. J., FELIU, A., MESTRE, L. & GUAZA, C. 2016. Microglia activation states and cannabinoid system: Therapeutic implications. *Pharmacol Ther,* 166**,** 40-55.

MECHA, M., FELIU, A., CARRILLO-SALINAS, F. J., RUEDA-ZUBIAURRE, A., ORTEGA-GUTIERREZ, S., DE SOLA, R. G. & GUAZA, C. 2015. Endocannabinoids drive the acquisition of an alternative phenotype in microglia. *Brain Behav Immun,* 49**,** 233-45.

MIGEON, B. R., MOSER, H. W., MOSER, A. B., AXELMAN, J., SILLENCE, D. & NORUM, R. A. 1981. Adrenoleukodystrophy: evidence for X linkage, inactivation, and selection favoring the mutant allele in heterozygous cells. *Proc Natl Acad Sci U S A,* 78**,** 5066-70.

MILLER, W. P., ROTHMAN, S. M., NASCENE, D., KIVISTO, T., DEFOR, T. E., ZIEGLER, R. S., EISENGART, J., LEISER, K., RAYMOND, G., LUND, T. C., TOLAR, J. & ORCHARD, P. J. 2011. Outcomes after allogeneic hematopoietic cell transplantation for childhood cerebral adrenoleukodystrophy: the largest single-institution cohort report. *Blood,* 118**,** 1971-8.

MILTON, N. G. 2002. Anandamide and noladin ether prevent neurotoxicity of the human amyloid-beta peptide. *Neurosci Lett,* 332**,** 127-30.

MINGHETTI, L. 2005. Role of inflammation in neurodegenerative diseases. *Curr Opin Neurol,* 18**,** 315-21.

MIRON, V. E., BOYD, A., ZHAO, J. W., YUEN, T. J., RUCKH, J. M., SHADRACH, J. L., VAN WIJNGAARDEN, P., WAGERS, A. J., WILLIAMS, A., FRANKLIN, R. J. M. & FFRENCH-CONSTANT, C. 2013. M2 microglia and macrophages drive oligodendrocyte differentiation during CNS remyelination. *Nat Neurosci,* 16**,** 1211-1218.

MORATO, L., GALINO, J., RUIZ, M., CALINGASAN, N. Y., STARKOV, A. A., DUMONT, M., NAUDI, A., MARTINEZ, J. J., AUBOURG, P., PORTERO-OTIN, M., PAMPLONA, R., GALEA, E., BEAL, M. F., FERRER, I., FOURCADE, S. & PUJOL, A. 2013. Pioglitazone halts axonal degeneration in a mouse model of X-linked adrenoleukodystrophy. *Brain,* 136**,** 2432-43.

MORATO, L., RUIZ, M., BOADA, J., CALINGASAN, N. Y., GALINO, J., GUILERA, C., JOVE, M., NAUDI, A., FERRER, I., PAMPLONA, R., SERRANO, M., PORTERO-OTIN, M., BEAL, M. F., FOURCADE, S. & PUJOL, A. 2015. Activation of sirtuin 1 as therapy for the peroxisomal disease adrenoleukodystrophy. *Cell Death Differ,* 22**,** 1742-53.

MOSER, A. B., BOREL, J., ODONE, A., NAIDU, S., CORNBLATH, D., SANDERS, D. B. & MOSER, H. W. 1987. A new dietary therapy for adrenoleukodystrophy:

biochemical and preliminary clinical results in 36 patients. *Ann Neurol,* 21**,** 240-9.

MOSER, A. B. & MOSER, H. W. 1999. The prenatal diagnosis of X-linked adrenoleukodystrophy. *Prenat Diagn,* 19**,** 46-8.

MOSER, H. W., LOES, D. J., MELHEM, E. R., RAYMOND, G. V., BEZMAN, L., COX, C. S. & LU, S. E. 2000. X-Linked adrenoleukodystrophy: overview and prognosis as a function of age and brain magnetic resonance imaging abnormality. A study involving 372 patients. *Neuropediatrics,* 31**,** 227-39.

MOSER, H. W. & MAHMOOD, A. 2007. New insights about hematopoietic stem cell transplantation in adrenoleukodystrophy. *Arch Neurol,* 64**,** 631-2.

MOSER, H. W., MOSER, A. B., FRAYER, K. K., CHEN, W., SCHULMAN, J. D., O'NEILL, B. P. & KISHIMOTO, Y. 1981. Adrenoleukodystrophy: increased plasma content of saturated very long chain fatty acids. *Neurology,* 31**,** 1241-9.

MOSER, H. W., RAYMOND, G. V., LU, S. E., MUENZ, L. R., MOSER, A. B., XU, J., JONES, R. O., LOES, D. J., MELHEM, E. R., DUBEY, P., BEZMAN, L., BRERETON, N. H. & ODONE, A. 2005. Follow-up of 89 asymptomatic patients with adrenoleukodystrophy treated with Lorenzo's oil. *Arch Neurol,* 62**,** 1073-80.

MOSSER, J., DOUAR, A. M., SARDE, C. O., KIOSCHIS, P., FEIL, R., MOSER, H., POUSTKA, A. M., MANDEL, J. L. & AUBOURG, P. 1993. Putative X-linked adrenoleukodystrophy gene shares unexpected homology with ABC transporters. *Nature,* 361**,** 726-730.

NAIDU, S., BRESNAN, M. J., GRIFFIN, D., O'TOOLE, S. & MOSER, H. W. 1988. Childhood adrenoleukodystrophy. Failure of intensive immunosuppression to arrest neurologic progression. *Arch Neurol,* 45**,** 846-8.

NETIK, A., FORSS-PETTER, S., HOLZINGER, A., MOLZER, B., UNTERRAINER, G. & BERGER, J. 1999. Adrenoleukodystrophy-related protein can compensate functionally for adrenoleukodystrophy protein deficiency (X-ALD): implications for therapy. *Hum Mol Genet,* 8**,** 907-13.

OEZEN, I., ROSSMANITH, W., FORSS-PETTER, S., KEMP, S., VOIGTLANDER, T., MOSER-THIER, K., WANDERS, R. J., BITTNER, R. E. & BERGER, J. 2005. Accumulation of very long-chain fatty acids does not affect mitochondrial function in adrenoleukodystrophy protein deficiency. *Hum Mol Genet,* 14**,** 1127-37.

OHLOW, M. J. & MOOSMANN, B. 2011. Phenothiazine: the seven lives of pharmacology's first lead structure. *Drug Discov Today,* 16**,** 119-31.

ORTEGA-GUTIERREZ, S., MOLINA-HOLGADO, E. & GUAZA, C. 2005. Effect of anandamide uptake inhibition in the production of nitric oxide and in the release of cytokines in astrocyte cultures. *Glia,* 52**,** 163-8.

OZ, M., LORKE, D. E. & PETROIANU, G. A. 2009. Methylene blue and Alzheimer's disease. *Biochem Pharmacol,* 78**,** 927-32.

PALAZUELOS, J., AGUADO, T., PAZOS, M. R., JULIEN, B., CARRASCO, C., RESEL, E., SAGREDO, O., BENITO, C., ROMERO, J., AZCOITIA, I., FERNANDEZ-RUIZ, J., GUZMAN, M. & GALVE-ROPERH, I. 2009. Microglial CB2 cannabinoid receptors are neuroprotective in Huntington's disease excitotoxicity. *Brain,* 132**,** 3152-64.

PALAZUELOS, J., DAVOUST, N., JULIEN, B., HATTERER, E., AGUADO, T., MECHOULAM, R., BENITO, C., ROMERO, J., SILVA, A., GUZMAN, M., NATAF, S. & GALVE-ROPERH, I. 2008. The CB(2) cannabinoid receptor controls myeloid progenitor trafficking: involvement in the pathogenesis of an animal model of multiple sclerosis. *J Biol Chem,* 283**,** 13320-9.

PARASCANDOLA, J. 1981. The theoretical basis of Paul Ehrlich's chemotherapy. *J Hist Med Allied Sci,* 36**,** 19-43.

PETRILLO, S., PIEMONTE, F., PASTORE, A., TOZZI, G., AIELLO, C., PUJOL, A., CAPPA, M. & BERTINI, E. 2013. Glutathione imbalance in patients with X-linked adrenoleukodystrophy. *Mol Genet Metab,* 109**,** 366-70.

PIRO, J. R., BENJAMIN, D. I., DUERR, J. M., PI, Y., GONZALES, C., WOOD, K. M., SCHWARTZ, J. W., NOMURA, D. K. & SAMAD, T. A. 2012. A dysregulated endocannabinoid-eicosanoid network supports pathogenesis in a mouse model of Alzheimer's disease. *Cell Rep,* 1**,** 617-23.

POTEET, E., WINTERS, A., YAN, L. J., SHUFELT, K., GREEN, K. N., SIMPKINS, J. W., WEN, Y. & YANG, S. H. 2012. Neuroprotective actions of methylene blue and its derivatives. *PLoS One,* 7**,** e48279.

PUJOL, A., FERRER, I., CAMPS, C., METZGER, E., HINDELANG, C., CALLIZOT, N., RUIZ, M., PAMPOLS, T., GIROS, M. & MANDEL, J. L. 2004. Functional overlap between ABCD1 (ALD) and ABCD2 (ALDR) transporters: a therapeutic target for X-adrenoleukodystrophy. *Hum.Mol.Genet.,* 13**,** 2997-3006.

PUJOL, A., HINDELANG, C., CALLIZOT, N., BARTSCH, U., SCHACHNER, M. & MANDEL, J. L. 2002. Late onset neurological phenotype of the X-ALD gene inactivation in mice: a mouse model for adrenomyeloneuropathy. *Hum Mol Genet,* 11**,** 499-505.

RAMIREZ, B. G., BLAZQUEZ, C., GOMEZ DEL PULGAR, T., GUZMAN, M. & DE CEBALLOS, M. L. 2005. Prevention of Alzheimer's disease pathology by cannabinoids: neuroprotection mediated by blockade of microglial activation. *J Neurosci,* 25**,** 1904-13.

RANSOHOFF, R. M. 2016. A polarizing question: do M1 and M2 microglia exist? *Nat Neurosci,* 19**,** 987-91.

RIVEST, S. 2009. Regulation of innate immune responses in the brain. *Nat Rev Immunol,* 9**,** 429-39.

ROJAS, J. C., BRUCHEY, A. K. & GONZALEZ-LIMA, F. 2012. Neurometabolic mechanisms for memory enhancement and neuroprotection of methylene blue. *Prog Neurobiol,* 96**,** 32-45.

RUIZ, M., JOVE, M., SCHLUTER, A., CASASNOVAS, C., VILLARROYA, F., GUILERA, C., ORTEGA, F. J., NAUDI, A., PAMPLONA, R., GIMENO, R., FOURCADE, S., PORTERO-OTIN, M. & PUJOL, A. 2015. Altered glycolipid and glycerophospholipid signaling drive inflammatory cascades in adrenomyeloneuropathy. *Hum Mol Genet,* 24**,** 6861-76.

RUSNAKOVA, V., HONSA, P., DZAMBA, D., STAHLBERG, A., KUBISTA, M. & ANDEROVA, M. 2013. Heterogeneity of astrocytes: from development to injury - single cell gene expression. *PLoS One,* 8**,** e69734.

SCHILDER, P. 1924. Die Encephalitis periaxialis diffusa. *Arch Psychiatr. Nervenkr.*, 71**,** 327–356.

SCHIRMER, R. H., ADLER, H., PICKHARDT, M. & MANDELKOW, E. 2011. "Lest we forget you--methylene blue...". *Neurobiol Aging,* 32**,** 2325 e7-16.

SCHLUTER, A., ESPINOSA, L., FOURCADE, S., GALINO, J., LOPEZ, E., ILIEVA, E., MORATO, L., ASHEUER, M., COOK, T., MCLAREN, A., REID, J., KELLY, F., BATES, S., AUBOURG, P., GALEA, E. & PUJOL, A. 2012. Functional genomic analysis unravels a metabolic-inflammatory interplay in adrenoleukodystrophy. *Hum Mol Genet,* 21**,** 1062-77.

SCHLUTER, A., FOURCADE, S., RIPP, R., MANDEL, J. L., POCH, O. & PUJOL, A. 2006. The Evolutionary Origin of Peroxisomes: An ER-Peroxisome Connection. *Mol Biol Evol,* 23**,** 838-845.

SHANI, N., JIMENEZ-SANCHEZ, G., STEEL, G., DEAN, M. & VALLE, D. 1997. Identification of a fourth half ABC transporter in the human peroxisomal membrane. *Hum Mol Genet,* 6**,** 1925-31.

SHENG, W. S., HU, S., MIN, X., CABRAL, G. A., LOKENSGARD, J. R. & PETERSON, P. K. 2005. Synthetic cannabinoid WIN55,212-2 inhibits generation of inflammatory mediators by IL-1beta-stimulated human astrocytes. *Glia,* 49**,** 211-9.

SHINNOH, N., YAMADA, T., YOSHIMURA, T., FURUYA, H., YOSHIDA, Y., SUZUKI, Y., SHIMOZAWA, N., ORII, T. & KOBAYASHI, T. 1995. Adrenoleukodystrophy: the restoration of peroxisomal beta-oxidation by transfection of normal cDNA. *Biochem Biophys Res Commun,* 210**,** 830-6.

SIEMERLING, E. & CREUTZFELDT, H. G. 1923. Bronzekrankheit und sklerosierende encephalomyelitis. *Arch. Psychiatr Nervenkr.,* 68**,** 217-244.

SINGH, H., DERWAS, N. & POULOS, A. 1987. Very long chain fatty acid beta-oxidation by rat liver mitochondria and peroxisomes. *Arch Biochem Biophys,* 259**,** 382-90.

SINGH, I., KHAN, M., KEY, L. & PAI, S. 1998. Lovastatin for X-linked adrenoleukodystrophy. *N Engl J Med,* 339**,** 702-3.

SINGH, I., PAINTLIA, A. S., KHAN, M., STANISLAUS, R., PAINTLIA, M. K., HAQ, E., SINGH, A. K. & CONTRERAS, M. A. 2004. Impaired peroxisomal function in the central nervous system with inflammatory disease of experimental autoimmune encephalomyelitis animals and protection by lovastatin treatment. *Brain Res,* 1022**,** 1-11.

SINGH, I. & PUJOL, A. 2010. Pathomechanisms underlying X-adrenoleukodystrophy: a three-hit hypothesis. *Brain Pathol,* 20**,** 838-44.

SINGH, J., KHAN, M. & SINGH, I. 2009. Silencing of Abcd1 and Abcd2 genes sensitizes astrocytes for inflammation: implication for X-adrenoleukodystrophy. *J Lipid Res,* 50**,** 135-47.

SINGHRAO, S. K., NEAL, J. W., MORGAN, B. P. & GASQUE, P. 1999. Increased complement biosynthesis by microglia and complement activation on neurons in Huntington's disease. *Exp Neurol,* 159**,** 362-76.

STACK, C., JAINUDDIN, S., ELIPENAHLI, C., GERGES, M., STARKOVA, N., STARKOV, A. A., JOVE, M., PORTERO-OTIN, M., LAUNAY, N., PUJOL, A., KAIDERY, N. A., THOMAS, B., TAMPELLINI, D., BEAL, M. F. & DUMONT, M. 2014. Methylene blue upregulates Nrf2/ARE genes and prevents tau-related neurotoxicity. *Hum Mol Genet,* 23**,** 3716-32.

STELLA, N. 2010. Cannabinoid and cannabinoid-like receptors in microglia, astrocytes, and astrocytomas. *Glia,* 58**,** 1017-30.

SU, K., BOURDETTE, D. & FORTE, M. 2013. Mitochondrial dysfunction and neurodegeneration in multiple sclerosis. *Front Physiol,* 4**,** 169.

TANG, Y. & LE, W. 2016. Differential Roles of M1 and M2 Microglia in Neurodegenerative Diseases. *Mol Neurobiol,* 53**,** 1181-94.

TURU, G. & HUNYADY, L. 2010. Signal transduction of the CB1 cannabinoid receptor. *J Mol Endocrinol,* 44**,** 75-85.

VALDEOLIVAS, S., PAZOS, M. R., BISOGNO, T., PISCITELLI, F., IANNOTTI, F. A., ALLARA, M., SAGREDO, O., DI MARZO, V. & FERNANDEZ-RUIZ, J. 2013. The inhibition of 2-arachidonoyl-glycerol (2-AG) biosynthesis, rather than enhancing striatal damage, protects striatal neurons from malonate-induced death: a potential role of cyclooxygenase-2-dependent metabolism of 2-AG. *Cell Death Dis,* 4**,** e862.

VAN GEEL, B. M., ASSIES, J., HAVERKORT, E. B., KOELMAN, J. H., VERBEETEN, B., JR., WANDERS, R. J. & BARTH, P. G. 1999. Progression of abnormalities in adrenomyeloneuropathy and neurologically asymptomatic X-linked adrenoleukodystrophy despite treatment with "Lorenzo's oil". *J Neurol Neurosurg Psychiatry,* 67**,** 290-9.

VAN GEEL, B. M., POLL-THE, B. T., VERRIPS, A., BOELENS, J. J., KEMP, S. & ENGELEN, M. 2015. Hematopoietic cell transplantation does not prevent myelopathy in X-linked adrenoleukodystrophy: a retrospective study. *J Inherit Metab Dis,* 38**,** 359-61.

VAN ROERMUND, C. W., VISSER, W. F., IJLST, L., VAN CRUCHTEN, A., BOEK, M., KULIK, W., WATERHAM, H. R. & WANDERS, R. J. 2008. The human peroxisomal ABC half transporter ALDP functions as a homodimer and accepts acyl-CoA esters. *Faseb J,* 22**,** 4201-8.

VANSTONE, J. R., SMITH, A. M., MCBRIDE, S., NAAS, T., HOLCIK, M., ANTOUN, G., HARPER, M. E., MICHAUD, J., SELL, E., CHAKRABORTY, P., TETREAULT, M., CARE4RARE, C., MAJEWSKI, J., BAIRD, S., BOYCOTT, K. M., DYMENT, D. A., MACKENZIE, A. & LINES, M. A. 2016. DNM1L-related mitochondrial fission defect presenting as refractory epilepsy. *Eur J Hum Genet,* 24**,** 1084-8.

VARIN, A. & GORDON, S. 2009. Alternative activation of macrophages: immune function and cellular biology. *Immunobiology,* 214**,** 630-41.

VOSS, E. V., SKULJEC, J., GUDI, V., SKRIPULETZ, T., PUL, R., TREBST, C. & STANGEL, M. 2012. Characterisation of microglia during de- and remyelination: can they create a repair promoting environment? *Neurobiol Dis,* 45**,** 519-28.

WAISMAN, A., LIBLAU, R. S. & BECHER, B. 2015. Innate and adaptive immune responses in the CNS. *Lancet Neurol,* 14**,** 945-55.

WAKABAYASHI, J., ZHANG, Z., WAKABAYASHI, N., TAMURA, Y., FUKAYA, M., KENSLER, T. W., IIJIMA, M. & SESAKI, H. 2009. The dynamin-related GTPase Drp1 is required for embryonic and brain development in mice. *J Cell Biol,* 186**,** 805-16.

WANDERS, R. J., VISSER, W. F., VAN ROERMUND, C. W., KEMP, S. & WATERHAM, H. R. 2007. The peroxisomal ABC transporter family. *Pflugers Arch,* 453**,** 719-34.

WANDERS, R. J. & WATERHAM, H. R. 2006. Biochemistry of mammalian peroxisomes revisited. *Annu Rev Biochem,* 75**,** 295-332.

WEN, Y., LI, W., POTEET, E. C., XIE, L., TAN, C., YAN, L. J., JU, X., LIU, R., QIAN, H., MARVIN, M. A., GOLDBERG, M. S., SHE, H., MAO, Z., SIMPKINS, J. W. & YANG, S. H. 2011. Alternative mitochondrial electron transfer as a novel strategy for neuroprotection. *J Biol Chem,* 286**,** 16504-15.

WHITCOMB, R. W., LINEHAN, W. M. & KNAZEK, R. A. 1988. Effects of long-chain, saturated fatty acids on membrane microviscosity and adrenocorticotropin responsiveness of human adrenocortical cells in vitro. *J Clin Invest,* 81**,** 185-8.

WIESINGER, C., KUNZE, M., REGELSBERGER, G., FORSS-PETTER, S. & BERGER, J. 2013. Impaired very long-chain acyl-CoA beta-oxidation in human X-linked adrenoleukodystrophy fibroblasts is a direct consequence of ABCD1 transporter dysfunction. *J Biol Chem,* 288**,** 19269-79.

WYSS-CORAY, T. & MUCKE, L. 2002. Inflammation in neurodegenerative disease--a double-edged sword. *Neuron,* 35**,** 419-32.